

Young

Predictive Geochemical Modeling of Interactions Between Uranium Mill Tailings Solutions and Sediments in a Flow-Through System

Model Formulations and Preliminary Results

Prepared by S. R. Peterson, A. R. Felmy, R. J. Serne, G. W. Gee

Pacific Northwest Laboratory
Operated by
Battelle Memorial Institute

Prepared for
U.S. Nuclear Regulatory
Commission

NOTICE

This report was prepared as an account of work sponsored by an agency of the United States Government. Neither the United States Government nor any agency thereof, or any of their employees, makes any warranty, expressed or implied, or assumes any legal liability of responsibility for any third party's use, or the results of such use, of any information, apparatus, product or process disclosed in this report, or represents that its use by such third party would not infringe privately owned rights.

Availability of Reference Materials Cited in NRC Publications

Most documents cited in NRC publications will be available from one of the following sources:

1. The NRC Public Document Room, 1717 H Street, N.W.
Washington, DC 20555
2. The NRC/GPO Sales Program, U.S. Nuclear Regulatory Commission,
Washington, DC 20555
3. The National Technical Information Service, Springfield, VA 22161

Although the listing that follows represents the majority of documents cited in NRC publications, it is not intended to be exhaustive.

Referenced documents available for inspection and copying for a fee from the NRC Public Document Room include NRC correspondence and internal NRC memoranda; NRC Office of Inspection and Enforcement bulletins, circulars, information notices, inspection and investigation notices; Licensee Event Reports; vendor reports and correspondence; Commission papers; and applicant and licensee documents and correspondence.

The following documents in the NUREG series are available for purchase from the NRC/GPO Sales Program: formal NRC staff and contractor reports, NRC-sponsored conference proceedings, and NRC booklets and brochures. Also available are Regulatory Guides, NRC regulations in the *Code of Federal Regulations*, and *Nuclear Regulatory Commission Issuances*.

Documents available from the National Technical Information Service include NUREG series reports and technical reports prepared by other federal agencies and reports prepared by the Atomic Energy Commission, forerunner agency to the Nuclear Regulatory Commission.

Documents available from public and special technical libraries include all open literature items, such as books, journal and periodical articles, and transactions. *Federal Register* notices, federal and state legislation, and congressional reports can usually be obtained from these libraries.

Documents such as theses, dissertations, foreign reports and translations, and non-NRC conference proceedings are available for purchase from the organization sponsoring the publication cited.

Single copies of NRC draft reports are available free upon written request to the Division of Technical Information and Document Control, U.S. Nuclear Regulatory Commission, Washington, DC 20555.

Copies of industry codes and standards used in a substantive manner in the NRC regulatory process are maintained at the NRC Library, 7920 Norfolk Avenue, Bethesda, Maryland, and are available there for reference use by the public. Codes and standards are usually copyrighted and may be purchased from the originating organization or, if they are American National Standards, from the American National Standards Institute, 1430 Broadway, New York, NY 10018.

Predictive Geochemical Modeling of Interactions Between Uranium Mill Tailings Solutions and Sediments in a Flow-Through System

Model Formulations and Preliminary Results

Manuscript Completed: July 1983
Date Published: August 1983

Prepared by
S. R. Peterson, A. R. Felmy, R. J. Serne, G. W. Gee

Pacific Northwest Laboratory
Richland, WA 99352

Prepared for
Division of Health, Siting and Waste Management
Office of Nuclear Regulatory Research
U.S. Nuclear Regulatory Commission
Washington, D.C. 20555
NRC FIN B2292

ABSTRACT

An equilibrium thermodynamic conceptual model consisting of minerals and solid phases was developed to represent a soil column. A computer program was used as a tool to solve the system of mathematical equations imposed by the conceptual chemical model. The combined conceptual model and computer program were used to predict aqueous phase compositions of effluent solutions from permeability cells packed with geologic materials and percolated with uranium mill tailings solutions. Initial calculations of ion speciation and mineral solubility and our understanding of the chemical processes occurring in the modeled system were used to select solid phases for inclusion in the conceptual model. The modeling predictions were compared to the analytically determined column effluent concentrations. Hypotheses were formed, based on modeling predictions and laboratory evaluations, as to the probable mechanisms controlling the migration of selected contaminants. An assemblage of minerals and other solid phases could be used to predict the concentrations of several of the macro constituents (e.g., Ca, SO₄, Al, Fe, and Mn) but could not be used to predict trace element concentrations. These modeling conclusions are applicable to situations where uranium mill tailings solutions of low pH and high total dissolved solids encounter either clay liners or natural geologic materials that contain inherent acid neutralizing capacities.

CONTENTS

ABSTRACT.....	iii
ACKNOWLEDGMENTS.....	ix
RECOMMENDATIONS FOR FUTURE WORK.....	xi
EXECUTIVE SUMMARY.....	1
INTRODUCTION.....	3
PRIOR EFFORTS.....	4
MATERIALS AND METHODS.....	5
EQUILIBRIUM COMPUTER MODELING APPROACH.....	9
GEOCHEMICAL COMPUTER CODE.....	9
ION SPECIATION/SOLUBILITY CALCULATIONS.....	9
CONCEPTUAL MODEL DEVELOPMENT.....	10
COMPARISON OF PREDICTED VERSUS EXPERIMENTAL RESULTS.....	12
COMPONENTS AND ASSOCIATED SOLID PHASES CONSIDERED.....	12
RESULTS AND DISCUSSION.....	15
pH and pe.....	15
Aluminum.....	17
Calcium.....	21
Sulfate.....	22
Iron.....	24
Manganese.....	28
Magnesium.....	31
Strontium.....	33
Silicon.....	34
Uranium.....	35
TRACE ELEMENTS OF POTENTIAL IMPORTANCE IN URANIUM MILL TAILINGS SOLUTIONS.....	36
Selenium.....	38
Arsenic.....	40
Molybdenum.....	42
Vanadium.....	45
Chromium.....	46
Lead.....	49
Nickel, Silver, Cadmium, and Zinc.....	49
SUMMARY AND CONCLUSIONS.....	51
REFERENCES.....	Ref.1
APPENDIX A.....	A.1
APPENDIX B.....	B.1
APPENDIX C.....	C.1

FIGURES

1	Comparison of the Experimental and Modeling Systems.....	11
2	Measured and Predicted Values of pH Plotted Versus Pore Volumes of Effluent for Permeability Column 5.....	16
3	Measured and Predicted Values of pe Plotted Versus Pore Volumes of Effluent for the Vacuum Extractor Columns	16
4	Measured and Predicted Concentrations of Aluminum Plotted Versus Pore Volumes of Effluent for the Vacuum Extractor Columns.....	19
5	Measured and Predicted Concentrations of Aluminum Plotted Versus Pore Volumes of Effluent for Permeability Column 5.....	20
6	Measured and Predicted Concentrations of Aluminum Plotted Versus Pore Volumes of Effluent for Permeability Column 8.....	20
7	Measured and Predicted Concentrations of Calcium Plotted Versus Pore Volumes of Effluent for the Vacuum Extractor Columns.....	23
8	Measured and Predicted Concentrations of Calcium Plotted Versus Pore Volumes of Effluent for Permeability Column 5.....	23
9	Measured and Predicted Concentrations of Calcium Plotted Versus Pore Volumes of Effluent for Permeability Column 8.....	24
10	Measured and Predicted Concentrations of Sulfate Plotted Versus Pore Volumes of Effluent for the Vacuum Extractor Columns.....	25
11	Measured and Predicted Concentrations of Sulfate Plotted Versus Pore Volumes of Effluent for Permeability Column 5.....	25
12	Measured and Predicted Concentrations of Sulfate Plotted Versus Pore Volumes of Effluent for Permeability Column 8.....	26
13	Measured and Predicted Values of Iron Plotted Versus Pore Volumes of Effluent for the Vacuum Extractor Columns.....	27
14	Measured and Predicted Concentrations of Manganese Plotted Versus Pore Volumes of Effluent for the Vacuum Extractor Columns.....	29
15	Measured and Predicted Concentrations of Manganese Plotted Versus pH for the Vacuum Extractor Columns.....	29
16	Measured and Predicted Concentrations of Manganese Plotted Versus Pore Volumes of Effluent for Permeability Column 5.....	30

17	Measured and Predicted Concentrations of Manganese Plotted Versus Pore Volumes of Effluent for Permeability Column 8.....	30
18	Measured and Predicted Concentrations of Magnesium Plotted Versus Pore Volumes of Effluent for the Vacuum Extractor Columns.....	31
19	Measured and Predicted Concentrations of Magnesium Plotted Versus Pore Volumes of Effluent for Permeability Column 5.....	32
20	Measured and Predicted Concentrations of Magnesium Plotted Versus Pore Volumes of Effluent for Permeability Column 8.....	32
21	Measured and Predicted Concentrations of Strontium Plotted Versus Pore Volumes of Effluent for the Vacuum Extractor Columns.....	34
22	Measured and Predicted Concentrations of Uranium Plotted Versus Pore Volumes of Effluent for the Vacuum Extractor Columns.....	36

TABLES

1	Characterization of the Morton Ranch Clay Liner and Overburden.....	6
2	Composition of Various Highland Mill and Synthetic Tailings Solutions Used in Laboratory Experiments, mg/l.....	7
3	Components for Which Possible Solid Phase Controls Were Included in the Conceptual Model.....	12
4	Solid Phases Assumed to Exist in the Original Geologic Materials.....	13
5	Solids That Were Allowed to Precipitate.....	13
6	Summary of Important Control Mechanisms.....	53

ACKNOWLEDGMENTS

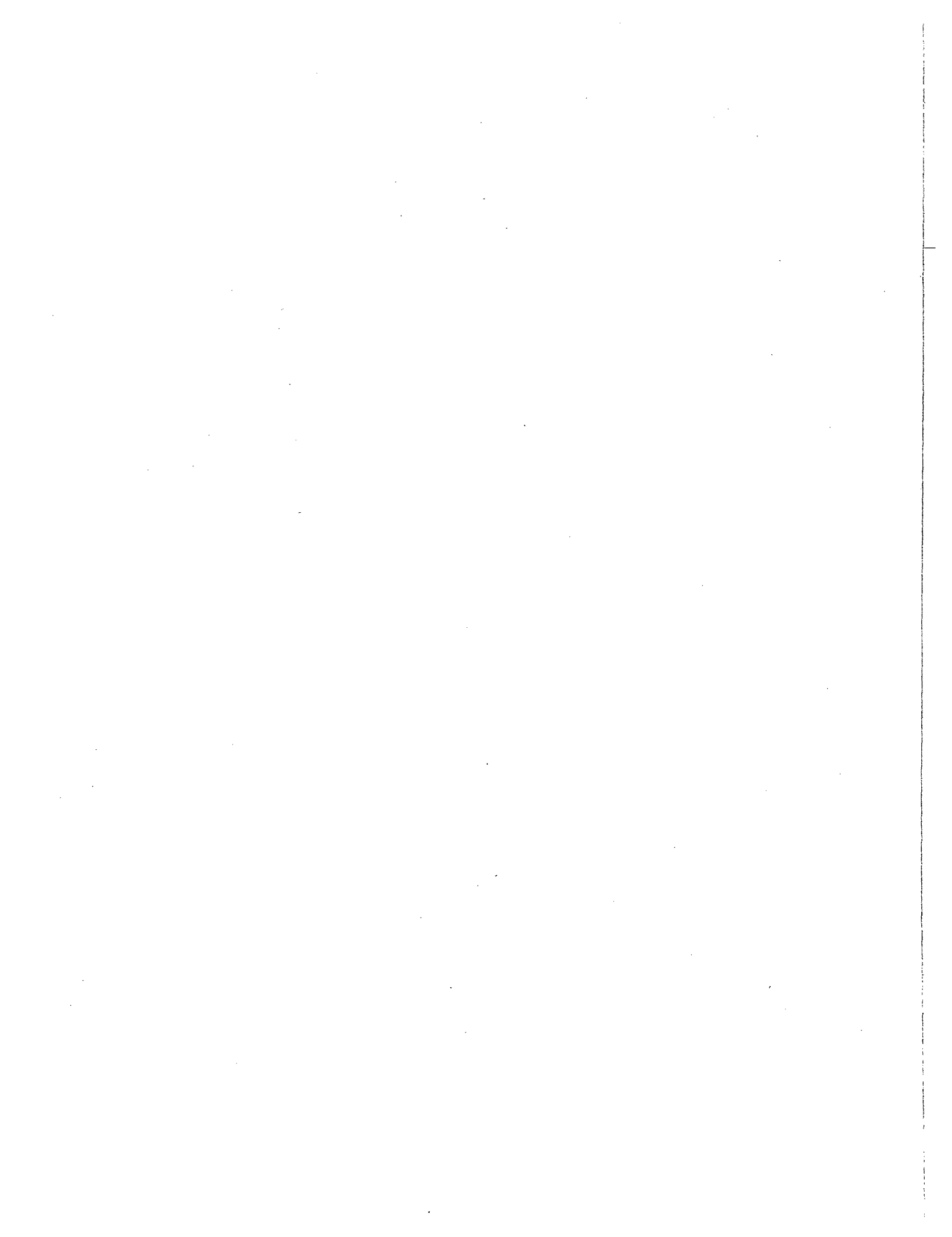
This study was funded by the U.S. Nuclear Regulatory Commission as part of the Uranium Recovery Research Program at Pacific Northwest Laboratory. We wish to thank C. W. Begej, A. C. Campbell, M. E. Dodson, R. L. Erikson, D. Gibson, A. W. Lautensleger, W. J. Martin, B. E. Opitz, D. E. Rinehart, R. W. Sanders, D. R. Sherwood, and J. M. Tingey for their help in setting up the necessary experiments and performing the analyses requisite to the completion of this report. We thank C. Brown, M. G. Foley, J. S. Fruchter, and J. A. Stottlemire for their technical and editorial review of this document. Special thanks are given to G. F. Birchard of the Nuclear Regulatory Commission technical staff for the guidance he has provided and for the meaningful comments he has given to this project. Finally, thanks are given to Ms. Deidre Berg for typing this manuscript and helping to organize the graphics and tables.

RECOMMENDATIONS FOR FUTURE WORK

A variety of theoretical and empirical adsorption models have been exercised to explain trace metal adsorption onto different hydrous oxide surfaces. However, further work needs to be done to explain trace metal adsorption phenomena in complex media such as uranium mill tailings solutions. According to previous work, and the results presented in this report, complexation/adsorption with hydrous oxide surfaces is an important mechanism controlling trace metal concentrations when uranium mill tailings solutions interact with sediments. Considerable success has been achieved in developing models that consider the adsorption of trace metals onto hydrous oxides (Davis and Leckie 1978, Hohl and Stumm 1976). Furthermore, the intrinsic stability constants have been published for the complexation of several trace metals with iron oxyhydroxides (Davis and Leckie 1978, Leckie et al. 1980, Balistrieri and Murray 1982). Two such surface complexation models: a constant capacitance model (Hohl and Stumm 1976) and the triple layer site binding model (Davis and Leckie 1978, Yates et al. 1974) are included in the MINTEQ computer code. The conceptual model presented here can be used to predict the mass of iron hydroxide that will precipitate when uranium mill tailings contact sediments that contain inherent acid neutralizing capacities. This conceptual model needs to be expanded to include the adsorption of trace metals onto the surface of iron oxyhydroxides.

Since the solubility and adsorption, hence mobility, of many elements are pH dependent it is imperative to develop geochemical models capable of predicting the pH front migration. This requires a more complete understanding and consideration of reactions that affect the pH. Reactions currently considered by our predictive model, in attempting to predict the pH front migration, such as precipitation/dissolution (especially calcite dissolution), complexation, and oxidation/reduction are based on thermodynamic constants. To improve our ability to predict the pH we need to simultaneously consider protonation reactions and reactions of the bulk electrolyte ions with the iron oxyhydroxide surface in a similar manner to trace metal adsorption.

Finally, additional field studies are needed to validate the geochemical modeling predictions and to further verify the applicability of the extrapolation of the laboratory results to the field. The field studies are needed at acidic tailings sites which have detailed site chemistry, including pore water solution chemistry data, and well-documented hydrology of the contaminant plume. Although most present sites, suitable for such a study, are associated with above-ground tailings ponds, the analysis at below grade pit disposal sites is possible if geochemical considerations are similar at pond and pit sites of interest.



PREVIOUS DOCUMENTS IN SERIES

This progress report is the seventh NUREG document prepared for this project, "Assessment of Leachate Movement from Uranium Mill Tailings" (FIN B2292). The project has two thrust areas, laboratory determination of contaminant retardation in sediments and clay liners and computer model development/simulation of water movement and contaminant migration. Validation of the laboratory measurements and geochemical modeling predictions is planned through a field study at a mill site. The project was initiated in April 1979. Other NUREG reports from this project are:

NUREG/CR-1494, "Interaction of Uranium Mill Tailings Leachate with Soils and Clay Liners: Laboratory Analysis/Progress Report," G. W. Gee, A. C. Campbell, D. R. Sherwood, R. G. Strickert and S. J. Phillips, June 1980.

NUREG/CR-1495, "Model Assessment of Alternatives for Reducing Seepage from Buried Uranium Mill Tailings at the Morton Ranch Site in Central Wyoming," R. W. Nelson, A. E. Reisenauer and G. W. Gee, June 1980.

NUREG/CR-2360, "TRUST: A Computer Program for Variably Saturated Flow in Multidimensional Deformable Media," A. E. Reisenauer, K. T. Key, T. N. Narasimhan and R. W. Nelson, January 1982.

NUREG/CR-2845, "DIGRD: An Interactive Grid Generating Program," H. P. Foote, W. A. Rice and C. T. Kincaid, October 1982.

NUREG/CR-2946, "The Long Term Stability of Earthen Materials in Contact with Acidic Tailings Solutions," S. R. Peterson, R. L. Erikson and G. W. Gee, November 1982.

NUREG/CR-3124, "Laboratory Measurements of Contaminant Attenuation of Uranium Mill Tailings Leachates by Sediments and Clay Liners," R. J. Serne, S. R. Peterson, and G. W. Gee, April 1983.



EXECUTIVE SUMMARY

This report documents the use of a solid phase assemblage to predict the aqueous effluent compositions from columns of subsoil materials percolated with uranium mill tailings solutions. Previous geochemical modeling efforts (Nordstrom et al. 1979, Gang and Langmuir 1974, Jenne et al. 1980, Peterson and Krupka 1981, Peterson et al. 1982, and Deutsch et al. 1982) have confined themselves to examining saturation indices in the quest for solid phases that could be in equilibrium with their dissolved constituents. Little effort has been expended to use these solid phases as a model of a heterogeneous material. Such a mineral assemblage can be reacted with a specified solution in a flow-through system and used to predict the resultant effluent concentrations. The solid phase assemblage was constructed not only from calculations of ion speciation/solubility but also from our understanding of the chemical processes occurring in the system.

In the experiments we modeled, columns of various configurations were packed with subsoils (either a silty clay loam or a sandy loam) and leached with one of two uranium mill tailings solutions. The two solutions were taken from the same site but differed in composition. The uranium mill tailings solutions contacted the aforementioned sediments for periods varying from three weeks up to approximately three years, depending upon the specific experiment. Transit times for a single pore volume of solution varied from 18 hours to roughly 45 days in the vacuum extractor and permeability columns, respectively. Measured effluent concentrations were compared to predicted effluent concentrations not only to judge the adequacy of the postulated mineral phase assemblage but also for elucidation of important chemical mechanisms.

The initial predictive modeling effort in this report is presented for the purpose of illustrating the methodology employed in predictive modeling and for demonstrating the applicability of this type of modeling to the movement of leachate from uranium mill tailings impoundments. Efforts are continuing at refining the conceptual model presented in this report to increase the predictability of the models. These efforts will be documented in subsequent reports.

The precipitation/dissolution reactions considered in the conceptual model were capable of predicting the column effluent concentrations of several of the macro constituents of the tailings solutions (SO_4 , Ca, Al, Mn, and Fe). Sulfate concentrations in the column effluents were generally one to two orders of magnitude above the secondary drinking water standards established by the U.S. Environmental Protection Agency. The conceptual model was able to predict these elevated concentrations.

The conceptual model was unsatisfactory when used to predict the concentrations of selected trace metals. Generally, trace metals were undersaturated relative to any solid phases that could control their concentrations. Data developed through laboratory and field studies lead us to believe that we can empirically quantify the migration of trace metals though we were unable to make satisfactory predictions based on this initial attempt at developing a

theoretical construct. Other mechanisms besides precipitation/dissolution (e.g., adsorption, ion exchange) appear to be controlling the concentration of many of the trace elements. Additional laboratory data must be developed to adequately predict the concentrations of these trace elements. Precipitation/dissolution reactions based on thermodynamic constants are sufficient to explain the effluent concentrations of some elements, while additional mechanisms, for which experimental data must be developed, are necessary for others.

The concentrations of many trace elements appear to be controlled by adsorption and/or coprecipitation with ferric oxyhydroxide surfaces. Several adsorption models of the hydrous oxide water interface have been formulated (Davis and Leckie 1978, Hohl and Stumm 1976) and have shown considerable success in modeling the adsorption of trace metals onto hydrous oxides. In addition, intrinsic stability constants for the reaction of several trace metals with iron oxyhydroxides have been published in the literature (Davis and Leckie 1978, Leckie et al. 1980, Balistrieri and Murray 1982). Thus, it appears that the conceptual chemical model presented here, can be expanded to predict the adsorption of several trace metals onto the surface of iron oxyhydroxides.

INTRODUCTION

Ion speciation and mineral solubility calculations have been used extensively to gain a better understanding of the geochemical processes controlling the chemical composition of natural waters. Several computer programs have been utilized to perform these calculations. Some of the more recent programs include MINEQL (Westall et al. 1976), PHREEQE (Parkhurst et al. 1980), WATEQ3 (Ball et al. 1981), and MINTEQ (Felmy et al. 1983). Several such computer programs have been successfully used to help evaluate possible solid phase controls on solution composition (Nordstrom et al. 1979, Gang and Langmuir 1974, Peterson and Krupka 1981, Peterson et al. 1982, and Deutsch et al. 1982). However, very little work has been done in exercising these geochemical computer codes in a flow-through system to predict the aqueous phase compositions resulting from solution interaction with an assemblage of solid phases. During such interactions, one or more solid phases may dissolve and thermodynamically more stable solid phases precipitate as the solution composition changes. The new set of stable solid phases, along with their associated masses, can then be reacted with a new volume of influent and the process repeated.

Conceptually, the hypothesized solid phase assemblage can be used to represent heterogeneous natural geologic materials. The solid phase assemblage consists of solids which are permitted to dissolve or precipitate in response to changes in the aqueous media. This solid phase assemblage, in conjunction with a computer program, is then used to simulate the contact of a specified solution with the geologic media. The resultant aqueous phase compositions and the change in mass of the solid phase assemblage are calculated as successive pore volumes of solution interact with the solid phase assemblage. The MINTEQ computer code (Felmy et al. 1983) was chosen for use in this study because of its ability to model this type of system.

The natural system modeled in this study was a flow-through system in which a silty clay loam and a sandy loam soil were contacted with uranium mill tailings solution. The mill tailings liquor is extremely acidic ($\text{pH} \approx 2$) and contains high concentrations of sulfate, iron, manganese, aluminum, silica, and several radionuclides and trace metals. The first few pore volumes of acid solution are neutralized upon contact with the geologic materials, which results in the precipitation of solid phases and the concurrent lowering of the aqueous phase concentrations. As successive pore volumes of solution flow through the columns, the natural buffering capacity of the soil material is eventually exhausted, the pH begins to drop, and the solution concentrations increase. The drop in pH can result in the dissolution of previously precipitated phases.

This system was chosen for predictive modeling because precipitation/dissolution of solid phases is expected to be the dominant mechanism controlling the aqueous concentrations of several constituents. Additional mechanisms (e.g., adsorption) must be incorporated into the conceptual model to effectively simulate the movement of constituents, such as trace metals, for which precipitation/dissolution is not a dominant control mechanism.

PRIOR EFFORTS

Previous efforts in applying geochemical modeling to uranium mill tailings are discussed in Peterson and Krupka (1981) and Peterson et al. (1982). Peterson and Krupka (1981) modeled batch solutions in which synthetic tailings solution, actual tailings solution, and H_2SO_4 interacted with natural and treated clay materials. This study illustrated the importance of obtaining accurate and adequate solution analyses. The modeling results indicated that several solids could be precipitating in the batch experiments. This precipitation was thought to be partially responsible for the reduction in permeability over time that was observed in other experiments involving laboratory permeability columns. Ion speciation/solubility modeling was found to be an effective tool in helping delineate the chemical reactions purportedly responsible for the observed reductions in permeability.

Peterson et al. (1982) modeled effluent solutions from permeability cells packed with the Morton Ranch clay liner and contacted with synthetic and actual tailings solutions. The purpose of this study was to compare the solubility controls identified in the static batch experiments with those controls identified in the dynamic column experiments to see if the same solubility controls were operating in both types of experiments. Many, but not all, of the same controls were found in the column experiments as were identified in the batch experiments. The information obtained in these studies was used to help formulate the conceptual chemical model used in this study.

MATERIALS AND METHODS

The materials and experimental methods used in obtaining the data used to compare with the modeling results have been abundantly documented elsewhere (Gee et al. 1980, Peterson et al. 1982, and Serne et al. 1983). Results of the physical and chemical characterization work performed on the geologic materials and uranium mill tailings solutions that were used to provide the interactions modeled in this document are presented in Tables 1 and 2.

Table 1 has been extracted from Peterson et al. (1982) and contains the physical and chemical characterizations of the Morton Ranch clay liner and the Morton Ranch overburden. These geologic materials were obtained from the Morton Ranch Uranium Mine and Mill site located in Converse County, Wyoming. The geology of the area has been documented in a United Nuclear Corporation Environmental Report (U.S. NRC 1979). All characterization work on these materials was done using standard soil testing procedures as outlined in Black (1965a,b). The Morton Ranch clay liner is classified in the USDA system as a silty clay loam; while the Morton Ranch overburden is classified as a sandy loam. The calcium carbonate value for the Morton Ranch clay liner reported here differs from that given in Peterson et al. (1982) (0.04%). This value was determined by a subcontractor (using Black 1965b procedures). Several new determinations of the calcium carbonate content of the Morton Ranch clay liner were made. The number reported here (0.3%) is an average of eight measurements. The latter value will be used throughout this report.

The chemical compositions of the tailings solutions used as influent for the column experiments are given in Table 2 which is compiled from data given in Peterson et al. (1982) and Serne et al. (1983). In general, macro cations were analyzed by Inductively Coupled Plasma emission spectroscopy (ICP) while trace elements were determined by graphite furnace atomic absorption (AA). Anions were analyzed by ion chromatography (IC) and titration while X-ray and γ -ray radioanalytical techniques were used to measure radionuclide activities. The Highland Mill tailings solutions were taken from the Exxon Highland Mill (H.M.) in Wyoming. The Highland Mill tailings solution percolated through permeability cells 5 and 8 was designated H.M. #1 while the H.M. tailings solution used for the vacuum extractor columns had a different chemical composition and was labeled H.M. #2. The reason for the differences in composition between the two solutions is mainly due to dilution of H.M. #2 with mine seepage water. The two solutions were sampled in different locations. Whereas H.M. #1 was collected at the front end of the tailings pipeline that carries tailings solution into the pond, H.M. #2 was taken directly from the pond into which mine seepage waters had been pumped. Highland Mill tailings solution #2 (H.M. #2) was spiked with radioactive tracers before it was used in the vacuum extractor columns and is listed in Table 2 as H.M. #2-radiotraced #1, along with the counts per second per milliliter (cps/ml) added of each radioactive spike. Permeability cell 1 was percolated with the synthetic tailings solution.

TABLE 1. Characterization of the Morton Ranch Clay Liner and Overburden

	<u>Morton Ranch Clay Liner</u>	<u>Morton Ranch Overburden</u>
Water Content (g/g) (%) (after air drying)	4.10	1.15
Particle Density (g/cm ³)	2.72	2.68
Particle Size Distribution (wt%)		
Sand (50-2000 μm)	12.0	76
Silt (2-50 μm)	54.0	15
Clay (<2 μm)	34.0	9
pH of Saturated Paste	8.2	8.5
Eh of Saturated Paste (volts)	+0.406	+0.345
EC of Saturated Extract (mmhos/cm)	0.70	0.19
Organic Matter (g/g) (%)	1.44	0.19
CaCO ₃ (g/g) (%)	0.3*	0.19
Cation Exchange Capacity (CEC) (meq/100g)	31.6	7.8
Water Soluble Cations (meq/100g) (1:1 Extract)		
K	ND	0.22
Na	ND	1.10
Ca	ND	2.72
Mg	ND	1.11

ND = Not determined.

* = Average of eight measurements.

TABLE 2. Composition of Various Highland Mill and Synthetic Tailings Solutions Used in Laboratory Experiments, mg/l

Constituents	H. M. Tailings Solution #1 (used in permeability cells 5, 8)	H. M. Tailings Solution #2 [used in vacuum extractors (measured)]	H. M. Tailings Solution #2 - Radiotraced #1 [for vacuum extractors (calculated)]	H. M. Tailings Solution #2-Radiotraced #1 [1:5 dilution (measured)]	Synthetic Tailings Solution (used in permeability cell 1)
Li	0.9	0.48	0.48	0.11	
B	0.19	0.19	0.19	0.05	
HCO ₃ /CO ₃	0.0	0.0	0.0	0.0	
NO ₃	16.5	8.5	27.7	19.4	15
F	4.0	4.0	4.0	<0.5	
Na	343	364	364	71	343
Mg	690	440	440	88	689
Al	600	396	396	79	603
Si	234	255	255	52	
P	30	6.8	6.8	1.0	
SO ₄	12,850	9,100	9,100	1,820	13,000
Cl	97	330	330	78	100
K	40	<3	<3	<3	
Ca	537	483	483	97	533
V	10.6	10.6	10.6	0.8	
Cr	2.7	1.5	1.5	0.3	
Mn	64	43	43	8.5	
Fe	2,215	560	560	126	2,200
Co	<1	1	1	0.2	
Ni	3.0	1.7	1.7	0.38	
Cu	2.3	1.3	1.3	0.27	
Zn	8.4	3.9	3.9	0.89	
As	3.50	0.45	0.45	0.10	
Se	0.6	1.18	1.18	0.24	
Sr	15.7	6.6	6.6	1.4	
Mo	0.35	<0.05	<0.05	<0.05	
Cd	0.04	0.04	0.04	<0.01	
Sb	<1	<1	<1	<1	
Ba	<0.05	<0.05	<0.05	<0.05	
La	ND ^(a)	5.0	5.0	0.93	
Pb	<0.05	<0.04	<0.04	<0.04	
U	40.0	7.2	7.2	1.54	
pH	1.8	2.19	2.15 ^(b)	ND	2.0
Eh(mv)	910	750	ND	ND	
<u>Radionuclides (cps/ml)</u>					
⁵¹ Cr			6.6 ^(b)	ND	
⁵⁴ Mn			43.1 ^(b)	ND	
⁵⁹ Fe			2.25 ^(b)	ND	
⁷³ As			17.0 ^(b)	ND	
⁷⁵ Se			8.16 ^(b)	ND	
^{110m} Ag			2.85 ^(b)	ND	
¹⁰⁹ Cd			4.01 ^(b)	ND	
²¹⁰ Pb			35.5 ^(b)	ND	
²²⁸ Ra			0	0	

(a) ND - not determined.
(b) Values were actually measured.

Permeability cells 1 and 5 were packed with the Morton Ranch clay liner material to 97% and 96% of maximum compaction, respectively, as determined by a standard proctor test (Black 1965a). This produced a bulk density of 1.79 g/cm^3 for column 1 and 1.76 for column 5. Column 1 was leached with the synthetic tailings solution and column 5 with the H.M. #1 solution. As mentioned, H.M. #1 was also used in column 8 which was packed with the Morton Ranch overburden to a bulk density of 1.92 g/cm^3 . Effluent solutions from columns 1, 5, and 8 were periodically collected and subsequently analyzed according to the procedures previously described. The setup and operation of the permeability cells is described in detail in Peterson et al. (1982).

The vacuum extractor columns were packed with the Morton Ranch clay liner to a density of 1.25 g/cm^3 , based on an oven dry-weight. The material in the vacuum extractor columns was packed to a lower density than that in the permeability cells to facilitate the movement of solution through the columns in a shorter time than was available for the permeability cells. The vacuum extractor experiments are described in Serne et al. (1983). The vacuum (mechanical) extractor consists, essentially, of a series of three syringes stacked on top of each other and connected to each other through apertures and flexible tubing. The upper syringe acts as a holding reservoir for the tailings solution and the middle syringe is packed with the sediment to be contacted. The plunger on the lower syringe is slowly extracted by a moveable plate, driven by an electric motor, which creates the vacuum responsible for pulling the tailings solution from the upper syringe into and through the middle syringe containing the sediment. The collected effluents from the vacuum extractor column were then analyzed by the same methods as were used for the permeability cell effluent solutions. Use of the vacuum extractor columns enables one to simulate flow paths of varying lengths containing intermittent sampling ports. Only effluent solutions from the first tier of columns were modeled in this study. As explained in Serne et al. (1983), the first six columns (1st tier) all received the H.M. #2-radiotraced #1 solution as an input solution. Vacuum extractor columns were found to be capable of closely duplicating the results obtained from the permeability cells and, in addition, appear to be a useful experimental tool for simulating long-term experiments in shorter time frames. The residence time of one pore volume in the vacuum extractor columns was ~16 hr while the same pore volume took about 45 days to percolate through column 5.

The analytically determined chemical compositions of the eluants from permeability columns 1, 5, and 8 and vacuum extractor columns 1-6, 8-12, and 15-18 are shown in Appendix A. These data are presented at increasing numbers of pore volumes to show the effects of the passage of tailings solutions upon the column effluent concentrations. Vacuum extractor columns 1-6, 8-12, and 15-18 were treated as three separate columns in that corresponding pore volumes from each set of columns (1-6, 8-12, and 15-18) were combined to form single samples. Each set of columns was treated similarly in that the same leaching solution contacted each column within a set at the same time.

EQUILIBRIUM COMPUTER MODELING APPROACH

The geochemical modeling is outlined in this section.

GEOCHEMICAL COMPUTER CODE

The geochemical computer code selected for use in this study was MINTEQ (Felmy et al. 1983). The MINTEQ code combines many of the "best" features from its two immediate predecessors, WATEQ3 (Ball et al. 1981) and MINEQL (Westall et al. 1976). MINTEQ is capable of performing calculations of ion speciation/solubility, adsorption, oxidation-reduction, gas phase equilibria, and precipitation/dissolution of solid phases. In addition, MINTEQ has the ability to accept a value for the starting mass of a solid phase. In other words, one can give a solid an initial finite mass as a starting value for the computer simulations and the code will dissolve that solid only until the starting mass is exhausted. This unique capability allows MINTEQ to model flow through systems in which the mass of solid precipitated in earlier pore volumes can be redissolved as later pore volumes percolate through the system in subsequent simulations. To perform the predictive geochemical modeling outlined in this report, it was imperative to have this capability incorporated into the computer code.

Another important consideration in selecting a geochemical code for use in this study was the completeness and credibility of the code's thermodynamic data base. The thermodynamic data base in MINTEQ was taken from the data base of WATEQ3 which has been developed and documented over a period of years by members of the United States Geological Survey (USGS) (Truesdell and Jones 1974, Ball et al. 1980, Ball et al. 1981). The MINTEQ thermodynamic data base used in this study was expanded from that of Felmy et al. (1983) to include thermodynamic data for solids and aqueous species of Ra, Se, Th, and Mo.

Several other important capabilities were considered before selecting the MINTEQ code for use in this study. MINTEQ has the ability to select and equilibrate the solution with the most thermodynamically stable solids in response to changes in solution composition. It was imperative that the code be able to select the most stable solids from the suite of solids in the conceptual chemical model. The MINTEQ computer program can also compute the pH and pe (negative log of electron activity) as the solution composition changes in response to precipitation and dissolution of solid phases. The pH is recomputed from a modified form of the electroneutrality condition commonly termed the proton condition (Morel and Morgan 1972) and the pe by initializing the mass totals for each oxidation state of an element and including a redox reaction between the components of each oxidation state. Further details of the computational methods are provided in Felmy et al. (1983) and Westall et al. (1976).

ION SPECIATION/SOLUBILITY CALCULATIONS

In the initial geochemical modeling work performed for this study, the solution analyses of selected pore volumes from the permeability and vacuum extractor cells were used for ion speciation/solubility calculations. MINTEQ

computes the activities of complexed and uncomplexed cationic and anionic species, neutral ion pairs, and the activities of cationic and anionic redox species. The activities are then used to perform solubility calculations in which ion activity products (AP) for solids and minerals are calculated. The activity products are then compared to the solubility products (K) of minerals and solids stored in the thermodynamic data base of MINTEQA2 to develop a saturation or disequilibrium index [$\log (AP/K)$]. This saturation index indicates the degree of undersaturation or oversaturation of a solution relative to solids and minerals of interest. If a solution is oversaturated with respect to a particular solid phase, the value of the saturation index is $\log (AP/K) > 0$. Oversaturation conditions are usually explained by kinetic and/or mineralogical factors that prevent the solid from precipitating at a rate sufficient to control the concentrations of its dissolved components. If the saturation index reflects undersaturation [$\log (AP/K) < 0$], it is concluded that either a less soluble solid is controlling the dissolved constituents' concentrations or that another mechanism, such as kinetics or adsorption, is controlling the concentrations of the component species below their solubility products. The activity coefficient corrections used in calculating the activity products were based upon either the extended Debye-Huckel equation with two adjustable parameters (Truesdell and Jones 1974) or, alternatively, the Davies equation (Davies 1962).

The saturation indices of the original leaching solutions and the effluent pore volumes of the various columns are given in Appendix B and indicate which solids and minerals may be dissolving or precipitating at a sufficient rate to control the concentrations of certain of their aqueous components. Some of the saturation indices (S.I.'s) listed for permeability columns 1 and 5 differ from those published in Peterson et al. (1982) as not all of the input data for the initial modeling of these solutions used data that had been corrected for matrix interferences that were found to exist in these high ionic strength, high sulfate solutions.

CONCEPTUAL MODEL DEVELOPMENT

The printout from MINTEQA2 contains a listing of the saturation indices of those solids and minerals in the thermodynamic data base for which the component activities can be computed. The saturation indices were used as indicators of whether or not to include certain solids in the conceptual model. If the saturation index for a certain solid was near zero, this was an indication that the solid might be in equilibrium with the solution and was evidence for including the solid in the conceptual model. If, however, the saturation index indicated a significant supersaturation relative to a solid, this was a strong indication that the solid was not forming rapidly enough to be in equilibrium with the solution and was evidence for excluding the solid from the conceptual model. Saturation indices are only one of several factors considered in developing a conceptual model of the system, i.e., a list of possible solid phase controls on solution composition. Consideration must also be given, based on one's experience and knowledge, to factors such as kinetics, degree of crystallinity, pH region being studied, redox status, and documented occurrence of the solid phase, especially in the media being studied.

The interaction of the acidic tailings solution with the clay liner material and overburden was simulated by reacting incremental pore volumes of solution with a solid phase assemblage, i.e., our conceptual model of the system. Since the computer program requires a 1-liter volume of solution, the initial masses of solids in the columns before acid addition were corrected to the unit liter by multiplying the analytically determined mass of solid by the same scalar that was used to convert a column pore volume to 1 liter of solution. Figure 1 compares the experimental and modeling systems.

The conceptual chemical model of the Morton Ranch clay liner consists only of solid phases. The conceptual chemical model of the clay liner plus tailings solution also includes aqueous speciation and redox reactions in solution. A number of important constraints were imposed on the conceptual chemical model. First, the adsorption of aqueous species onto clay surfaces and/or precipitated solid phases, such as amorphous ferric hydroxide, is ignored. Second, the computer program is a thermodynamic equilibrium model and, as such, does not consider kinetics. Third, only solid phases of fixed composition can be considered. Fourth, the computer program employs ion speciation theory to compute aqueous speciation while other ion interaction theories, such as those of Harvie and Weare (1980), may be more applicable to these high acid-sulfate solutions.

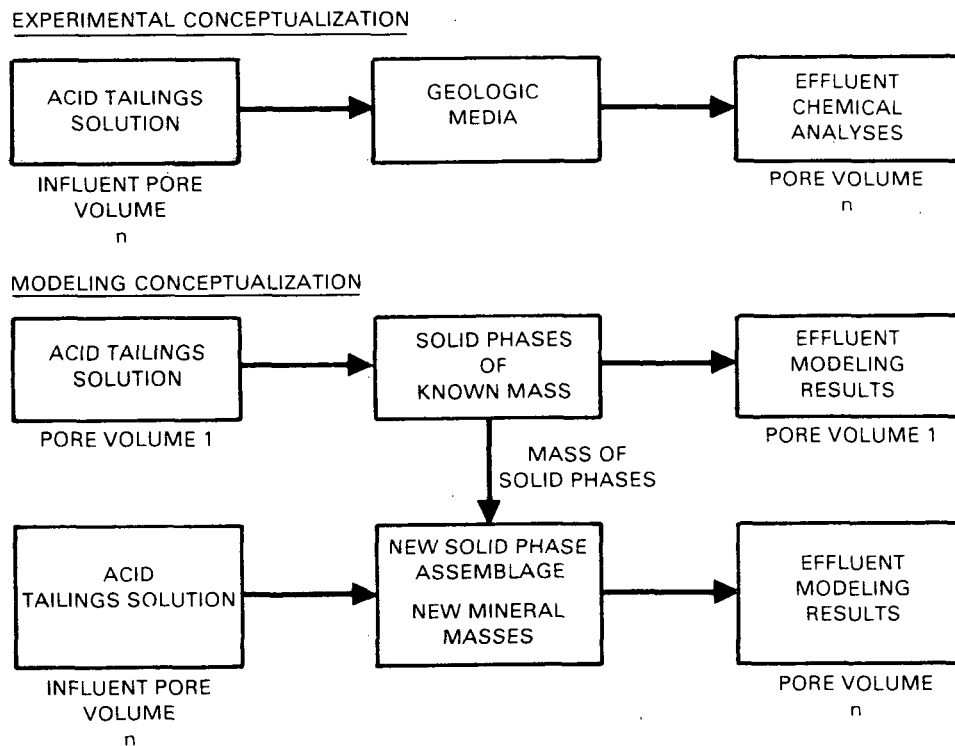


FIGURE 1. Comparison of the Experimental and Modeling Systems

Since aqueous complexation reactions generally reach equilibrium rapidly, the conceptual model includes all aqueous complexes which could form from any combination of the constituents in the original tailings solutions (Table 2). For the initial predictive modeling described in this document, all the tailings solution constituents were used, while in subsequent modeling efforts, yet to be published, only certain components were considered for the oxidation-reduction and aqueous complexation reactions.

The only gas phase considered in the conceptual model was CO₂. Since the pH of the effluent was measured after contact with the atmosphere, the partial pressure of CO₂ was fixed at the atmospheric value of 10^{-3.5} (percent by volume).

COMPARISON OF PREDICTED VERSUS EXPERIMENTAL RESULTS

The modeling results generated by the MINTEQ code using the conceptual model can then be compared to the experimental results. If the modeling results and experimental data compare favorably, then it is possible that we are describing the most important chemical reactions contributing to the retardation and mobilization of the chemical species in the leachate moving through the column. If the predicted and experimental data don't agree sufficiently, we can assume that our model of the system is incorrect, incomplete, or that other mechanisms, in addition to precipitation/dissolution governed by thermodynamics, are contributing appreciably to retardation or mobilization of particular elements.

COMPONENTS AND ASSOCIATED SOLID PHASES CONSIDERED

The predictive modeling was done only for the constituents in Table 3 plus pH and pe. These, of course, are not the only elements included in the speciation reactions. All components analyzed in the original leaching solutions were included in the speciation reactions and can potentially react with the elements included in Table 3. For example, phosphate is among the components in the original tailings solution and so can form complexes with any of the components included in Table 3 for which the requisite thermodynamic data are available, though no predictions are made, with our conceptual model, as to phosphate concentrations.

To initiate the predictive modeling, we assumed that five solids were present in the geologic materials before contact with the acidic tailings solutions. These solids are identified in Table 4.

TABLE 3. Components for Which Possible Solid Phase Controls Were Included In the Conceptual Model

Aluminum	Magnesium	Manganese	
Iron	Calcium	Lead	
Silicon	Sulfate	Strontium	Uranium

TABLE 4. Solid Phases Assumed to Exist in the Original Geologic Materials (for initial pore volume simulation)

Solid Phases	Steps(a)
Calcite (CaCO_3)	2 + 3
Dolomite ($\text{CaMg}(\text{CO}_3)_2$)	2 + 3
Silica (amorphous precipitate) (SiO_2 , Pt)	1 to 3
Amorphous ferric hydroxide $\text{Fe}(\text{OH})_3$	1 to 3
Amorphous aluminum hydroxide $\text{Al}(\text{OH})_3$	1 to 3

(a) Selective extraction (Serne et al. 1983).

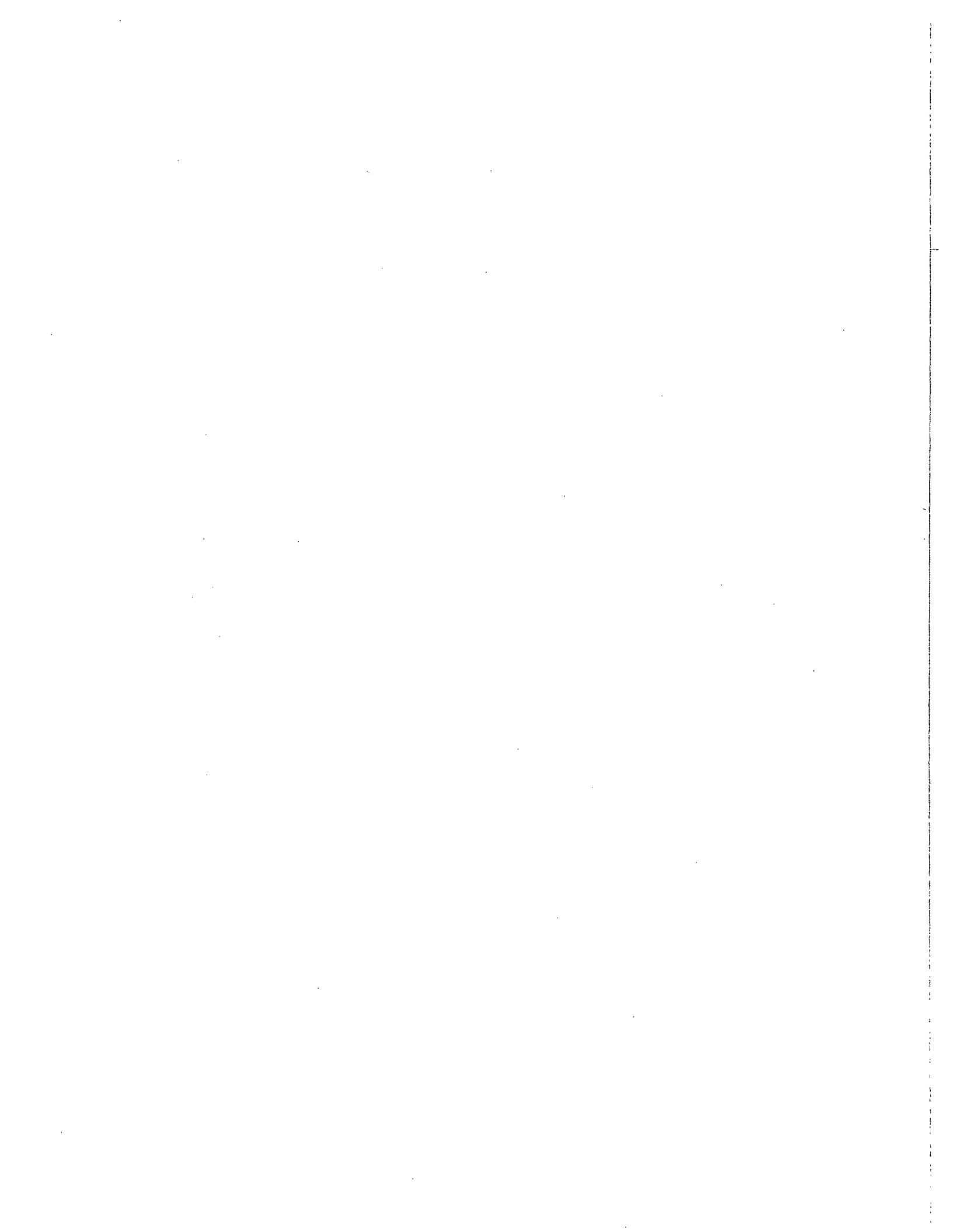
The mass of each solid phase entered into the model was established from the work of Serne et al. (1983) in which semi-selective extraction techniques were used to differentiate between certain solid phases in the Morton Ranch clay liner. The extraction steps used in calculating the mass of material entered as an initial mass in the model are shown in Table 4.

The solid phases that were allowed to precipitate out of solution if their activity products were exceeded are shown in Table 5. Again, these were the solids placed in this category to simulate the passage of the first pore volume of solution through the column. The solids in equilibrium with the solution changed as successive pore volumes of tailings solutions passed through the columns.

The thermodynamic data for the reactions involving the solid phases of Tables 4 and 5 are listed in Felmy et al. (1983).

TABLE 5. Solids That Were Allowed to Precipitate (listing at beginning of first pore volume simulation)

Gypsum	($\text{CaSO}_4 \cdot 2\text{H}_2\text{O}$)	Rhodochrosite	(MnCO_3)
Celestite	(SrSO_4)	Schoepite	$\text{UO}_3 \cdot 2\text{H}_2\text{O}$
AlOHSO_4		Anglesite	PbSO_4
Siderite	(FeCO_3)		



RESULTS AND DISCUSSION

In the following pages various predictions are made as to the effluent concentrations of several constituents using the conceptual model discussed in this report. The predictive geochemical modeling results were compared to the experimentally determined concentrations of effluents from permeability columns 5 and 8 containing the Morton Ranch clay liner and Morton Ranch overburden, respectively, and also to the first tier of vacuum extractor columns (columns 1-6) (also see Appendix C). The discussion proceeds constituent by constituent. Moreover, we discuss several trace metals, that are not included in the preliminary conceptual model, which are important to uranium mill tailings solutions and hypothesize as to their possible controlling mechanisms.

The major emphasis of this report is on comparing the predictive geochemical modeling results with the vacuum extractor data. cursory descriptions will also ensue comparing the predictive geochemical modeling results with solution data from the permeability cells. The rationale for taking this approach springs from several considerations. For consistency and brevity it was thought best to limit our discussion, on the main, to the vacuum extractor columns. Our objective in this report is to demonstrate the concept of predictive modeling of multicomponent aqueous media and also to present a preliminary conceptual model for the purpose of demonstrating this approach. The vacuum extractor column data were chosen for the focus of attention because of greater confidence in their effluent analytical data. No Eh determinations were made on the permeability columns' effluents. The given Eh values, for the permeability columns, were estimated based on experience with analogous experiments. Also, we have greater confidence in the ICP and AA data for the vacuum extractor columns since, by the time the vacuum extractor column effluents were analyzed, we felt we had identified and made corrections for the spectral and physical interferences found in these low pH, high sulfate, high ionic strength uranium mill tailings solutions. In addition, the influent solution for the permeability columns was thought to have some anomolous values, especially iron, because of the methods used in transporting the solutions (Peterson et al. 1982).

pH and pe

In this exploratory predictive modeling effort, pH and pe were allowed to vary according to the speciation and dissolution/precipitation reactions taking place. Figures 2 and 3 contain plots of the measured and predicted values of the pH and pe, respectively, plotted versus pore volumes of effluent for permeability column 5 (Figure 2) and the vacuum extractor columns (Figure 3).

In the conceptual chemical model the initial buffering capacity was attributed to calcite and dolomite. The mass of calcite and dolomite was estimated from the total carbonate analysis. Attributing all of the buffering capacity to just carbonate minerals was inadequate to explain the observed pH front breakthrough. As a result, the predicted pH front breakthroughs occur before the measured pH front breakthroughs. The pH front breakthrough is defined, for purposes of this report, as occurring when the effluent pH drops below a value of roughly 6.5.

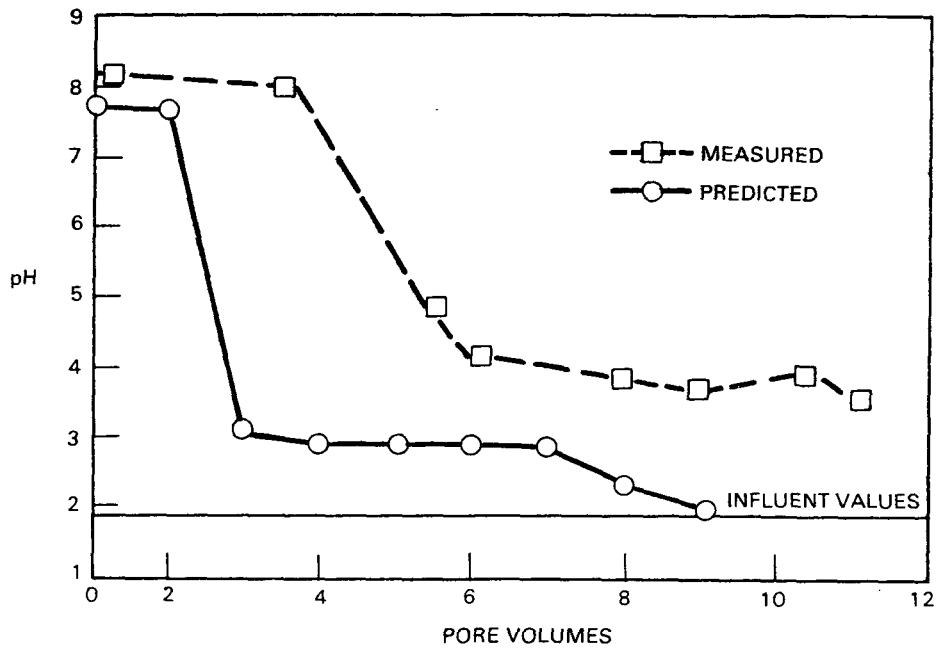


FIGURE 2. Measured and Predicted Values of pH Plotted Versus Pore Volumes of Effluent for Permeability Column 5

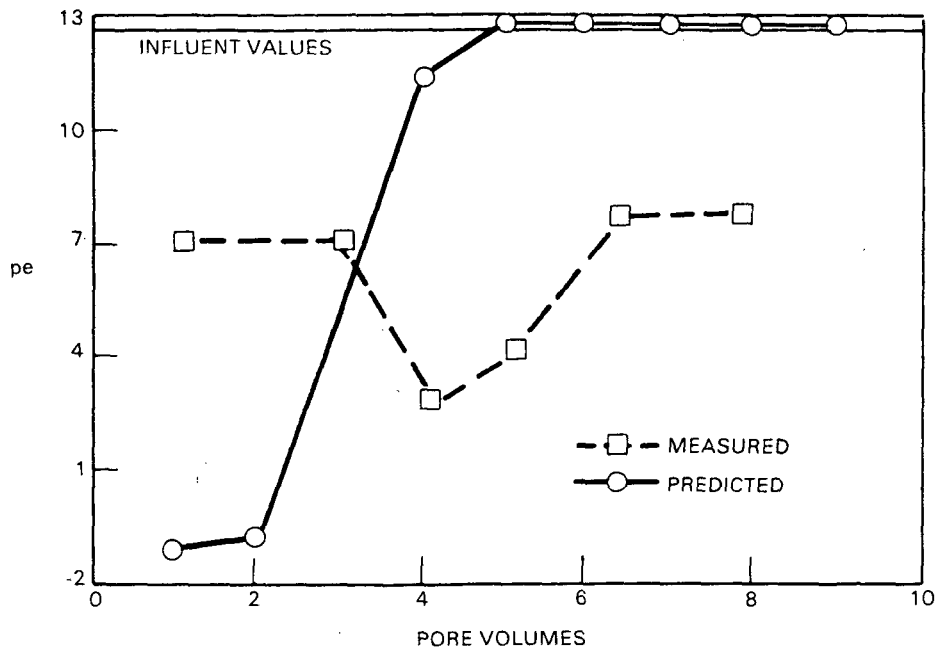
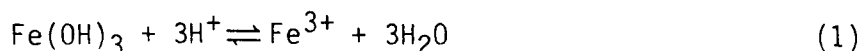


FIGURE 3. Measured and Predicted Values of pe Plotted Versus Pore Volumes of Effluent for the Vacuum Extractor Columns

The fact that the predicted pH and pe varied from the measured values influenced all of the following modeling predictions. In ongoing refinements to the conceptual model presented here, the pH and pe are being held constant to remove the effect of the variability of these two parameters from the conceptual model. The conceptual model presented here is an exploratory attempt at predictive modeling, the main purpose of which is to demonstrate the methodology of the approach, the applicability of this kind of modeling to uranium mill tailings, and identify critically needed data.

Peterson et al. (1982) and Relyea and Martin (1982) termed the ability of the soil to maintain the effluent pH values above the influent values, even after the initial buffering capacity of the soil was exhausted, the residual buffering capacity. The existence of this residual buffering capacity was partly attributed to the dissolution of amorphous solids [e.g., amorphous $\text{Fe}(\text{OH})_3$] that had previously precipitated at earlier pore volumes and higher pH values. This reaction is shown in Equation (1).



The conceptual model supported this hypothesis in that the residual buffering capacity in permeability cell 5 (Figure 2) and the predicted residual buffering were within a half log unit of one another. The predictive buffering capacity in the conceptual model was caused by the dissolution of previously precipitated amorphous ferric hydroxide (ferrihydrite) and the predicted pH never dropped to influent values until ferrihydrite had completely redissolved.

The failure to accurately predict the pe affects the ability of the conceptual model to predict the concentration of redox sensitive elements (e.g., iron, uranium). The large drop in computed pe resulted from the precipitation of ferrihydrite and a resultant change in the $\text{Fe}^{3+}/\text{Fe}^{2+}$ ratio. Since $\text{Fe}^{3+}/\text{Fe}^{2+}$ was the predominant redox buffer in our system a change in the $\text{Fe}^{3+}/\text{Fe}^{2+}$ ratio resulted in the large drop in pe. In later work we will attempt to improve our ability to predict pe by including an initial amount of dissolved oxygen in the conceptual chemical model. The dissolved oxygen would tend to buffer the system and prevent the large drop in pe.

Aluminum

The aqueous geochemistry of the $\text{Al}_2\text{O}_3\text{-SO}_3\text{-H}_2\text{O}$ system is complex and a large number of stable and metastable solid phases may affect the aqueous aluminum concentrations. Aluminum chemistry is important because of the high concentration of aluminum (396 mg/l in vacuum extractor influent solutions and 600 mg/l in the permeability columns' influent solutions)) in the influent tailings solutions. Hydrolysis of Al^{3+} and the precipitation of solid phases as the pH rises will be a major factor in determining the predicted pH and thus the acid front breakthrough curves as detailed in Peterson et al. (1982). Also, due to the wide range of pH values existing in the column effluent solutions, the conceptual chemical model must include solid phases which are stable at higher pH values and solids that will be stable under more acidic

conditions. The computer program, MINTEQ, will select and precipitate or dissolve thermodynamically stable solids as the aqueous composition, pH, and pe change.

Gibbsite and kaolinite usually control the activity of aluminum in natural systems (Lindsay 1979). However, under low pH and high sulfate concentrations different solids are likely to be stable. Acid mine waters and acid sulfate soil samples were observed (Van Breeman 1973) to be consistently undersaturated with respect to gibbsite and kaolinite. Nordstrom (1982), after completing an extensive review of stability relations in the $Al_2O_3-SO_3-H_2O$ system concluded that gibbsite and kaolinite were not stable in acid sulfate waters and proposed that jurbanite ($AlOHSO_4 \cdot 5H_2O$) may set on upper limit on aluminum solubility in acid sulfate waters. Nordstrom (1982) also concluded that even if other solids such as gibbsite and alunite are thermodynamically stable solid phases, amorphous basaluminite ($Al_4SO_4(OH)_{10} \cdot 5H_2O$) is likely to precipitate from solution and may persist for long periods of time. Jurbanite would become stable under more acidic conditions than basaluminite. Van Breeman (1973) postulated that a solid with the composition of $AlOHSO_4$ controlled aluminum activity in low pH, high sulfate waters.

Based on the foregoing discussion and on ion speciation/solubility calculations (Appendix B) $AlOHSO_4$ was chosen as a solid phase for inclusion in the conceptual model. In currently ongoing modeling efforts, jurbanite and basaluminite are being included in the conceptual chemical model.

At higher pH values, several authors have reported the formation of aluminum hydroxides. May et al. (1979) in studies of gibbsite solubility found greater solubility for a natural gibbsite than a synthetic gibbsite. The rate of attainment of equilibrium for both the natural and synthetic material depended upon solution pH. When equilibrium was approached from oversaturation and the solution pH was between 5 and 6.5, both materials were close to the final solubility value after only 28 hrs. Of particular interest was the slow approach to equilibrium (16 days) at pH values greater than 6.7, for which the authors believed boehmite, or diaspore, was the stable phase.

Singh (1974, 1976) attempted to precipitate gibbsite from solution by neutralization of $AlCl_3$ with NaOH. The precipitated gibbsite did not become stable until after one year of aging.

Hem et al. (1973), in studying the aqueous silica and aluminum system, found that the presence of silica inhibited the formation of gibbsite. In the pH range 4.5 to 6.0, the highest silica concentration at which gibbsite would form was 9 mg/l as SiO_2 . An aluminum-silica precipitate with a lower solubility than gibbsite formed and was identified as halloysite. In the pH range 6.5 to 9.5 and low dissolved silica (<10 mg/l), bayerite was produced upon aging though the crystallinity was slow to develop.

Wada and Kubo (1975), in experiments to study the precipitation of amorphous aluminosilicates, found that such precipitates would form rapidly with the composition of the formed precipitate dependent upon the initial SiO_2/Al_2O_3 ratio and reaction time.

The high silica concentration in the column influents would thus appear to favor the precipitation of an amorphous aluminosilicate over a pure aluminum hydroxide phase. However, since the composition of any amorphous aluminosilicate is unknown, and accurate thermodynamic data are not available, we were unable to include any amorphous aluminosilicate in the conceptual model.

Also, at least in the case of the vacuum extractor columns, the precipitation of solids such as boehmite (May et al. 1979) or bayerite (Hem et al. 1973) would either reach equilibrium too slowly or their formation would be inhibited by the presence of silica. As mentioned, Hem et al. (1973) clearly demonstrated the inhibition of gibbsite precipitation by silica. This is also supported by the aqueous speciation modeling of the vacuum extractor column effluents where the solutions are oversaturated with respect to gibbsite (S.I. values as high as 3.78).

Thus, we have selected amorphous aluminum hydroxide for inclusion in the conceptual chemical model. The thermodynamic solubility product for amorphous aluminum hydroxide was originally taken from Latimer (1952) and appears to set an upper limit on aluminum concentrations in natural waters as described by Gang and Langmuir (1974) and Nordstrom (1982).

Figures 4, 5 and 6 contain plots of the predicted concentrations of aluminum versus the actual concentrations. The predicted and actual concentrations of aluminum are plotted versus pore volumes of effluent for the vacuum extractor columns, permeability column 5 and permeability column 8. The aluminum concentrations of the influent solution are also indicated on each figure.

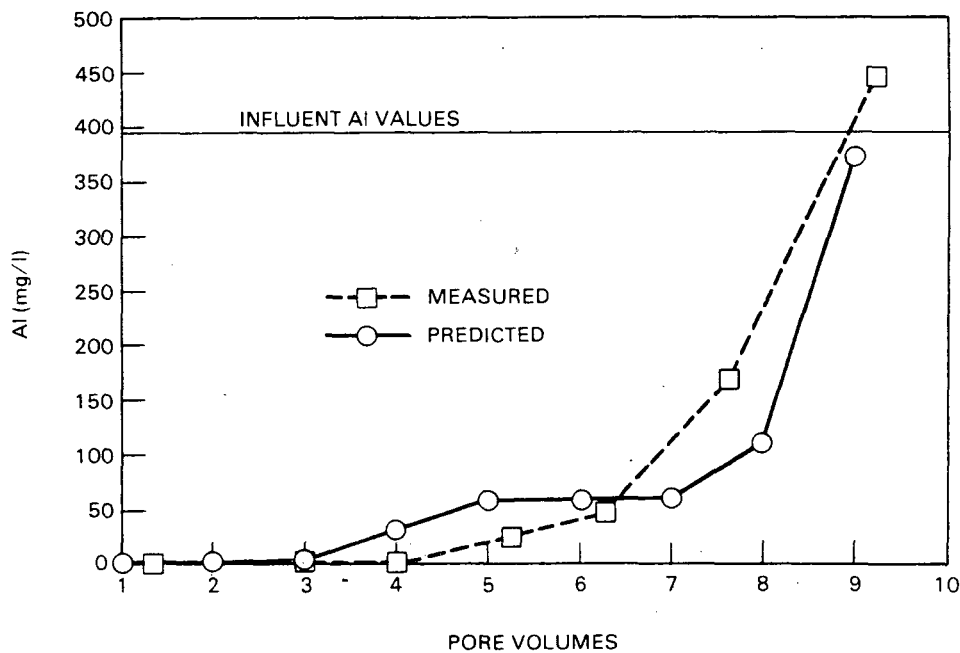


FIGURE 4. Measured and Predicted Concentrations of Aluminum Plotted Versus Pore Volumes of Effluent for the Vacuum Extractor Columns

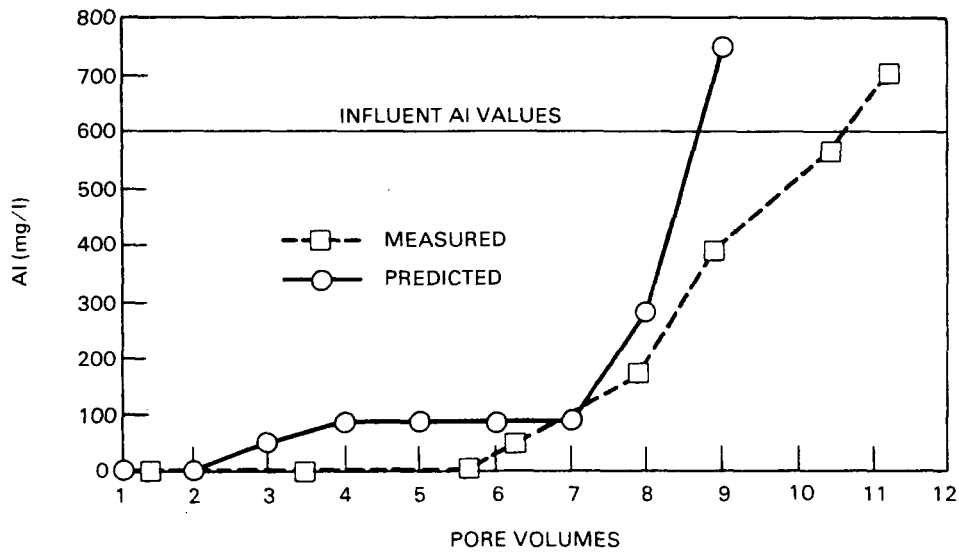


FIGURE 5. Measured and Predicted Concentrations of Aluminum Plotted Versus Pore Volumes of Effluent for Permeability Column 5

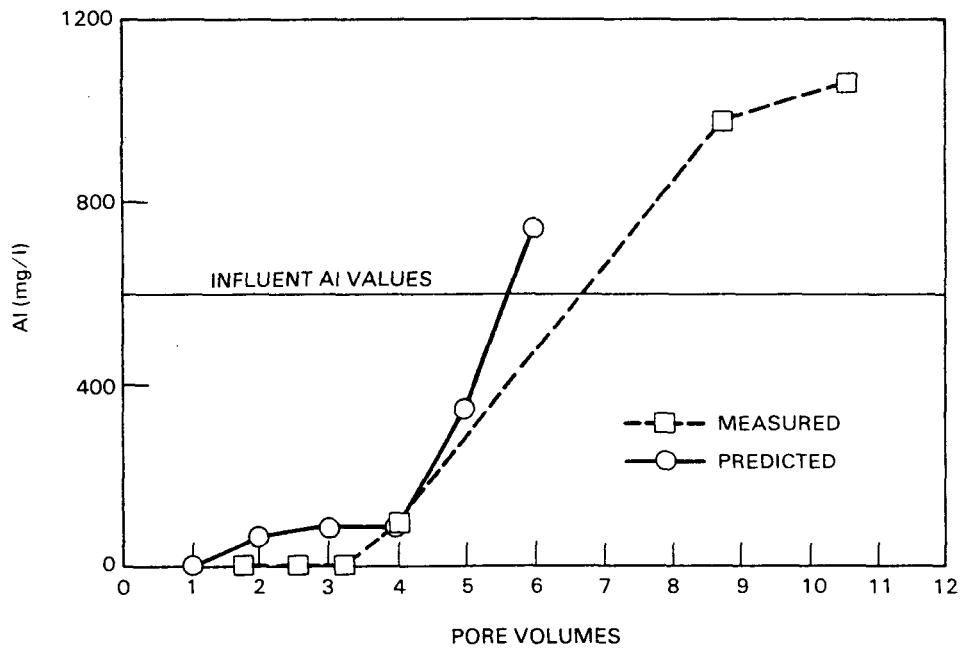


FIGURE 6. Measured and Predicted Concentrations of Aluminum Plotted Versus Pore Volumes of Effluent for Permeability Column 8

The predicted effluent concentrations for permeability cells 5 and 8 were plotted for fewer numbers of pore volumes than the measured values since complete acid breakthrough pH occurred earlier in the predictive simulations. Once the effluent pH values had dropped close to the influent values the predictive simulations were stopped.

The results from all three column types (vacuum extractor, permeability column 5, and permeability column 8) are similar in that the predicted concentrations of aluminum tracked the measured concentrations. Predicted concentrations began to increase more quickly than the measured concentrations in every instance.

Significant differences existed in all three column types. The cation exchange capacity of the Morton Ranch clay liner used in the vacuum extractor columns and permeability cell 5 was 31.6 milliequivalents/100 g compared to the 7.8 milliequivalents/100 g of the Morton Ranch overburden used in permeability cell 8. The transit time for a pore volume to pass through the columns varied from about 45 days for permeability cell 5 to 18 hours for the vacuum extractor columns. This indicates the generic applicability of the conceptual model developed. It also suggests that adsorption and kinetic considerations are not significantly affecting the effluent aluminum concentrations, which are governed by the precipitation/dissolution reactions mandated by the solid phases included in the conceptual chemical model.

In all three columns the measured aluminum values surpassed the influent values at higher numbers of pore volumes (lower pH values), indicating that the aluminum that initially precipitated at high pH values is redissolving at lower pH values. Equilibrium precipitation/dissolution, governed by solid phase controls appears to be the dominant mechanism controlling aluminum concentration and appears capable of satisfactorily predicting effluent concentrations.

It should be noted that our computed pH was significantly different than the measured pH at similar pore volumes and the solids included in our conceptual chemical model may not give the same predictions if the pH were more accurate. A later report will address this problem.

Calcium

Three calcium bearing solids were selected for inclusion in the conceptual chemical model: calcite, dolomite, and gypsum. Calcite and dolomite were entered into the model as precipitated solids with initial masses based on carbonate analyses. As related earlier in this report, the calcium carbonate value reported in Peterson et al. (1982) for the Morton Ranch clay liner was thought to be in error. Based on an average of several new determinations, a calcium carbonate equivalent of 0.3% is reported in this document. Steps two and three of the selective extraction procedures (Serne et al. 1983) indicated that more calcium was in the soil as a solid phase than that represented by the 0.3% that was measured. For entering an initial finite mass of calcium carbonate in the conceptual model a value of 0.36% calcium carbonate was used, which is intermediate between the calcium values indicated by the calcium carbonate equivalent measurement and the selective extraction techniques (Steps 2 and 3).

In the initial aqueous speciation/solubility modeling most of the effluent solutions exhibited a consistent, slight oversaturation with respect to gypsum. Oversaturation with respect to gypsum has been observed in enough instances that a re-evaluation of the solubility product of gypsum was undertaken by D. K. Nordstrom of the U.S. Geological Survey. After a perusal of gypsum solubility data, Nordstrom (personal communication E. A. Jenne, February 1981) believes that the best value for gypsum may be a $\log_{10}K$ of -4.60 ± 0.02 . We have used this value for the solubility product of gypsum in our conceptual model. The vast majority of the column effluent saturation indices for gypsum are in equilibrium with gypsum solubility determined by the solubility product of Nordstrom. Gypsum was identified in all five subsections of the dissected permeability cell 5 and was not identified in the uncontacted material. Gypsum was also found to have precipitated in the field at the Lucky Mc mill site in Wyoming (Erikson and Sherwood 1982, Peterson et al. 1982) after an evaporation pond contacted acidic tailings solution for a period of ten years. Therefore, gypsum was included in the conceptual chemical model. After simulation of the passage of the first pore volume of tailings solution through the columns, gypsum precipitated from solution.

Fluorite (CaF_2) was not included because aqueous speciation/solubility modeling indicated significant oversaturation was being maintained during the time frames of interest.

Predicted versus measured values of calcium are plotted against pore volumes of effluent for the vacuum extractor columns, permeability cell 5, and permeability cell 8 in Figures 7, 8, and 9. All of the column types (vacuum extractor, permeability cell 5, and permeability cell 8) had initial measured effluent concentrations that were above the predicted values. The predicted values all tended to underestimate the calcium concentrations initially and then approached the measured values more closely at later pore volumes. In this particular conceptual model, all of the calcium carbonate initially added to the soil dissolved during the first pore volume in all column types.

The conceptual chemical model did not accurately predict the extremely high concentrations of calcium in the first few pore volumes of the three columns. There are two possible reasons for this lack of agreement: 1) large amounts of exchangeable Ca^{2+} are brought into solution as a result of contact with the tailings solution, or 2) there is a greater mass of calcite in the original soil than determined by carbonate analysis or more of the original carbonate should be assigned to calcite rather than dolomite. The first hypothesis, release of exchangeable calcium, appears to be the most likely since there is a large reservoir of exchangeable calcium (Serne et al. 1983) in the Morton Ranch clay liner. Future modeling efforts will address this point further.

Sulfate

Predicted and measured values of sulfate are plotted against pore volumes of effluent for the vacuum extractor columns, permeability cell 5, and

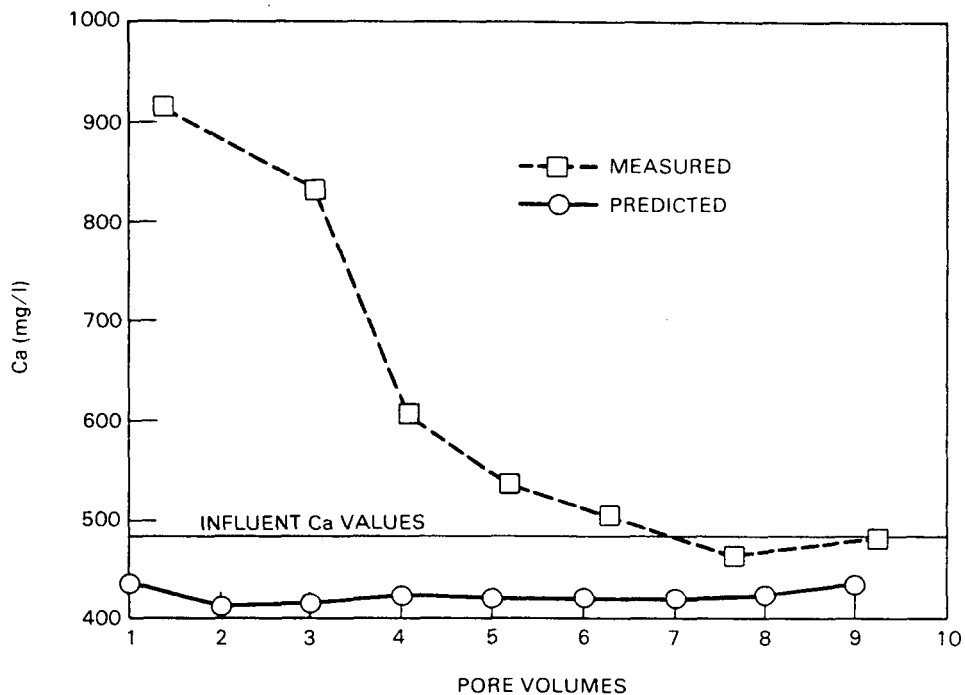


FIGURE 7. Measured and Predicted Concentrations of Calcium Plotted Versus Pore Volumes of Effluent for the Vacuum Extractor Columns

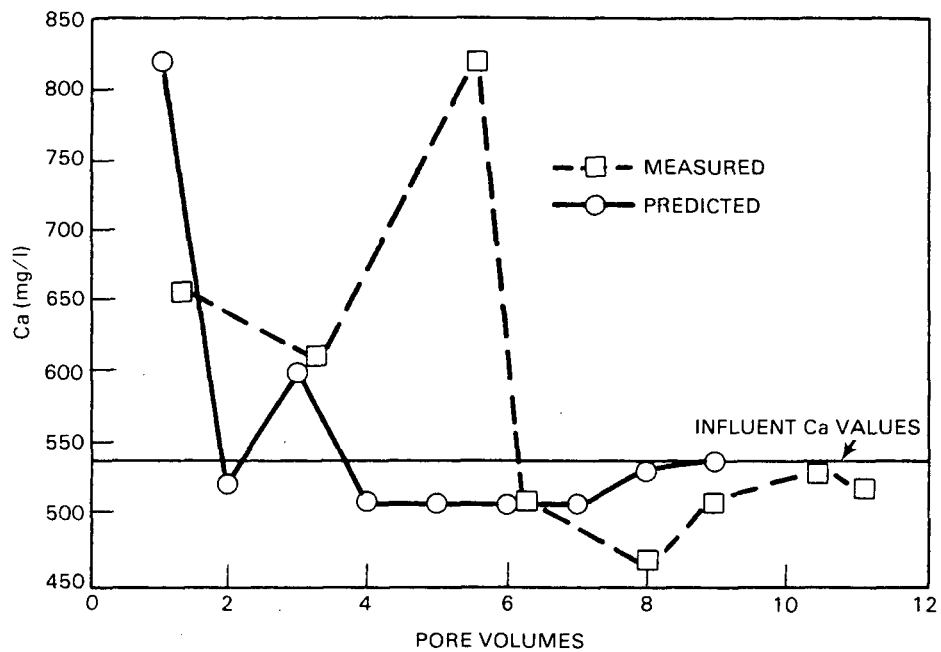


FIGURE 8. Measured and Predicted Concentrations of Calcium Plotted Versus Pore Volumes of Effluent for Permeability Column 5

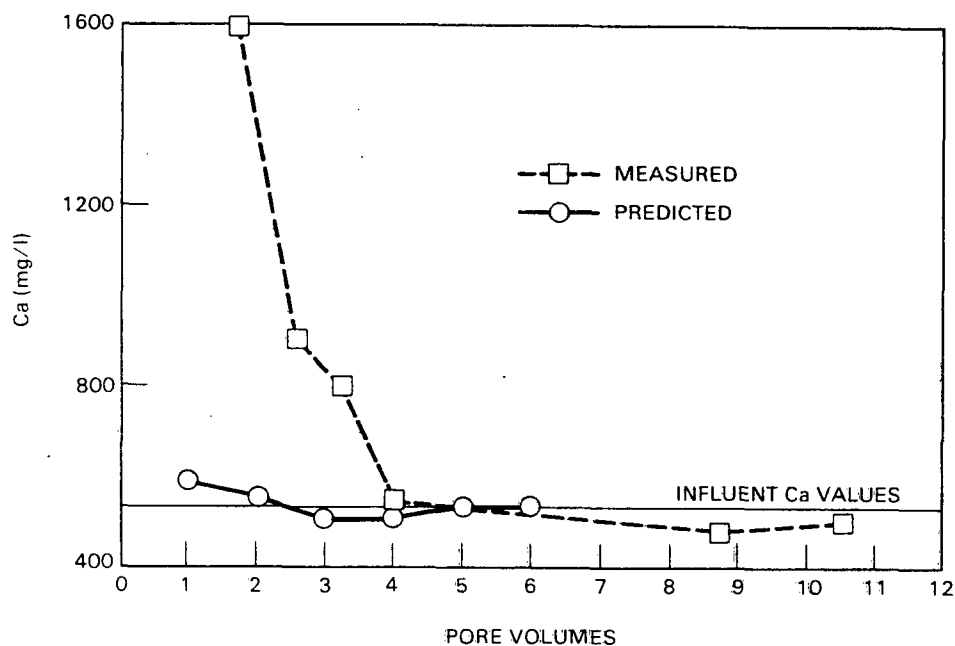


FIGURE 9. Measured and Predicted Concentrations of Calcium Plotted Versus Pore Volumes of Effluent for Permeability Column 8

permeability cell 8 in Figures 10, 11, and 12. Predicted sulfate concentrations tend to be the reciprocal of calcium concentrations, i.e., low sulfate concentrations coincide with high calcium concentrations and, conversely, high sulfate concentrations occur concomitantly with low calcium concentrations. This would indicate that a solid phase, such as calcium sulfate, is imposing a constant activity product upon the calcium and sulfate activities. Where the model predictions were high in the initial pore volumes for sulfate, they also concurrently underpredict calcium, at the same time maintaining equilibrium with gypsum. This result clearly demonstrates that, for certain systems, knowledge of the formation of a particular solid is not always sufficient to completely describe the aqueous concentrations of its dissolved components. Additional laboratory data, such as characterizing the exchange reactions of calcium with other electrolyte ions, may be necessary. All effluent solutions had sulfate concentrations that were significantly above the EPA National Secondary Drinking Water Standard (40 CFR 143) for sulfate. These high concentrations were predicted by the conceptual model.

Iron

The solubility of iron oxyhydroxides is complicated by several factors. Some of these factors include varying particle size and relative humidity (Murray 1979, Langmuir 1971), aqueous iron concentrations (Langmuir and

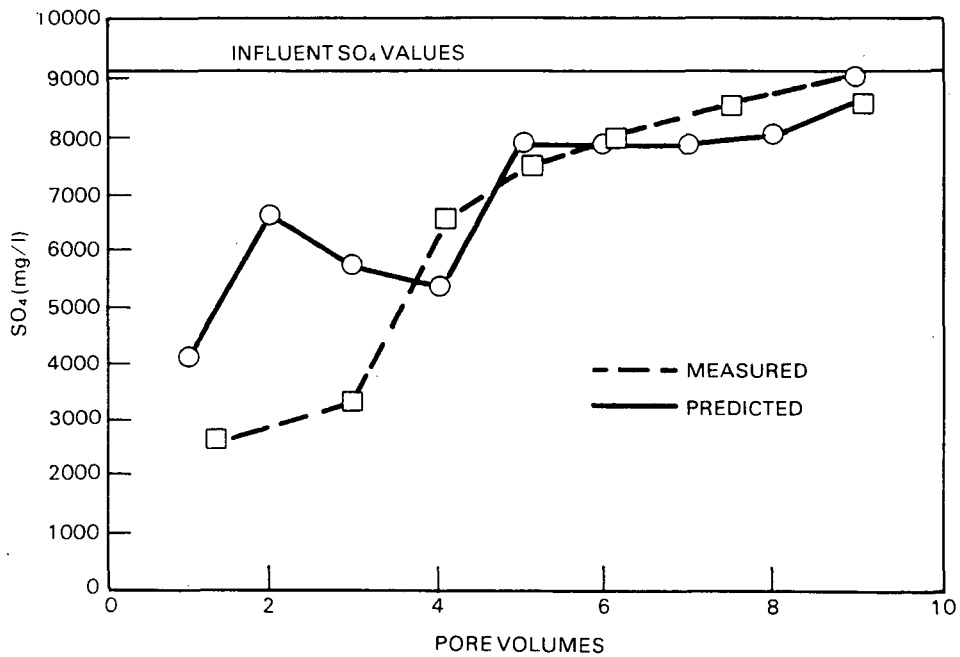


FIGURE 10. Measured and Predicted Concentrations of Sulfate Plotted Versus Pore Volumes of Effluent for the Vacuum Extractor Columns

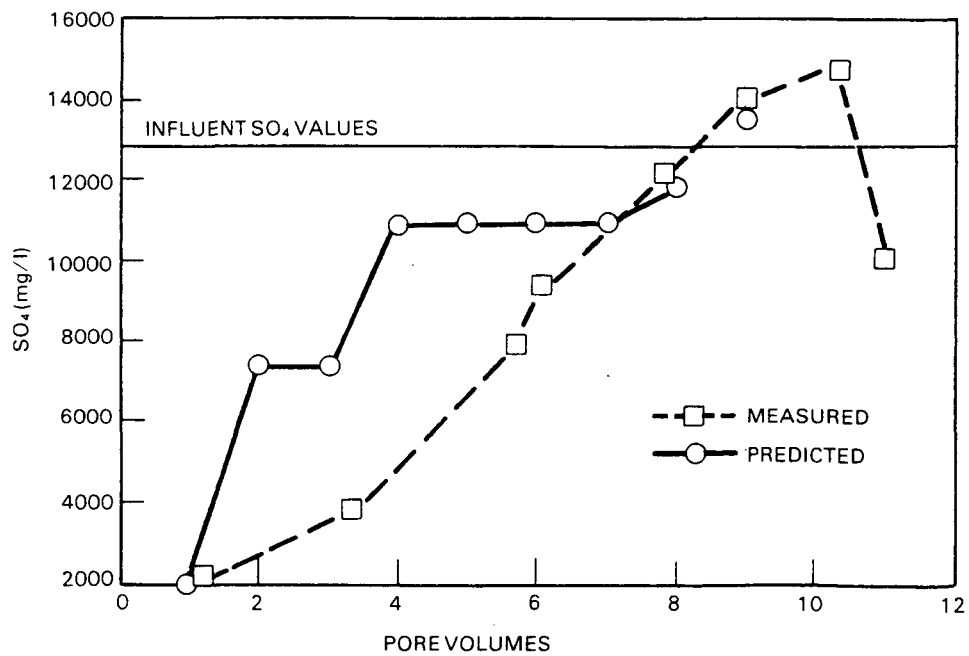


FIGURE 11. Measured and Predicted Concentrations of Sulfate Plotted Versus Pore Volumes of Effluent for Permeability Column 5

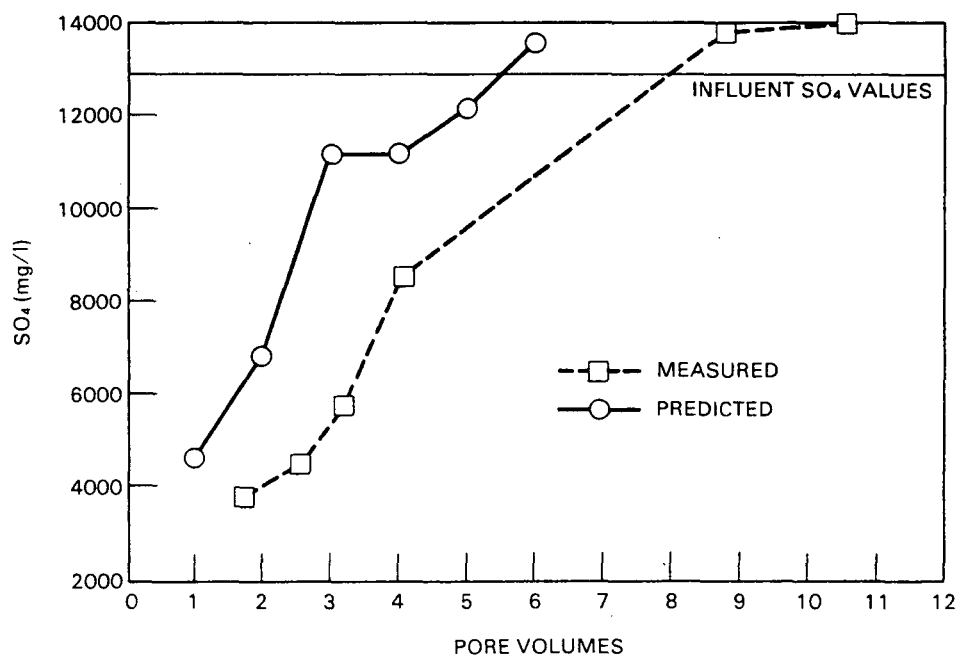


FIGURE 12. Measured and Predicted Concentrations of Sulfate Plotted Versus Pore Volumes of Effluent for Permeability Column 8

Whittemore 1971), reaction kinetics (Murray 1979, Langmuir 1969, Nordstrom 1979) and the incorporation of silica (Schwertmann and Thalmann 1976) or possibly aluminum (Fey and Dixon 1981) into the precipitated oxyhydroxide. The incorporation of silica has been shown by Schwertmann and Thalmann (1976) to favor precipitation of amorphous ferric hydroxide $[\text{Fe}(\text{OH})_3]$. Also, Fey and Dixon (1981) show that substitution of aluminum for iron into goethite increases the disorder in the crystal. Thus, both processes favor the formation of an amorphous material.

Nordstrom et al. (1979) found that iron concentrations in acid mine waters appeared to be controlled by amorphous ferric hydroxide. Amorphous ferric hydroxide (ferrihydrite) also appeared to place an upper limit on iron concentrations in batch studies where uranium mill tailings solutions contacted clay materials for up to 16 months (Peterson and Krupka 1981). Most of the column effluent solutions in this study were slightly oversaturated with respect to amorphous ferric hydroxide. A slight downward modification of the estimated Eh values for permeability column 5 would bring all of these solutions into equilibrium with an iron activity controlled by amorphous ferric hydroxide. We have thus selected amorphous ferric hydroxide for inclusion in this conceptual model and use an equilibrium constant (Felmy et al. 1983), which was calculated for a freshly precipitated amorphous ferric hydroxide.

Siderite (FeCO_3) was also included in the conceptual chemical model and could possibly form at high pH values if the computed pe should decrease to low values during the simulation.

The aqueous speciation/solubility modeling of column effluents computed that the solutions were oversaturated by several orders of magnitude with respect to Na, K, and H jarosite (an iron bearing sulfate compound). These findings agree with the results obtained from batch experiments by Peterson and Krupka (1981) and from acid mine water by Nordstrom et al. (1979). Jarosite was identified as having precipitated, by X-ray diffraction, in permeability column 5 (Peterson et al. 1982) but the rate of formation appears to be inhibited by some kinetic barrier and, therefore, jarosite was excluded from the conceptual model.

As explained in Serne et al. (1983), there was some question about the ability of the Highland Mill Tailings solution, percolated through permeability columns 5 and 8, to maintain the originally measured iron concentrations due to possible subsequent precipitation. Therefore, we restrict our discussion on iron to the vacuum extractor columns.

The form of the curve of the predicted Fe effluent solution values imitates the shape of the measured curve, except that the predicted values begin to rise sooner than the measured values (see Figure 13). Both predicted and measured values start below the influent values at early pore volumes, exceed the influent values at intermediate pore volumes, and then begin to fall toward the influent values at higher pore volumes.

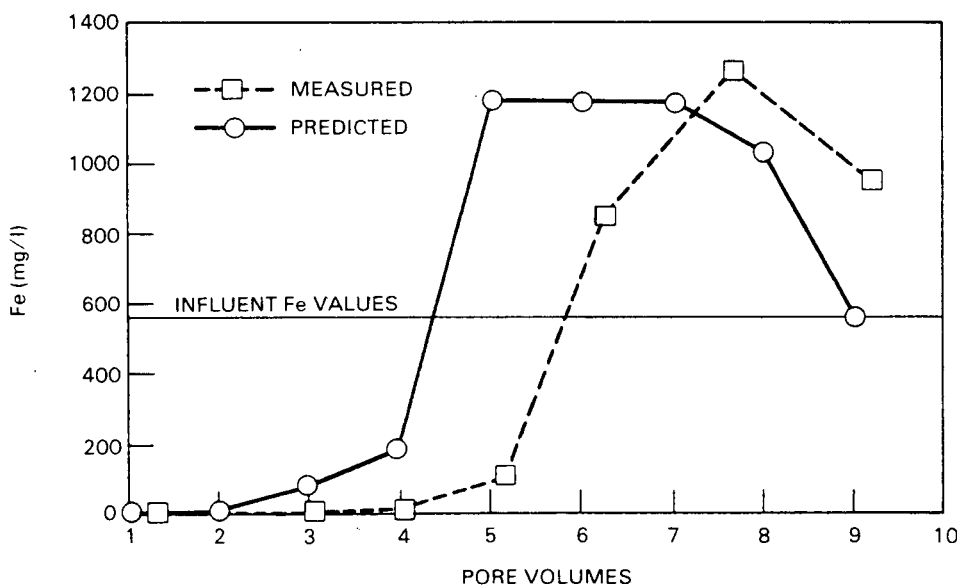


FIGURE 13. Measured and Predicted Values of Iron Plotted Versus Pore Volumes of Effluent for the Vacuum Extractor Columns

As indicated by the predicted values, one mechanism that will explain the shape of the curves of the measured values is the precipitation/dissolution of amorphous ferric hydroxide as conceived in the conceptual model. At high pH values, amorphous ferric hydroxide precipitates and then begins to redissolve at intermediate pore volumes as the pH falls, bringing the effluent iron concentration levels above the influent levels. After all of the originally precipitated material redissolves the effluent values fall toward the influent values because the lower pH values will now maintain all of the influent iron in solution. Therefore, the difference in the measured and predicted values could be a result of our inability to accurately predict pH, rather than inappropriate choices of solids for the conceptual chemical model.

Manganese

Rhodochrosite (MnCO_3) was included in the conceptual chemical model since it has been shown to readily precipitate from solution (Johnson 1982).

Many of the batch solutions and column effluent solutions were close to equilibrium with MnHPO_4 . It was difficult to draw any conclusions from the vacuum extractor column effluents since many of the phosphate numbers were reported as less than values. Jenne et al. (1980) suggest that MnHPO_4 could be a possible Mn control in a variety of environments. Although MnHPO_4 has been discussed in the literature (Lindsay 1979), a cursory review of X-ray and mineralogical references has produced no evidence for the existence of this solid in natural systems (Peterson et al. 1982). For this reason we excluded MnHPO_4 from the conceptual model although the possibility of MnHPO_4 formation is being pursued in further refinements of this preliminary conceptual model. The concentrations of phosphate in the Highland Mill tailings solutions used in the permeability columns and vacuum extractor columns are high enough (30 and 6.8 mg/l as P, respectively) that the possibility of a MnHPO_4 precipitate affecting the Mn concentration cannot be dismissed a priori.

Figures 14 through 17 contain plots of the measured and predicted concentrations of manganese for the three column types. The shapes of the predicted and measured solution concentrations for manganese are similar. One mechanism that could explain this shape is precipitation/dissolution of a solid phase, as hypothesized in the model. Again, we have the initial manganese effluent levels dropping below the influent levels at early pore volume, rising above the influent levels at intermediate pore volumes and, finally, falling toward the influent levels at the later pore volumes. One way of accounting for this phenomenon is through a precipitation/dissolution spike. Ion exchange could also account for the shape of the curves. The concentration of manganese is plotted versus pH for the vacuum extractor columns 1-6 in Figure 15. The close correlation between the measured and predicted values suggests that the precipitation/dissolution of manganese could very well be controlled by rhodochrosite in these solutions. This remobilization due to dissolution of precipitated material could also explain the behavior of the radiotraced manganese in the vacuum extractor columns (Serne et al. 1983).

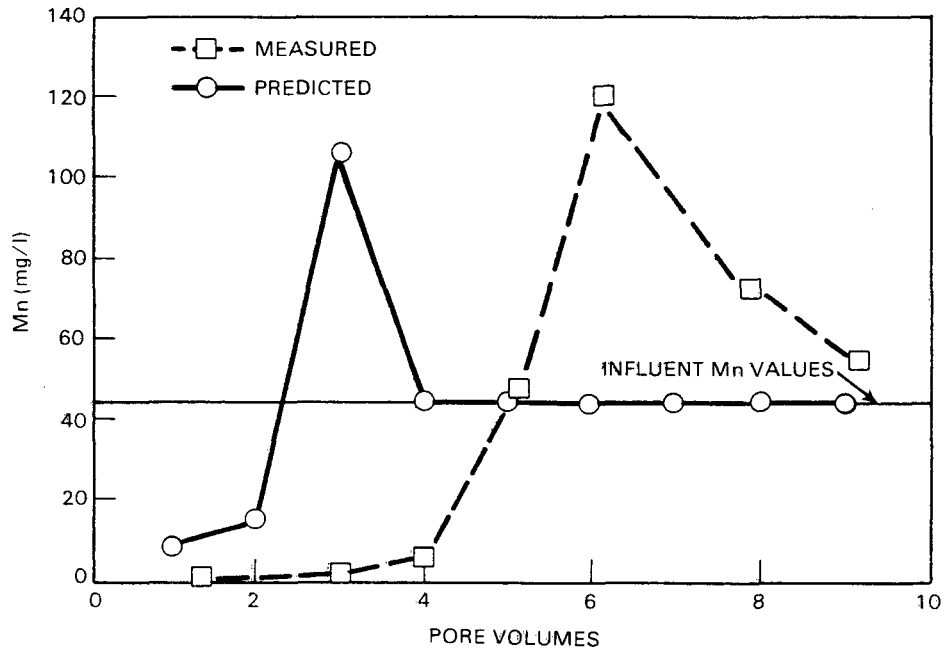


FIGURE 14. Measured and Predicted Concentrations of Manganese Plotted Versus Pore Volumes of Effluent for the Vacuum Extractor Columns

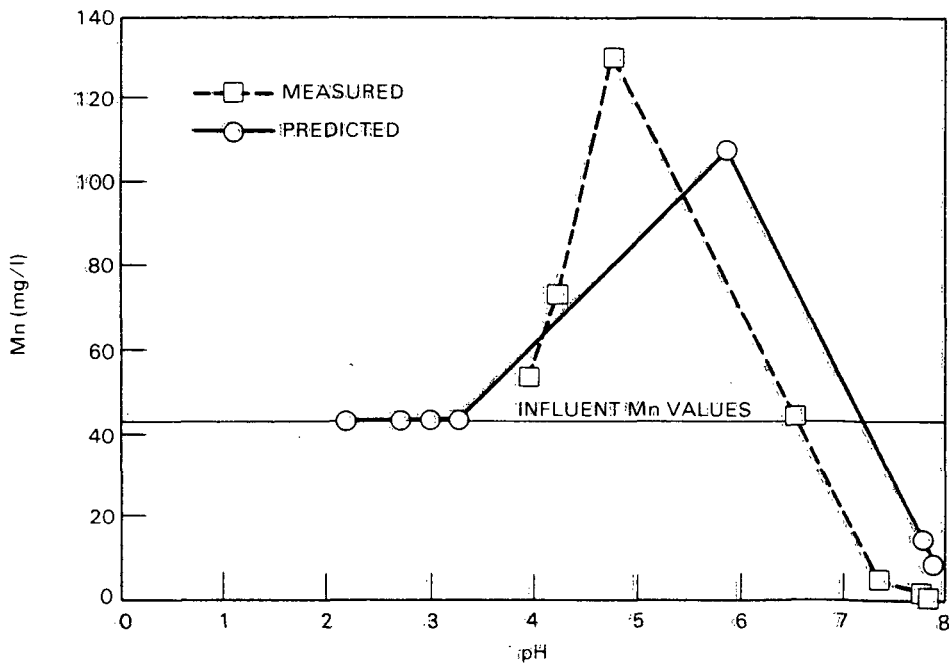


FIGURE 15. Measured and Predicted Concentrations of Manganese Plotted Versus pH for the Vacuum Extractor Columns

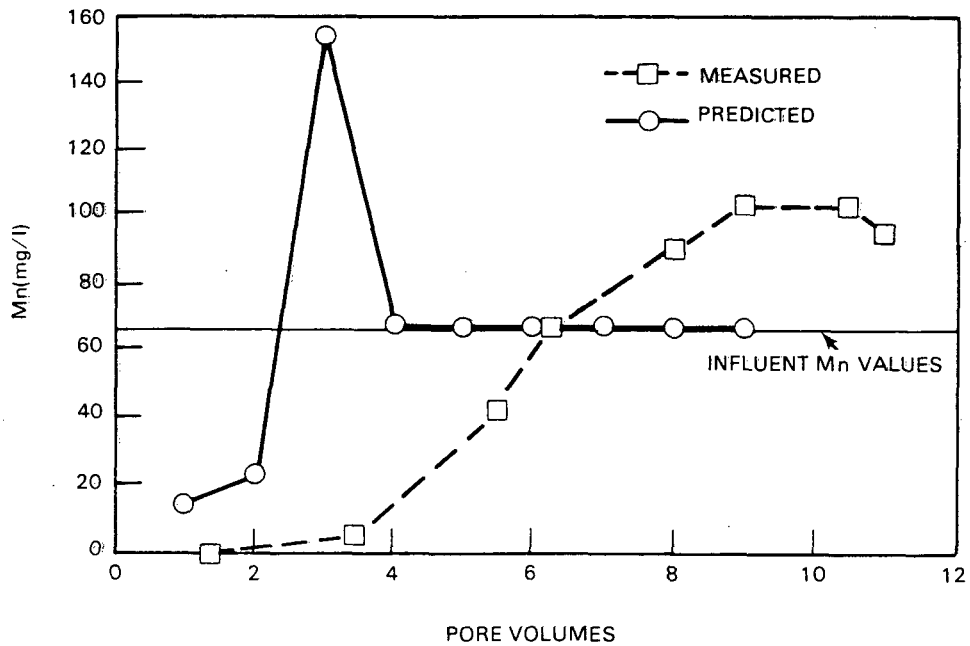


FIGURE 16. Measured and Predicted Concentrations of Manganese Plotted Versus Pore Volumes of Effluent for Permeability Column 5

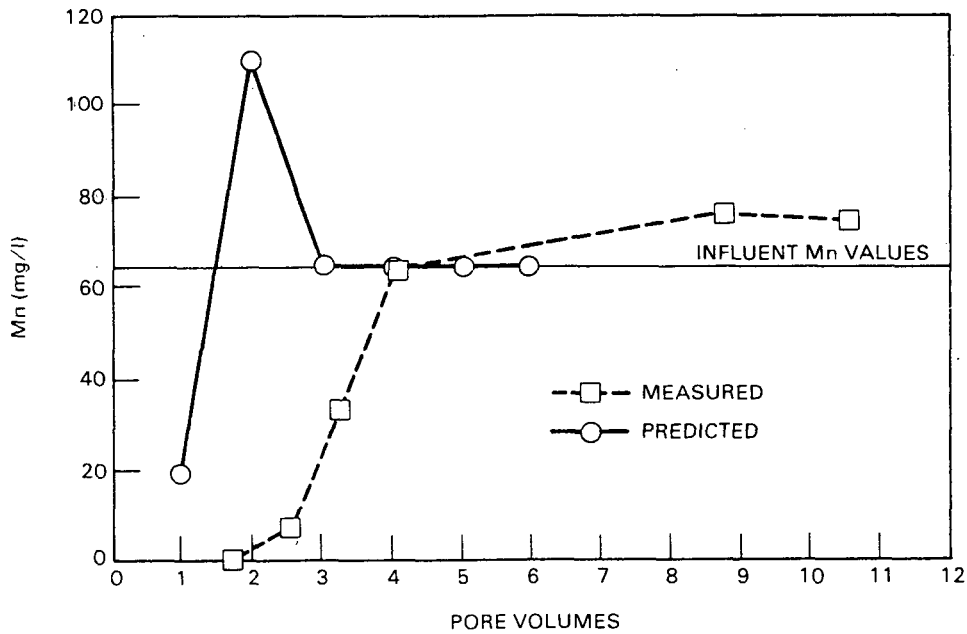


FIGURE 17. Measured and Predicted Concentrations of Manganese Plotted Versus Pore Volumes of Effluent for Permeability Column 8

Ion exchange behavior could also explain the results obtained from the permeability and vacuum extractor columns. Semi-selective extraction procedures applied to the vacuum extractor columns (Serne et al. 1983) indicated that much of the manganese was exchangeable. This possibility is being pursued in future work.

Magnesium

In this preliminary conceptual chemical model the only magnesium solid considered was dolomite $[CaMg(CO_3)_2]$. Ongoing modeling efforts are considering other magnesium solids. Dolomite was entered as a precipitated material with a finite initial mass. That is, dolomite existed in the columns prior to their (the columns') contact with the acidic tailings solutions.

Figures 18, 19, and 20 are plots of the predicted and measured concentrations of magnesium versus pore volumes of effluent for the permeability and vacuum extractor columns. The initial column mass of dolomite explains the immediate rise of the predicted magnesium effluent concentrations to values above those of the influent concentrations. The percolate tailings solution used in the permeability columns contained 690 mg/l of magnesium, while that of the vacuum extractor columns held 440 mg/l of magnesium. After dolomite

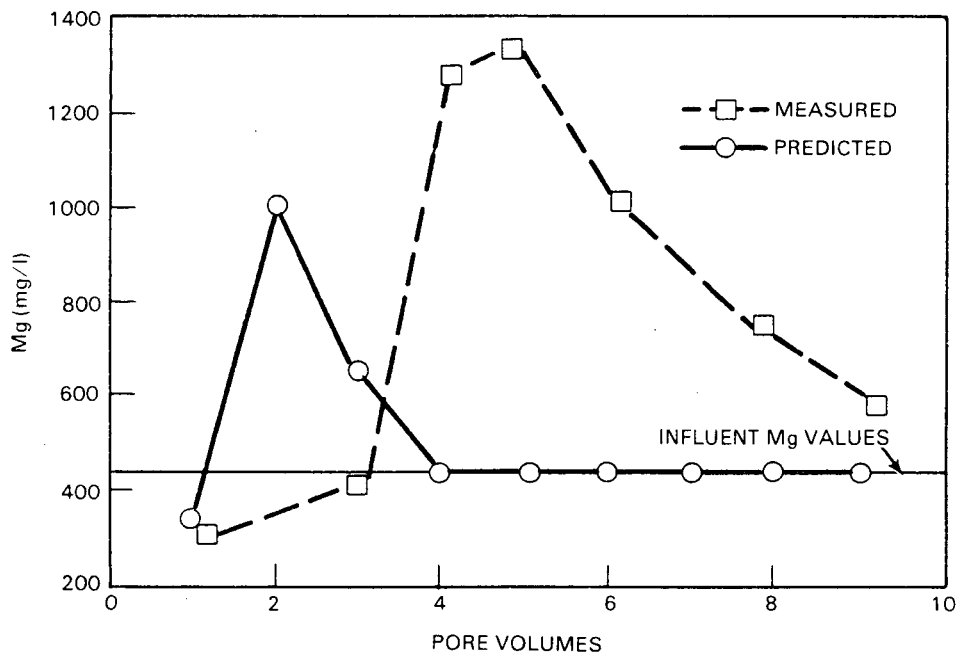


FIGURE 18. Measured and Predicted Concentrations of Magnesium Plotted Versus Pore Volumes of Effluent for the Vacuum Extractor Columns

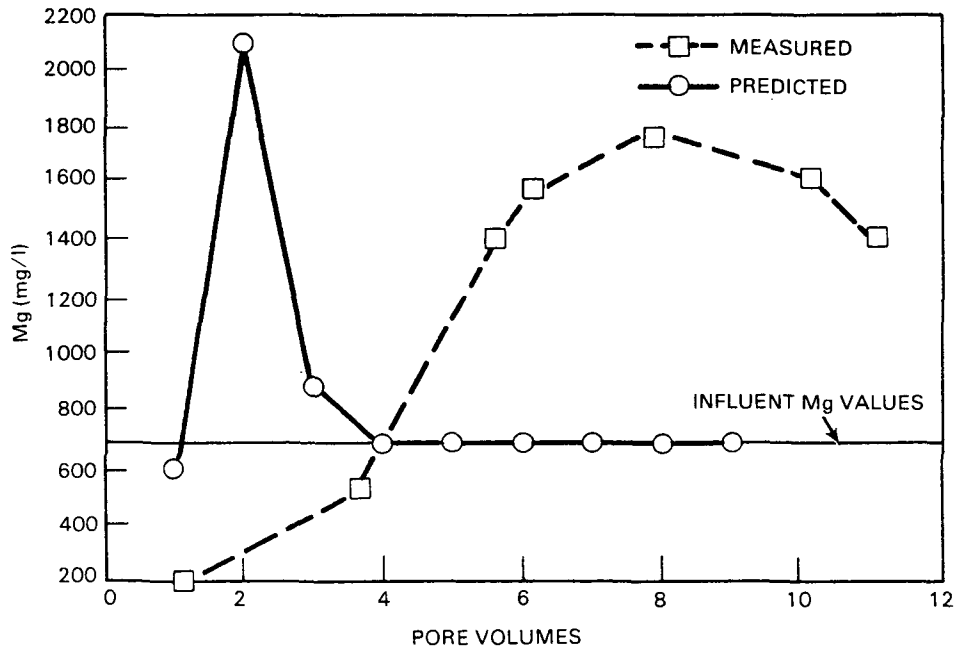


FIGURE 19. Measured and Predicted Concentrations of Magnesium Plotted Versus Pore Volumes of Effluent for Permeability Column 5

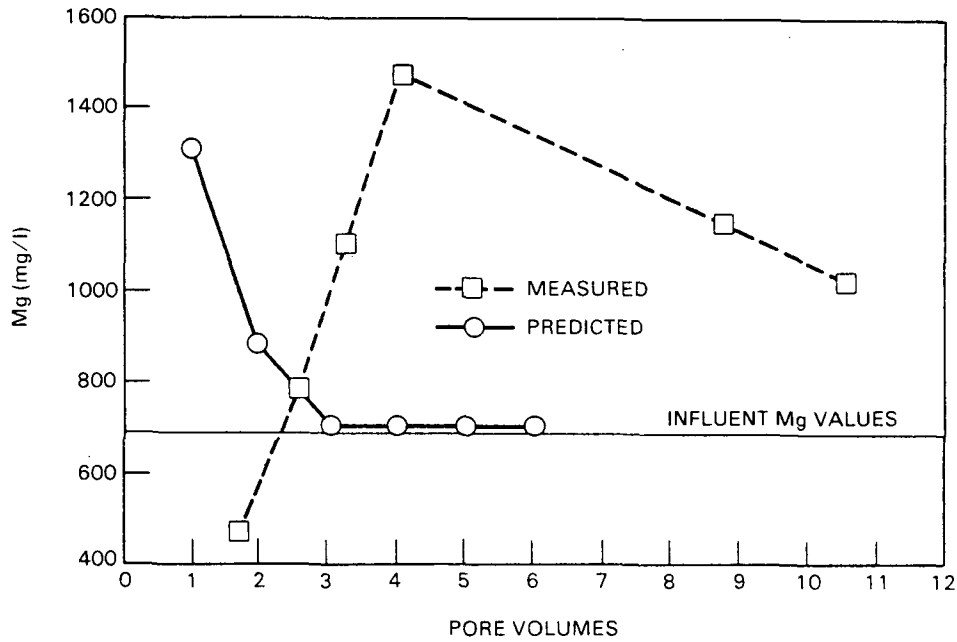


FIGURE 20. Measured and Predicted Concentrations of Magnesium Plotted Versus Pore Volumes of Effluent for Permeability Column 8

dissolves, the predicted values quickly fall to the influent values. The predicted values always tend to lead the measured values, i.e., they lead the rise or fall of the measured values.

Other magnesium solids need to be studied before much can be said about what controls the magnesium concentrations in solution. A precipitation/dissolution reaction cannot, at the present time, be discounted as a possible dominant mechanism. Another possible important mechanism is ion-exchange.

Strontium

Many of the column effluent solutions were near equilibrium with celestite (SrSO_4), according to ion speciation solubility calculations. Celestite was thus chosen as a solid in the conceptual model and allowed to precipitate when its solubility product was exceeded.

Precipitating gypsum provides another pathway by which strontium can be removed from solution. Strontium could either coprecipitate with gypsum or be incorporated into the gypsum crystal lattice to form a solid solution, or both. Since we presently have no way of quantifying either of these effects, such strontium removal mechanisms were not considered in the model. One would also expect ion exchange to be a removal mechanism that could affect the strontium concentrations. Serne et al. (1983) found from semi-selective extraction techniques that most of the strontium appeared to be present as ion exchangeable and weak acid soluble strontium.

In all cases (i.e., for both permeability and vacuum extractor columns), the measured strontium concentrations exceeded the predicted strontium concentrations. The predicted strontium levels in the vacuum extractor columns followed the influent strontium lines because the strontium and sulfate activity products were too low for the model to precipitate celestite (see Figure 21). The percolate used in the permeability columns had a higher strontium concentration than that used in the vacuum extractor columns and, thus, celestite was predicted to precipitate in the permeability columns, followed by a small dissolution spike as the pH front breakthrough occurred.

If we assume that our analytical data are correct, we then infer from the consistently high strontium concentrations (above influent values) that the original, uncontacted geologic materials are a source of strontium. Semi-selective extraction data indicate that this could indeed be the case (Serne et al. 1983). In every instance, X-ray fluorescence detected less strontium in the sediment after the leaching and extractions were performed on the sediments than before. This difference between the before and after contact was significant at the 99 percent level. Strontium indigenous to the sediment was sometimes present at levels exceeding one hundred parts per million. Thus, ion exchange of strontium could be a significant factor affecting strontium concentrations in solution. This ion exchange may explain the lack of agreement with the modeling predictions.

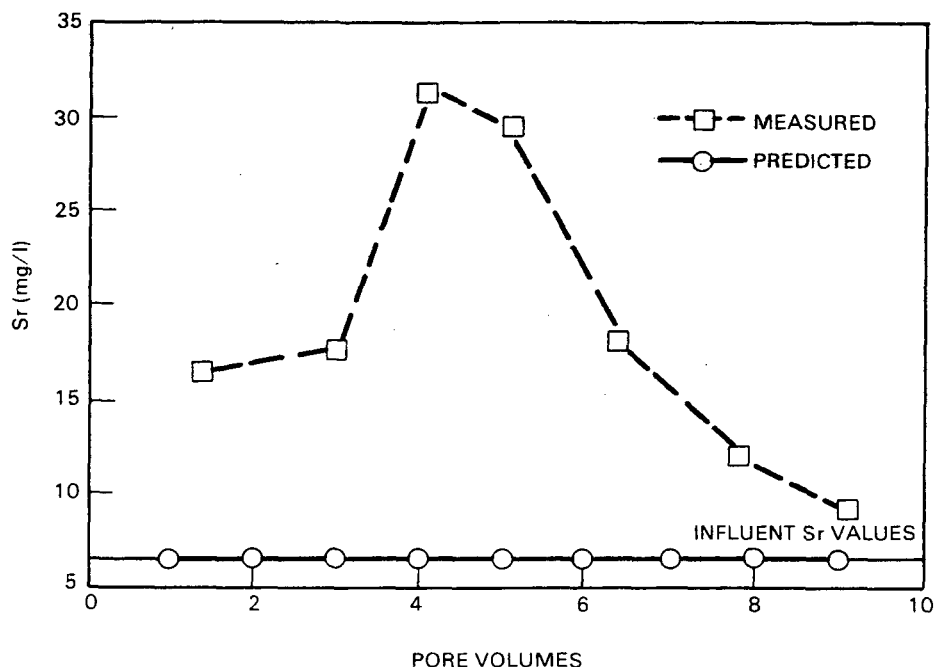


FIGURE 21. Measured and Predicted Concentrations of Strontium Plotted Versus Pore Volumes of Effluent for the Vacuum Extractor Columns

Silicon

Silicon is present in extremely high concentrations in the original tailings solutions. The original Highland Mill tailings solutions percolated through the permeability columns and vacuum extractor columns contained 234 and 255 mg/l of silicon, respectively (501 and 545 mg/l respectively of SiO_2). These inordinately high concentrations are almost five times higher than the solubility of an amorphous silica precipitate determined by Morey et al. (1964) and at least four times higher than any values found by the same authors in available literature (Morey et al. 1964). Morey et al. showed that amorphous silica can take up to three months to reach equilibrium when approached from oversaturation. However, in Morey's experiments, there was a rapid initial decrease in the degree of oversaturation and, after a few days, the silicon concentration reached a value of approximately 160 ppm silicon as SiO_2 . The degree of oversaturation in the original H.M. tailings solutions therefore appears too large to result from a lack of sufficient time for the solution silicon values to reach equilibrium.

Morey et al. (1964) measured molybdenum blue reactive silica which is, presumably, either a monomeric or a dimeric form of silica in contrast to our ICP analysis, which measures total silicon. Fournier (1973) found that silica polymers readily formed in some of his acid waters.

In view of the foregoing information we remeasured the silica concentrations in the tailings solutions that were percolated through the vacuum extractor columns to determine molybdate reactive and unreactive silica. The total of the unreactive plus reactive silica was determined to be 280 ppm as SiO_2 and reactive silica as one-half of the total or 140 ppm as SiO_2 . It would appear that there was a problem in reporting the ICP silica values given in Table 2. Unfortunately, the new value for silica was measured after the conceptual chemical model and the predictive chemical modeling for this report were completed. Modeling efforts currently underway use the new value of silica. These further efforts will be documented in future reports. The silicon concentrations in the effluent solutions do not show the extreme oversaturation with respect to amorphous silica that was observed in the original, acidic uranium mill tailings solutions.

An amorphous silica precipitate described by Morey et al. (1964) was included in the conceptual chemical model. It was believed that the amorphous precipitate should set an upper limit on dissolved silica concentrations.

No silica plots are included here because of the apparent problem with the silicon data. Not only are the silicon data ostensibly incorrect but thermodynamic data were available only for the monomeric form of silica and polymeric silica evidently comprised a major portion of the total silica in solution. Because of the large input silica values, the model continuously precipitated amorphous SiO_2 and thus the predicted silica values remained at a relatively constant concentration of 50 mg/l. In the column effluents, the SiO_2 values increased at higher pore volumes when the pH began to drop. This effect is not predicted by the modeling.

Uranium

Schoepite ($\text{UO}_3 \cdot 2\text{H}_2\text{O}$) was included in the conceptual model. Ion speciation/solubility calculations show near equilibrium with respect to schoepite.

An extensive discussion of uranium solubility as affected by a schoepite control is unwarranted because of the problem in predicting the Eh or pe. Schoepite should, based on saturation indices, predict uranium concentrations much better than is indicated by Figure 22. The considerable difference between observed and predicted values arises because the predicted pe values are lower than the measured values and thus schoepite is continuously undersaturated. Therefore, the predicted uranium values remain at influent levels.

In future simulation modeling, the pe needs to be fixed in order to remove this variable from our plots of predicted versus measured uranium concentrations.

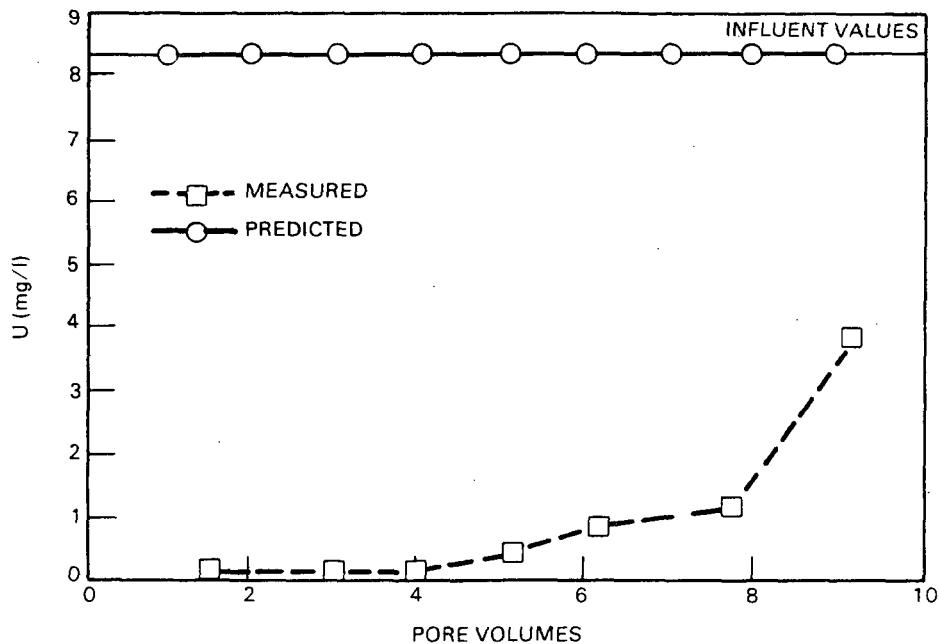


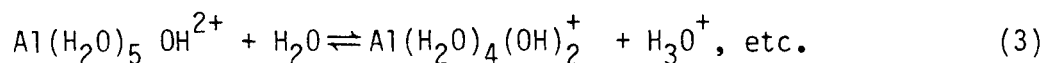
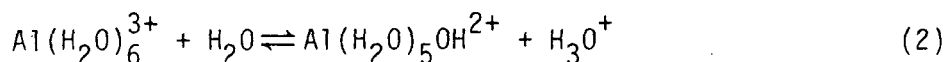
FIGURE 22. Measured and Predicted Concentrations of Uranium Plotted Versus Pore Volumes of Effluent for the Vacuum Extractor Columns

TRACE ELEMENTS OF POTENTIAL IMPORTANCE IN URANIUM MILL TAILINGS SOLUTIONS

The chemistry of many of the trace elements examined here does not appear to be dominated by precipitation/dissolution reactions. As a result, a conceptual chemical model composed of only minerals and other solid phases is inadequate for predictive modeling of trace elements.

The milling of uranium ore deposits invariably exposes large quantities of previously unexposed ores and minerals to accelerated weathering conditions. Although trace elements in uranium ores may be too sparse to be of commercial interest, these same elements may exist in significant concentrations compared to background levels. For instance, enhanced levels of Pb, As, Se, Mo, Al, Cd, Ba, U, Cr, and Fe have been observed in uranium mill tailings and in areas associated with uranium mines (Ford, Bacon, and Davis 1977i, 1977e, 1977j, 1977c, 1977h; Peterson et al. 1982; Legrande and Runnels 1975). The reactions of trace elements are too complex to allow a complete description of their chemistries. What we will do in the following pages is briefly discuss some of the trace elements that may be important in uranium recovery operations and review their chemistries to assess trace element movement and to help discern the dominant transport mechanisms in uranium mill tailings. To completely describe trace element chemistry we must have data on the nature and number of species formed, their chemical stabilities, and kinetics of their formation. Interfacial processes, such as adsorption or ion exchange, may play an important role in defining the chemistry of elements associated with uranium mill tailings.

Metals exhibit varying degrees of acidity when dissolved in aqueous solutions. Many metal cations hydrate in such a manner that the water molecule becomes an integral part of the cationic structure in solution. Examples are $\text{Al}(\text{H}_2\text{O})_6^{3+}$ and $\text{Zn}(\text{H}_2\text{O})_4^{2+}$. In their hydrated forms, polyvalent cations can operate as efficient proton donors. The reason why a solution becomes acidic when a metal salt is added can be explained by the following reactions with aluminum.



Thus, many polyvalent metal cations can be regarded as polyprotic acids. One important consequence is that a solution of a trace metal salt will always contain numerous hydroxo-complexes which are products of the hydrolysis reaction unless the pH is low enough to suppress the hydrolysis or high enough to precipitate the metal. In the pH range of natural waters the hydroxo complexes of trace metals are predominate while at the pH of many uranium mill tailings solutions the formation of many hydroxo complexes would be suppressed. The alkaline earth cations do not form hydroxo complexes except at very high pH, because of their weak acidic nature.

The adsorptive behavior of hydrolyzable trace metal ions in aqueous solutions is strongly pH dependent. For many metals there is a critical pH range, often less than 1 unit wide, where the adsorption goes from almost nothing being adsorbed to almost everything being adsorbed. Iron oxides may act as adsorption surfaces (Jenne 1977, Means et al. 1978) and were thought to be precipitating in uranium mill tailings reacted with clay liners by Peterson et al. (1982).

Several adsorption models of the hydrous oxide water interface have been formulated (Davis and Leckie 1978, Hohl and Stumm 1976) and have shown considerable success in modeling the adsorption of trace metals onto hydrous oxides. Two of these surface complexation models: a constant capacitance model (Hohl and Stumm 1976) and the triple layer site binding model (Davis and Leckie 1978, Yates et al. 1974) are included in the MINTEQ computer code. Intrinsic stability constants for the reaction of several trace metals with iron oxyhydroxides have also been published in the literature (Davis and Leckie 1978, Leckie et al. 1980, Balistrieri and Murray 1982). Thus, it appears that the conceptual chemical model presented here can be expanded to include adsorption of several trace metals onto the surface of iron oxyhydroxides. We might also improve our ability to predict pH and Ca, Mg, and SO_4 concentrations by simultaneously including protonation reactions and reactions of the bulk electrolyte ions with the iron oxyhydroxide surface.

Selenium

Environmental Occurrence

Selenium is often environmentally associated with elements such as copper, lead, silver, and uranium, but it is not found in high enough concentrations to make it profitable to extract by itself. It is usually obtained as a by-product from the extraction of ores such as uranium ores. Concentrations of selenium that exceed EPA drinking water standards have been observed in waters near tailings impoundments by Ford, Bacon, and Davis (1977b, 1977g, 1977e, 1977d, and 1977f). Frost and Griffin (1977) cited Garland and Mosher (1975) in stating that Se has been reported to be a pollutant of groundwater as far away as five kilometers from a dump on Long Island, New York.

Most soils have selenium contents ranging from 0.01-0.2 ppm (Weswig 1972). In certain areas of the country, such as South Dakota, soil selenium levels appear quite high. Conversely, the northeast and northwest sectors of the country have selenium deficient soils. The upper limit for selenium in drinking water is 10 ppb (U.S.E.P.A. 1980).

Environmental Chemistry

The environmental aqueous chemistry of selenium is very complex. Selenium in aqueous solution can exist as a variety of aqueous species and in three different oxidation states (-2, +4, +6).

Under reducing conditions the dominant aqueous species would be $\text{H}_2\text{Se}^\circ$ and HSe^- . The $\text{H}_2\text{Se}^\circ$ form would dominate below a pH of approximately 3.8 and HSe^- would dominate above a pH value of 3.8. Selenite species would predominate under intermediate to slightly oxidizing conditions with HSeO_3^- the major species in the pH range of approximately 3 to 8.5. Below a pH of roughly three, selenous acid (H_2SeO_3) would be the dominant form; above a pH value of about 8.5, SeO_3^{2-} would dominate. The selenate species (SeO_4^{2-}) would only form under highly oxidizing conditions and become increasingly important as the pH increases under a fixed pe regime.

Kinetics can play a significant role in the interconversions between the various oxidation states of selenium. The oxidation of elemental selenium to selenite is rather slow and difficult to achieve unless the elemental selenium is finely dispersed (Geering et al. 1968). Conversely, the reduction of selenite to elemental selenium proceeds quite rapidly (Howard 1977). The rate of transformation of selenite to selenate is sluggish (Geering et al. 1968) and will probably not occur under natural weathering conditions; though under the redox status extant in some of the acidic uranium mill tailings solutions some selenate can form.

Howard (1977) states that HSeO_3^- and SeO_3^{2-} are strongly adsorbed by hydrated surfaces of ferric oxides in pH values ranging from 2 to 8. Frost and Griffin (1977) found that the HSeO_3^- ion appears to be the Se(IV) species predominately adsorbed by clay minerals. Above a pH of 8, adsorption decreases, according to Howard (1977), until complete desorption occurs at pH 11. Howard quotes several authors as stating that adsorption on hydrous ferric oxides

removes from 95 to 99% of the selenium (IV) oxyanions from solution at pH 8 and below (at least down to where the iron solid dissolves). Howard (1977) quotes Rosenfeld and Beath (1964) and Carey et al. (1967) as suggesting that in alkaline environments, SeO_3^{2-} is oxidized to the Se(VI) state, or SeO_4^{2-} , which is not strongly adsorbed nor does it form insoluble compounds and is, therefore, quite mobile. Singh et al. (1981), in contrast to the above, found that selenate was always adsorbed more than selenite in laboratory experiments involving soils with a range of characteristics and differing competitive anions.

The low solubility of selenium in soils was attributed by Lakin (1961) to the formation of a ferric selenite but it is unclear whether this ferric selenite was a crystalline solid or a ferric oxide-selenite adsorption complex. Geering et al. (1968), after studying the solubility of selenium in seven different soils, indicated that the mechanism controlling the solution concentration of selenium was the formation of a ferric oxide-selenite. Howard (1977) also supports the view that ferric oxyhydroxides control the concentrations of selenium in natural waters and not the formation of a solid phase.

Experimental and Geochemical Modeling Results

The original Highland Mill Tailings solution contacted with the vacuum extractor columns is predominately selenite although some selenate should be present. The vacuum extractor columns will be emphasized here since the movement of radiotraced and stable selenium was closely followed through these columns. Most of the selenite and selenate in the initial percolate for the vacuum extractor columns should be in the H_2SeO_3 and SeO_4^{2-} forms, respectively, though a considerable portion, roughly one-third, of the selenite should exist as HSeO_3^- . If the Eh values are assumed to be reliable, then the selenate species remain relatively minor species compared to selenite, except for the first two effluent solutions (pore volumes 1.36 and 3.04), in which the selenite and selenate species should be present in roughly equal concentrations.

The slow rate at which selenite is converted to selenate could help explain some of the results that were observed in vacuum extractor experiments (Serne et al. 1983). In the vacuum extractor experiments, radiotracers were added to the tailings solutions to provide a convenient method for determining quantitatively the behavior of trace elements. The radiotracer chosen to simulate the movement of selenium was ^{75}Se . The total elemental concentration ratios (C/C_0 , where C_0 = influent concentrations and C = measured concentration in the effluent solution) for stable Se were much higher than the concentration ratios observed for the ^{75}Se tracer. The ^{75}Se tracer did not appear to act as an effective tracer of stable Se. The Se tracer was added as selenite which, as subsequently explained, tends to be less mobile than selenate which supposedly comprised a fraction of the Se in the original tailings solution. The slow conversion of selenite to selenate would prevent the radiotraced selenite solution from oxidizing to selenate during the time frame of the vacuum extractor experiments even though the redox status of the solution might warrant a partial transformation of selenite to selenate. It took roughly

18 hours for a pore volume of solution to percolate through the vacuum extractor columns. Thus, the more mobile selenate present in the original tailings solution would move through the columns to a greater degree than the ^{75}Se tracer, which accounts for the observed differences between ^{75}Se and stable Se concentration ratios.

Our aqueous speciation/solubility calculations affirm the thinking of Geering et al. (1968) and Howard (1977) in that selenium solid phases were almost invariably undersaturated relative to the solution composition. Furthermore, it appears that adsorption onto ferric oxyhydroxides is a likely mechanism of selenium retention in the vacuum extractor columns.

Semi-selective extraction techniques used on vacuum extractor columns (Serne et al. 1983) contacted with uranium mill tailings solutions indicated that the largest percentage of selenium was removed concomitantly with those chemical reagents that purported to dissolve amorphous iron and aluminum oxides and crystalline iron oxides.

Selenium solids were not included in the conceptual chemical model. Ion speciation/solubility calculations always computed the effluent solutions to be undersaturated relative to selenium solid phases. Other mechanisms appear to be controlling selenium concentrations and will be incorporated into future modeling efforts.

In future predictive modeling, the conceptual model presented here will be expanded to include the adsorption of selenium onto iron oxide surfaces through use of a surface complexation model.

Arsenic

Environmental Occurrence

Most arsenic found in the air and water is in the parts per billion (ppb) concentration range while arsenic present in the earth's crust is found in concentrations of 2 to 5 parts per million (ppm) (Buhler 1972, Wagner 1972). The maximum permissible concentration (MPC) established for arsenic in drinking water is 50 ppb (U.S.E.P.A. 1980). Normal arsenic concentrations in drinking water are in the <10 ppb range except for instances of high pollution (Braman 1975).

Water samples in areas near uranium mill tailings have been observed to exceed the MPC for arsenic (Ford, Bacon and Davis 1977c, 1977d, 1977g). In several instances the excess has been credited to arsenic leaching from uranium mill tailings impoundments.

Wageman (1978) used the typical concentrations of arsenic in freshwater systems along with the concentrations of 14 different metals found in these same systems to examine possible solid phase controls on arsenic solubility. Four metals emerged from this study as possible candidates. The four were Ba, Cu, Fe and Cr. After these metals were examined more closely, it appeared that Ba, at concentrations found in ground waters, could be a possible solid phase

control, with chromium and iron emerging as slightly less likely controls. Wageman (1978) goes on to say that isomorphous substitution of arsenic for phosphate is found in such minerals as apatite $[\text{Ca}_5(\text{PO}_4)_3(\text{OH},\text{F})]$, libethenite $[\text{Cu}_2(\text{OH})(\text{PO}_4)]$, and in other complex arsenates analogously to the phosphates. The affinity of arsenic for iron may be due to the formation of such compounds. The existence of such an arsenic compound has not been identified but the analogous phosphate compound does exist as $\text{FeH}_2\text{PO}_4(\text{OH})_2$ (Sillen and Martell 1964). The data in the literature are too sparse regarding barium and arsenic to come to any sort of conclusion as to the ability of a barium-arsenic solid to control the concentration of dissolved arsenic in solution.

Environmental Chemistry

Arsenic is stable in four oxidation states (-3, 0, +3, +5) under varying Eh and pH conditions, though metallic arsenic exists only rarely and the -3 oxidation state occurs only under extremely reducing conditions. The dominant oxidation states in natural aquatic systems are +3 and +5.

Arsenic removal from solution was observed to be pH dependent. Gulledge and O'Connor (1973) attributed this pH dependency to the arsenic's changing speciation with changing pH. Frost and Griffin (1977) concluded that H_2AsO_4^- was the principal As(V) species adsorbed by clay minerals.

Hounslow (1980) noted that the rate of oxidation of arsenite to arsenate may be sluggish. Cherry et al. (1979) observed that the Fe^{3+} oxidation of As(III) to As(V) was barely discernible at high pH values but becomes appreciable at lower pH values.

Inorganic forms of arsenic are variably toxic depending on whether they are in the trivalent or pentavalent state. Arsenic in the reduced state [As(III)] is much more toxic, more soluble, and mobile than in the As(V) oxidation state. Hounslow (1980) states that arsenic in the reduced state is 60 times more toxic than arsenic in the oxidized state.

Akins and Lewis (1976) cite Jacobs et al. (1970) as saying that the arsenic concentration in soils is directly proportional to the Fe_2O_3 content of the soils. The removal of Fe and Al compounds from the soil either drastically reduced or completely eliminated the arsenic adsorption. Akins and Lewis (1976) found that most of the arsenic in the soils studied was in the Fe-arsenate form with other forms such as Al- and Ca-arsenates predominating when the iron concentration was low. Water soluble arsenic was proportional to the total arsenic present in the soils and inversely proportional to the iron and aluminum present. Gulledge and O'Connor (1973) observed that ferric hydroxide $[\text{Fe}(\text{OH})_3]$ was able to remove more arsenic(V) from solution than aluminum hydroxide. Hem (1977) stated that precipitation of ferric arsenate and coprecipitation with ferric hydroxide may be a major factor in As attenuation in geothermal waters.

Results from the work of Frost and Griffin (1977) indicated that As and Se would be mobile in leachate passing through relatively pure clay materials under alkaline conditions. As noted earlier in this report, ferric hydroxides

appear to precipitate when uranium mill tailings solutions come in contact with sediments because pH increases due to the natural buffering capacity of the clay. Ferric oxyhydroxides could help reduce high arsenic concentrations in the tailings solution as it (the solution) percolates through the sediments.

Experimental and Geochemical Modeling Results

The As in the solution used in both the permeability and vacuum extractor columns was predominantly in the +5 oxidation state, based on Eh measurements, with approximately one-third and one-half, respectively, existing initially as the $H_2AsO_4^-$ species. The $H_2AsO_4^-$ species should be the predominant species between pH values of approximately 2 to 7 under the Eh conditions commonly found in these tailings solutions.

The kinetics of the conversion of arsenite to arsenate should not produce any difference in the migration of radiotraced arsenic and stable arsenic, as happened with selenium since both sources of arsenic were purportedly in the +5 oxidation state. Both stable and radiotraced arsenic tied up very quickly in the columns.

Selective extraction data (Serne et al. 1983) demonstrated that hydrous iron oxides were contributing to the removal of arsenic in these tailings solutions/sediment interactions. The extraction results indicated that amorphous iron oxide could be an important sink for arsenic with crystalline iron oxides and manganese oxides also contributing.

Arsenic solid phases were found to be undersaturated relative to the solution composition for effluent solutions for which ion speciation/solubility modeling was performed. Many of the column effluents had arsenic concentrations that were below the detection limits of the instrument.

In summary, arsenic was immobilized at all pH values in the vacuum extractor columns and based upon semi-selective extraction work, we believe the attenuation mechanisms to be adsorption of arsenic onto iron oxides. Formation of an insoluble ferric hydroxy arsenate could also be occurring but could not be tested owing to a lack of thermodynamic data.

Future work will involve incorporating a surface complexation model into our conceptual model to account for the adsorption of arsenic onto ferric oxides.

Molybdenum

Environmental Occurrence

The concentration of molybdenum in soils usually varies within the narrow range of 0.6 to 3.5 ppm. The Federal Water Quality Committee suggested that soils not be continuously irrigated with water containing greater than 75 $\mu g/l$ Mo because of toxicity associated with plant uptake of molybdenum. Fine soils that are sporadically irrigated may use water that contains up to 50 $\mu g/l$ molybdenum (F.W.P.C.A. 1968). The proposed standard for drinking water is

50 ppb (U.S.E.P.A. 1980). Molybdenum concentrations as high as 900 mg/l have been observed in tailings water from a uranium mill in southern Colorado (Legrande and Runnells 1975).

Environmental Chemistry

Few molybdenum minerals are known to occur naturally in soils. The most common of these is molybdenite (MoS_2). Molybdite (MoO_3) and ilsemannite (Mo_3O_8), which form from molybdenite, are also found naturally (Vlek and Lindsay 1977). Secondary minerals listed by Vlek and Lindsay (1977) include powellite (CaMoO_4), wulfenite (PbMoO_4), and ferrimolybdate [$\text{Fe}_2(\text{MoO}_4)_3 \cdot n\text{H}_2\text{O}$].

The solubilities of the metal molybdates CuMoO_4 , ZnMoO_4 , $\text{Fe}_2(\text{MoO}_4)_3$, and PbMoO_4 will depend upon the activities of the free metal ions in solution. Assuming that the activities of Cu, Zn, Fe, and Pb are controlled by CuFe_2O_4 , soil Zn (Sadiq and Lindsay 1980), $\text{Fe}(\text{OH})_3(\text{am})$, and PbCO_3 , then the relative solubilities of associated molybdenum compounds in decreasing order are CuMoO_4 , ZnMoO_4 , MoO_3 , H_2MoO_4 , $\text{Fe}_2(\text{MoO}_4)_3$, and PbMoO_4 (Rai et al. 1983).^{*} Lindsay used thermodynamic considerations such as these to speculate that wulfenite should be the most stable form of Mo in soils. In their experiments, however, MoO_4^{2-} concentrations in the soil decreased when wulfenite (PbMoO_4) was added to the soil. This led Vlek and Lindsay (1977) to conclude that adsorption may be controlling molybdenum concentrations.

Kaback and Runnells (1980) observed undersaturation of Mo in Tenmile Creek near Climax, Colorado, with respect to solid phases thought to be capable of controlling Mo solubility. It was thought that molybdenum in the creek was adsorbed on amorphous ferric hydroxide (ferrihydrite) coatings. Approximately 70% of the molybdenum was associated with amorphous ferric hydroxide iron. Increased concentrations of molybdenum have previously been identified with iron oxide accumulations in soils (Taylor and Giles 1970, Karimian and Fox 1978). Aluminum oxides, halloysite, nontronite, and kaolinite are also capable of removing molybdenum from solution (Karimian and Fox 1978). Theng (1971) found that the theory of Hingston et al. (1967, 1968) explained the sorption of molybdate onto crystalline and amorphous soil clays. This theory postulated that the fully undissociated acid (H_2MoO_4) and the most anionic species (MoO_4^{2-}) are not adsorbed. These forms only adsorb when both proton donating (e.g., HMoO_4^-) and proton accepting (MoO_4^{2-}) species are in solution. Pasricha and Randhawa (1977) found that Fe-soils adsorbed more molybdenum than Al-soils. Molybdenum is similar to selenium in that adsorption by soils, clays, and hydrous oxides decreases with increasing pH up to approximately pH 7.5, above which virtually no adsorption of Mo takes place (Reisenauer et al. 1962).

At the pH values and redox potentials of the acid uranium mill tailings solutions used in the vacuum extractor columns the predominant molybdenum species should be MoO_4^{2-} , with HMoO_4^- assuming predominance at pH values less than approximately 3.9 and at pe plus pH values over 8. Neutralization of uranium

^{*}Document in draft form.

mill tailings could increase the mobility of molybdenum by increasing its solubility and also by decreasing its adsorptive potential.

Experimental and Geochemical Modeling Results

In the vacuum extractor experiments (Serne et al. 1983), Mo was similar to selenium in that the first effluent sample from each vacuum extractor tier most often showed the highest molybdenum concentrations. The initial effluents from each column had the highest pH values. Molybdenum tends to be mobile at high pH values which could account for the high concentrations observed in the earliest effluents. The precipitation of iron and aluminum oxyhydroxides could have contributed to the attenuation of Mo after the pH began to drop.

At the pH values and redox potentials of the acidic uranium mill tailings solutions used in the vacuum extractor columns, the predominant molybdenum species should be MoO_4^{2-} , with HMO_4^- assuming predominance at pH values less than approximately 3.9 and at pe plus pH values over 8. Neutralization of uranium mill tailings could increase the mobility of molybdenum by increasing its solubility and also by decreasing its adsorptive potential.

No molybdenum solid phases were included in the conceptual model due to the consistent undersaturation of the solution relative to these solid phases.

Most of the effluent solutions from the vacuum extractor and permeability columns had Mo concentrations below the detection limits of the analytical instruments we used. Using atomic absorption with graphite furnace (Serne et al. 1983), the detection limit commonly attained in these acidic uranium mill tailings solutions for molybdenum was ~ 0.06 mg/l. Even if the solubility of MoO_4^{2-} were governed by the most insoluble of the solid phases, such as wulfenite (PbMoO_4) and the Pb^{2+} activities were comparable to those measured in the column effluents, the molybdenum concentrations should be high enough to be measured. It appears that some other mechanism, besides precipitation/dissolution is controlling the concentration of molybdenum in these effluent solutions. We believe that adsorption maintains molybdenum concentrations below the levels that could be maintained by any possible solid phase control. The molybdenum concentration of the Highland Mill tailings solution used to contact the permeability columns was 0.35 mg/l and was always below detection limits in the column effluents.

The molybdenum solid phases considered would maintain molybdenum concentrations at higher values than those determined analytically. The literature indicates that adsorption on the surface of iron oxides is most likely responsible for controlling molybdenum concentrations. As with selenium and arsenic, this retardation mechanism will be addressed in future predictive modeling efforts as we add a surface complexation model to our conceptual model.

Vanadium

Environmental Occurrence

Vanadium is found in uranium bearing sandstones such as carnotite ($K_2O \cdot 2UO_3 \cdot V_2O_5 \cdot 3H_2O$), uravanite ($2UO_3 \cdot 3V_2O_5 \cdot 15H_2O$), and tyuyamunite ($CaO \cdot 2UO_3 \cdot V_2O_5 \cdot 4H_2O$). Previously, a large percentage of the vanadium mined in the United States was extracted as a by-product from uranium ores. Recent reductions in the mining of uranium ores have, however, necessitated seeking vanadium from other sources. High levels of vanadium have been observed in tailings at tailings disposal sites (Ford, Bacon and Davis 1977a, 1977c, 1977h and 1977j).

Environmental Chemistry

Vanadium can exist in oxidation states of +2, +3, +4, and +5, but bivalent vanadium will decompose water at 25°C under all pH conditions and, therefore, would not be expected to form in nature. Trivalent vanadium is also somewhat unstable with respect to the atmosphere. Even the naturally occurring montroseite will be altered to an appreciable extent in the laboratory (Evans and Garrels 1958).

Hem (1977) states that ferrous vanadate precipitates could be capable of maintaining vanadium concentrations at approximately $10^{-8.00}$ to $10^{-9.00}$ moles/l in systems that are relatively rich in iron. In 16 of 27 public water systems for which specific vanadium concentrations were reported, the values calculated for dissolved iron, based upon a ferrous vanadate solubility control, were within ± 0.2 log units of the reported concentrations. However, vanadium concentrations were measured in 100 of these public water systems and the reported values ranged from 70 ppb down to below detection limits (Durfor and Becker 1964). Therefore, the 16 values described by Hem (1977) as being close to equilibrium with ferrous vanadate only represent a small fraction of the total measured values.

Taylor and Giles (1970) found vanadium associated with iron oxides in laterite soils.

Experimental and Geochemical Modeling Results

No vanadium solid phases were entered into the conceptual model. Most of the effluent solutions from the vacuum extractor and column experiments had vanadium concentrations below the detection limits (0.05 mg/l) of the graphite furnace atomic absorption (AA/GF) used to analyze vanadium in the solutions or that were below an indicated value (see Appendix A). Those solutions that did have measureable concentrations of vanadium, such as the original Highland Mill tailings solution used to contact the permeability and vacuum extractor columns, were always undersaturated with respect to the minerals considered by the MINTEQ code (Felmy et al. 1983). Even with 10.6 mg/l U in the initial tailings solution, all the solutions were undersaturated with respect to various minerals and solid phases. Carnotite and tyuyamunite become more soluble at pH

values above 8.5 through the formation of uranyl carbonate complexes and $(\text{UO}_2)_3(\text{OH})_5^+$ and at values below 5 by the formation of the UO_2^{2+} and protonated vanadium species.

Pentavalent vanadium should be the dominant form in neutralized uranium mill tailings solutions with quadravalent vanadium becoming progressively more important as pH values decline. The +5 vanadium form is the major form supposedly existing in the Highland Mill tailings solution percolated through the permeability columns, while the +4 state is slightly more important in the Highland Mill tailing solutions that contacted the vacuum extractor columns. In both solutions, the major species in the +5 form is VO_2^+ with the VO_2SO_4^- species also contributing significantly to the total. The dominant forms of the +4 vanadium in both solutions are VO^{2+} and VOSO_4^0 , with these two species being about equally predominant.

We speculate that the mechanism governing the apparent limited movement of vanadium is adsorption of vanadium onto soil particles and onto ferric oxide surfaces. The immobilized vanadium appears to be tightly bound as no vanadium appeared to move even after the pH of the effluent solutions dropped toward those of the influent values (Serne et al. 1983).

Thus it appears that vanadium could be modeled, similarly to selenium, arsenic, and molybdenum, through the addition of a surface complexation model to our conceptual model.

Chromium

Environmental Occurrence

Chromium has a multiplicity of uses in modern society making it possible for this element to enter the food chain through varied avenues. Chromium is used in electroplating solutions, paints, dyes, and drugs (Artiole and Fuller 1979 citing Udy 1956). Chromium(VI) is considered quite toxic while chromium(III) is relatively innocuous. Durum and Haffty (1963) report median chromium values of 5.8 ppb for large rivers of North America with the values ranging from 0.72 to 84 ppb.

Environmental Chemistry

Minerals containing chromium as a major constituent are few in number though chromium commonly replaces cations of comparable size. Chromium(III) closely resembles Al^{3+} and Fe^{3+} in its ionic size and frequently substitutes for these ions in the solid structure. Grove and Ellis (1980) maintain that $\text{Cr}(\text{OH})_3$ will precipitate above a pH of 6 even though Cr_2O_3 is thermodynamically more stable.

In the presence of soils, chromium was removed from solution at a lower pH value than would be possible were the removal controlled solely by precipitation of $\text{Cr}(\text{OH})_3$ (Bartlet and Kimble 1976b). Chromium(III) appeared to be held very tightly by the clay soil. In the presence of aluminum, chromium(VI)

precipitated out of solution as the pH rose above 4 to 5 and was almost totally removed from solution at a pH of 6 (Bartlet and Kimble 1976a). The solution concentration of chromium increased as the pH rose above 8. Since this follows quite closely the solubility of aluminum, the chromium removal mechanism was probably one of aluminum coprecipitation. Artiole and Fuller (1979) also found a positive correlation between increased chromium retention and the presence of the metal hydroxides of iron. The solution concentrations of chromium were noted by Griffin et al. (1977) to vary with speciation in such a way that they were led to believe that HCrO_4^- was the Cr(VI) species predominantly adsorbed. Adsorption of Cr(III) increased as the pH of the soil suspensions increased. About 300 to 600 times more Cr(III) was adsorbed in these systems than Cr(VI). The lack of adsorption of chromium above a pH of 8.5 suggested that CrO_4^{2-} is not readily adsorbed.

Chromate has been found to have similar adsorption properties to those of other tetroxo anions such as phosphate. Adsorption is enhanced by low pH conditions and further enhanced by reduction to the Cr(III) form in certain soil types (Mayer and Schick 1981). Mayer and Schick (1981) postulated that adsorption of Cr(VI) was a two step process involving reduction of Cr(VI) to Cr(III) followed by adsorption. This reduction-adsorption mechanism is favored by low pH and high organic matter in soils. Artiole and Fuller (1979) maintained that the most common oxidation state of chromium is the +6 form and thought that Fe^{2+} acted as an electron donor to reduce the Cr(VI) to Cr(III). The presence of electron donors such as Fe(II) and organic matter was speculated, by these researchers, to be of paramount importance in the retention of chromium as precipitated or adsorbed Cr(III) which would otherwise be more mobile in the +6 state. Nakayama et al. (1981) showed that manganese oxides existing under conditions prevalent in sea water could catalyze the oxidation of Cr(III) to Cr(VI). Direct oxidation of Cr(III) by dissolved oxygen appeared, from the studies of Nakayama (1981), to not always be possible because of the extremely slow kinetics of the reaction. Bartlet and James (1979) were surprised to find that Cr(III) oxidized to Cr(VI) quite readily in soils since they expected Cr(III) to be the prevalent form under normal soil conditions. The big factor in this oxidation again appeared to be the presence of oxidized manganese which acted as an electron acceptor in the reactions. Bartlet and James (1979) noted that earlier investigations had failed to notice the oxidation of Cr(III) to Cr(VI) because they used dried, crushed, soil instead of the fresh moist soils used by Bartlet and James (1979). These researchers found that atmospheric oxygen will oxidize small amounts of Cr(III) above a pH of 9, but not at the pH values commonly occurring in soils. In every case, drying the soil increased the amount of reduced manganese relative to oxidized manganese, thus decreasing the ability of manganese to oxidize Cr(III) to Cr(VI). Cary et al. (1977) observed a slightly deeper penetration of Cr(VI) into alkaline soils than into acid soils.

In experiments conducted by Plotnikov and Safonov (1979) on the precipitation of chromium with iron it was observed that the coprecipitation curve for chromium approximated the precipitation curve for pure chromium(III) hydroxide. This indicates that chromium may have begun to precipitate as the hydroxide. Theis and Richter (1979) modeled field measurements of leachate from an active power plant disposal site and concluded that chromium concentrations were

determined by precipitation of discrete phases. This precipitated phase was also presumed to be the chromium hydroxide phase. Chromites, mixed oxides of Cr(III) and Fe(II), are thought to be more stable than chromium oxides by Cary et al. (1977).

Griffin et al. (1977) studied how pH affects adsorption of chromium from landfill leachate by montmorillonite and kaolinite clays. Below a pH of 4.0, adsorption appeared to be the most important mechanism for removing chromium from solution. In the pH range of 4 to 5 a combination of adsorption-precipitation mechanisms became important. Above a pH of 5, Griffin et al. (1977) found that precipitation was the major chromium attenuating mechanism. The precipitate formed was identified by color and by X-ray diffraction, as chromic hydroxide. Bartlett and Kimble (1976a) in studying the behavior of chromium in soils found that the solubility behavior of Cr(III) varied with pH and phosphate concentration in much the same way as Al. The solubility of Cr(III) decreased with increasing pH. Precipitation was complete at a pH of about 5.5. The precipitate was thought to consist of macro molecules of Cr in six coordination complexes with water and hydroxyl groups.

Matzat and Shirak (1978) quote others in stating that chromic hydroxide should precipitate at chromium concentrations higher than approximately $10^{-11.7}M$ in natural waters which is lower than the levels analytically observed.

Experimental and Geochemical Modeling Results

No thermodynamic data for chromium were available in the MINTEQ data base and, therefore, no geochemical modeling of this element could be performed. Thus, no chromium solid phases were included in the conceptual model. It is anticipated that these data will be added soon as Schmidt and Jenne* (1983) recently completed an extensive review of the literature on chromium thermodynamic data.

The original Highland Mill tailings solutions percolated through the permeability and vacuum extractor columns had 2.7 and 1.5 mg/l chromium, respectively. These concentrations are higher than that expected to be maintained by $Cr(OH)_3$ at the oxidation potentials of these solutions. Many of the effluent solutions from the permeability and vacuum extractor cells had concentrations that were below the detection limit (0.03 mg/l) of our instruments for these solutions. Several chromium solids, e.g., $Cr(OH)_3$ and $Fe_2Cr_2O_4$, are able to maintain chromium concentrations below the detection limits of our instruments depending upon the exact pH and pe determined. Other possible solubility controls under oxidizing conditions are Cr_2O_3 and $PbCr_2O_4$.

In our experiments with radiotraced chromium (Serne et al. 1983), the chromium tied up in the upper portions of the columns and remained immobile even after the pH of the effluent solution had dropped to values around 3.0. Both radiotracer and stable chromium data agreed upon the extent of migration

*Document in draft form.

of chromium through the columns. As discussed, chromium adsorption is enhanced at low pH values and also by reduction of chromium to the Cr(III) form.

Semi-selective extraction of dissected soil columns (Serne et al. 1983) revealed that chromium was only removed, except for one sample, by those extraction procedures designed to remove only amorphous iron and aluminum and crystalline iron oxides. This indicates that adsorption onto iron oxides is a possible mechanism removing chromium from solution at higher pH values. At lower pH values, where dissolution of iron oxides occurs, adsorption onto clay surfaces may become important.

Chromium thermodynamic data need to be added to the MINTEQ computer code to look for solid phases that could be in equilibrium with the solution composition. Depending upon the outcome of the search for solid phases that may be in equilibrium with the solution, we may need to consider the adsorption of chromium onto iron oxides in the manner discussed for the other trace elements.

Lead

Few effluent solutions from the permeability and vacuum extractor columns had measureable concentrations of lead. Thus, it was impossible to predict with any certainty lead solubility controls. Earlier studies (Peterson and Krupka 1981, Peterson et al. 1982) indicated that anglesite ($PbSO_4$) could be in equilibrium with uranium mill tailings after contact with clay and other geologic materials. Due to the less than detectable (see Table 2) lead concentrations in the original Highland Mill tailings solution used in both the permeability and vacuum extractor columns no lead values were input and consequently, no lead precipitated from the solutions in the predictive modeling efforts. Based on the sulfate activities computed for tailings solutions percolated through the permeability columns, the lead concentrations maintained in solution by anglesite would be extremely low ($\sim 0.6 \text{ mg/l}$) but still significantly above the EPA established drinking water standard of 0.05 mg/l (U.S.E.P.A. 1978) and the detection limits of our primary instruments. It appears, however, that attenuation mechanisms are operating to limit lead concentrations to very low levels.

Radiotraced lead was found to be more strongly retained than other transition metals and tied up in the upper portions of the columns. No detectable ^{210}Pb was found in the vacuum extractor column effluents. The semi-selective extraction data (Serne et al. 1983) indicated that ^{210}Pb was predominantly associated with crystalline or amorphous iron and aluminum oxides, with some Pb being exchangeable. Since ^{210}Pb remains immobilized, even after the soil's initial buffering capacity has been exhausted and iron oxides began to redissolve, lead appears to be immediately bound to cation exchange sites or to other soil minerals upon dissolution of the iron oxides.

Nickel, Silver, Cadmium, and Zinc

No potential solubility controls were developed for the transition elements nickel, silver, cadmium, and zinc. No detectable silver was in either the original tailings solutions or in any of the effluent solutions from the

permeability and vacuum extractor columns. Cadmium and nickel were invariably undersaturated with regard to any solid phases that could be controlling the concentrations of these elements. [See MINTEQ data base documentation for a listing of those solid phases considered (Truesdell and Jones 1974, Ball et al. 1981). Most of the solution species of nickel, cadmium and zinc should exist in solution as uncomplexed metal ions and metal ions complexed with sulfate. In the high pH range, zinc was slightly oversaturated with respect to $ZnSiO_3$ and willemite and became progressively undersaturated as the pH fell toward influent values.

Silver was quickly immobilized in the columns and remained immobilized at all pH values. Nickel, cadmium and zinc on the other hand, though bound at high pH values, became mobile at pH values less than 4.5 (Serne et al. 1983).

A conclusion to be drawn from these migration data and the selective extraction data is that to accurately and quantitatively account for the migration of cadmium, silver, zinc and nickel one must take into consideration their pH dependent immobilization onto precipitated hydrous oxides and other phases already present in the column. Based on results from the study documented in this report, precipitation/dissolution reactions based on thermodynamic equilibrium relationships are insufficient to characterize the movement of these elements. The measured column effluent concentrations of these elements are generally too low to have an effective solid phase control.

SUMMARY AND CONCLUSIONS

An assemblage of solid phases known or suspected to be present was used to create a conceptual model of the sediments being contacted with acidic uranium mill tailings. The conceptual model was used to predict the aqueous phase compositions of an acidic uranium mill tailings solution as it flowed through permeability and vacuum extractor columns. The model predictions were then compared to laboratory data for these same systems. This represents an exploratory attempt to use a conceptual model, such as described above, to simulate the interaction of acidic uranium mill tailings solutions with geologic sediments. This particular conceptual model (solid phase assemblage) is being presented here for the purpose of demonstrating the methodology and applicability of the approach. Refinements to the conceptual model are currently being undertaken and will be documented in future publications. The solid phase assemblage was used to simulate the passage of successive pore volumes of acidic uranium mill tailings solutions through geologic materials. Currently, the conceptual model can only predict the concentrations of elements whose dominant controlling mechanism is precipitation/dissolution.

The data used to compare the model predictions came from laboratory columns. These columns were packed with either a silty clay loam or a sandy loam and percolated with uranium mill tailings solutions of different compositions. The effluent solutions from these columns were collected at various pore volumes and analyzed for selected constituents to obtain time dependent concentrations.

The precipitation/dissolution reactions considered in the conceptual model were capable of predicting the column effluent concentrations of several of the macro constituents of the tailings solutions (SO_4 , Ca, Al, Mn, and Fe). Sulfate concentrations in the column effluents were generally one to two orders of magnitude above the secondary drinking water standards established by the U.S. Environmental Protection Agency. The conceptual model was able to predict these elevated concentrations.

The conceptual model was unsatisfactory when used to predict the concentrations of selected trace elements. Generally, trace elements were undersaturated relative to any possible solid phase controls that could exist. Data developed through laboratory and field studies lead us to believe that we can empirically quantify the migration of trace elements, though we were unable to make satisfactory predictions based on this initial attempt at developing a theoretical construct. Other mechanisms (e.g., specific adsorption, ion exchange) besides precipitation/dissolution appear to be controlling the concentrations of many of the trace elements. Additional data must be developed to adequately predict the concentrations of these trace elements. Precipitation/dissolution reactions based on thermodynamic constants are sufficient to explain the effluent concentrations of some elements, while additional mechanisms, for which experimental data must be developed, are necessary for others.

Future work will address the need to develop the necessary thermodynamic adsorption data. These data will be utilized, in conjunction with a solid phase assemblage, to predict the concentrations of many trace elements. Additional work is also necessary to acquire a more complete understanding of the reactions that need to be included in the conceptual model to increase its ability to predict pH and pe. This should allow our solid phase assemblage to predict the concentrations of additional elements (e.g., uranium) and improve the accuracy of predicting Al, Fe, Mn, and Ca.

The concentrations of many trace elements appear to be controlled by adsorption and/or coprecipitation with ferric oxide surfaces. Several adsorption models of the hydrous oxide water surface have been formulated (Davis and Leckie 1978, Hohl and Stumm 1976) and have shown considerable success in modeling the adsorption of trace metals onto hydrous oxides. In addition, stability constants for the reaction of several trace metals with iron oxyhydroxides have also been published in the literature (Davis and Leckie 1978, Leckie et al. 1980, Balistrieri and Murray 1982). Thus, it appears that the conceptual chemical model presented here, which can estimate the mass of precipitated ferric oxide by means of our solid phase assemblage, can be expanded to predict the adsorption of several trace metals onto the surface of iron oxyhydroxides. Table 6 is a summary of important control mechanisms for selected constituents of uranium mill tailings solutions.

TABLE 6. Summary of Important Control Mechanisms

	<u>Solubility</u> <u>Controlling Solid</u>	<u>Surface Adsorption</u> <u>Cation-Anion Exchange</u> <u>Hydrous Oxides</u>	<u>Unknown</u>
Al	X		
Ca	X	X	
SO ₄	X		
Fe	X		
Mn	X	X	
Mg	x(a)	x(a)	
Sr		X	
Si			X
U	X	x(a)	
Se		X	
As	x(a)	X	
Mo		X	
V		X	
Cr	x(a)	X	
Pb		X	
Ni		X	
Ag		X	
Cd		X	
Zn		X	

(a) Mechanism may be important but its importance cannot be determined at this time.

REFERENCES

- Akins, M. B., and R. J. Lewis. 1976. "Chemical Distribution and Gaseous Evolution of Arsenic-74 Added to Soils as DSMA - ⁷⁴As." Soil Sci. Soc. Am. J. 40(5):655-658.
- Artiole, J., and W. H. Fuller. 1979. "Effect of Crushed Limestone Barriers on Chromium Attenuation in Solids." J. Environ. Qual. 8(4):503-510.
- Ball, J. W., D. K. Nordstrom and E. A. Jenne. 1980. Additional and Revised Thermochemical Data and Computer Code for WATEQ2 - A Computerized Chemical Model for Trace and Major Element Speciation and Mineral Equilibria of Natural Waters. U.S. Geologic Survey, Water Resources Investigations WRI-78-116, 109 pp.
- Ball, J. W., E. A. Jenne, and M. W. Cantrell. 1981. WATEQ3: A Geochemical Model with Uranium Added. U.S. Geol. Survey, Open File Report 81-1183.
- Bartlett, R. J., and J. M. Kimble. 1976a. "Behavior of Chromium in Soils: I. Trivalent Forms." J. Environ. Qual. 5(4):379-383.
- Bartlett, R. J., and J. M. Kimble. 1976b. "Behavior of Chromium in Soils: II. Hexavalent Forms." J. Environ. Qual. 5(4):383-386.
- Bartlett, R., and B. James. 1979. "Behavior of Chromium in Soils: III. Oxidation." J. Environ. Qual. 8(1):31-35.
- Balistrieri, L. S. and J. W. Murray. 1982. "The Adsorption of Cu, Pb, Zn, and Cd on Goethite from Major Ion Seawater." Geochimica et Cosmochimica Acta 46:1253-1265.
- Black, C. A. 1965a. Methods of Soil Analysis. Part 1. Physical and Mineralogical Properties Including Statistics of Measurement and Sampling. American Society of Agronomy, Monograph 9.
- Black, C. A. 1965b. Methods of Soil Analysis. Part. 2. Chemical and Microbiological Properties. American Society of Agronomy, Monograph 9.
- Braman, R. S. 1975. "Arsenic in the Environment." In Arsenical Pesticides, pp. 108-123. ACS Symposium Series No. 7. American Chemical Society, Washington, D.C.
- Breeman, N. Van. 1973. "Dissolved Aluminum in Acid Sulfate Soils and in Acid Mine Waters." Soil Sci. Soc. Am. Proc. 37:694-697.
- Buhler, D. R. 1972. "Environmental Contamination by Heavy Metals." In Heavy Metals in the Environment, pp. 1-35. Oregon State University Water Resources Research Institute. SEMN WR 016.73.

- Cary, E. E., G. A. Wiedzoreck, and W. H. Allaway. 1967. "Reactions of Selenite-Selenium Added to Soils that Produce Low-Selenium Forages." Soil Sci. Soc. Am. Proc. 31:21-26.
- Cary, E. E., W. H. Allaway, and O. E. Olson. 1977. "Control of Chromium Concentrations in Food Plants. 2. Chemistry of Chromium in Soils and Its Availability to Plants." J. Agric. Food Chem. 25(2):305-309.
- Cherry, J. A., A. U. Shaikh, D. E. Tallman, and R. V. Nicholson. 1979. "Arsenic Species as an Indicator of Redox Conditions in Groundwater." Journal of Hydrology 43:373-392.
- Davies, C. W. 1962. Ion Association. Butterworths Pub., Washington, D.C., 190 pp.
- Davis, J. A. and J. O. Leckie. 1978. "Surface Ionization and Complexation at the Oxide/Water Interface: II. Surface Properties of Amorphous Iron Oxyhydroxide and Adsorption of Metal Ions." J. Colloid Interface Sci. 67:90-107.
- Deutsch, W. J., E. A. Jenne, and K. M. Krupka. 1982. "Solubility Equilibria in Basalt Aquifers: The Columbia Plateau, Eastern Washington, U.S.A." Chemical Geology 36:15-34.
- Durfor, C. N., and E. Becker. 1964. Public Water Supplies of the 100 Largest Cities in the United States, 1962. U.S. Geol. Surv. Water-Supply Paper 1812, 384 pp.
- Durum, W. H., and H. Haffty. 1963. "Implications of the Minor Element Content of Some Major Streams of the World." Geochimica et Cosmochimica Acta 27:1-14.
- Erikson, R. J., and D. R. Sherwood. 1982. "Interaction of Acidic Leachate with Soil Minerals at Lucky Mc Pathfinder Mill, Gas Hills, Wyoming. In Proceedings of the Fifth Symposium on Uranium Mill Tailings Management. Civil Engr. Dept. Colorado State University, Ft. Collins, Colorado.
- Evans, H. T. and R. M. Garrels. 1958. "Thermodynamic Equilibria of Vanadium in Aqueous Systems as Applied to the Interpretation of Colorado Plateau Ore Deposits." Geochimica et Cosmochimica Acta 15:131-149.
- Felmy, A. R., D. C. Girvin, and E. A. Jenne. 1983. MINTEQ: A Computer Program for Calculating Aqueous Geochemical Equilibria, EPA-68-03-3089 (Draft).
- Fey, M. V., and J. B. Dixon. 1981. "Synthesis and Properties of Poorly Crystalline Hydrated Aluminum Goethites." Clays and Clay Minerals 29(2):91-100.

- Ford, Bacon and Davis Utah Inc. 1977a. Phase II - Title I Engineering Assessment of Inactive Uranium Mill Tailings, Durango Site, Durango, Colorado. GJT-6, National Technical Information Service, Springfield, Virginia.
- Ford, Bacon and Davis Utah Inc. 1977b. Phase II - Title I Engineering Assessment of Inactive Uranium Mill Tailings, Falls City Site, Falls City, Texas. GJT-16, National Technical Information Service, Springfield, Virginia.
- Ford, Bacon and Davis Utah Inc. 1977c. Phase II - Title I Engineering Assessment of Inactive Uranium Mill Tailings, Grand Junction Site, Grand Junction, Colorado. GJT-9, National Technical Information Service, Springfield, Virginia.
- Ford, Bacon and Davis Utah Inc. 1977d. Phase II - Title I Engineering Assessment of Inactive Uranium Mill Tailings, Green River Site, Green River, Utah. GJT-1, National Technical Information Service, Springfield, Virginia.
- Ford, Bacon and Davis Utah Inc. 1977e. Phase II - Title I Engineering Assessment of Inactive Uranium Mill Tailings, Lowman Site, Lowman, Idaho. GJT-17, National Technical Information Service, Springfield, Virginia.
- Ford, Bacon and Davis Utah Inc. 1977f. Phase II - Title I Engineering Assessment of Inactive Uranium Mill Tailings, Phillips/United Nuclear Site, Ambrosia Lake, New Mexico. GJT-13, National Technical Information Service, Springfield, Virginia.
- Ford, Bacon and Davis Utah Inc. 1977g. Phase II - Title I Engineering Assessment of Inactive Uranium Mill Tailings, Riverton Site, Riverton, Wyoming. GJT-19, National Technical Information Service, Springfield, Virginia.
- Ford, Bacon and Davis Utah Inc. 1977h. Phase II - Title I Engineering Assessment of Inactive Uranium Mill Tailings, Shiprock Site, Shiprock, New Mexico. GJT-2, National Technical Information Service, Springfield, Virginia.
- Ford, Bacon and Davis Utah Inc. 1977i. Phase II - Title I Engineering Assessment of Inactive Uranium Mill Tailings, Slick Rock Site, Slick Rock, Colorado. GJT-7, National Technical Information Service, Springfield, Virginia.
- Ford, Bacon and Davis Utah Inc. 1977j. Phase II - Title I Engineering Assessment of Inactive Uranium Mill Tailings, Tuba City Site, Tuba City, Arizona. GJT-5, National Technical Information Service, Springfield, Virginia.
- Fournier, R. O. 1973. "Silica in Thermal Waters: Laboratory and Field Investigations." In Proceedings of Symposium on Hydrogeochemistry and Biogeochemistry, Volume I-Hydrogeochemistry, Tokyo, Japan, September 7-9, 1970, The Clarke Company, Washington, D.C.

- Frost, R. R., and R. A. Griffin. 1977. "Effect of pH on Adsorption of Arsenic and Selenium from Landfill Leachate by Clay Minerals." Soil Sci. Soc. Am. J. 41:53-57.
- FWPCA. 1968. Report of the Committee on Water Quality Criteria. Fed. Water Pollut. Contr. Admin., U.S. Dept. of Interior.
- Gang, M. W., and D. Langmuir. 1974. "Controls on Heavy Metals in Surface and Ground Waters Affected by Coal Mine Drainage: Clarion River - Redbank Creek Watershed, Pennsylvania." In Proceedings of Fifth Symposium on Mine Drainage Research, pp. 39-63. Coal and the Environment Technical Conference, October 22-24.
- Garland, G. A., and D. C. Mosher. 1975. "Leachate Effects from Improper Land Disposal." Waste Age 6:42-48.
- Gee, G. W., A. C. Campbell, D. R. Sherwood, R. G. Strickert, and S. J. Phillips. 1980. Interaction of Uranium Mill Tailings Leachate with Soils and Clay Liners. NUREG/CR-1494, National Technical Information Service, Springfield, Virginia.
- Geering, H. R., E. E. Car, L. H. P. Jones, and W. H. Allaway. 1968. "Solubility and Redox Criteria for the Possible Forms of Selenium in Soils." Soil Sci. Soc. Am. Proc. 32:35-40.
- Griffin, R. A., A. K. Au, and R. R. Frost. 1977. "Effect of pH on Adsorption of Chromium from Landfill-Leachate by Clay Minerals." J. Environ. Sci. Health A12(8):431-449.
- Grove, J. H., and B. G. Ellis. 1980. "Extractable Iron and Manganese as Related to Soil pH and Applied Chromium." Soil Sci. Soc. Am. J. 44:243-246.
- Gulledge, J. H., and J. T. O'Connor. 1973. "Removal of Arsenic(V) from Water by Adsorption on Aluminum and Ferric Hydroxides." JAWWA 65(8):548-552.
- Harvie, C. E., and J. H. Weare. 1980. "The Prediction of Mineral Solubilities in Natural Waters: the Na-K-Mg-Ca-Cl-SO₄-H₂O System from Zero to High Concentration at 25°C." Geochimica et Cosmochimica Acta 44:981-987.
- Hem, J. D., C. E. Roberson, C. J. Lind, and W. L. Polzer. 1973. Chemical Interactions of Aluminum with Aqueous Silica at 25°C. Geological Survey Water-Supply Paper 1827-E.
- Hem, J. D. 1977. "Reactions of Heavy Metals at Surfaces of Hydrous Iron Oxide." Geochimica et Cosmochimica Acta 41:527-538.
- Hingston, F. J., R. J. Atkinson, A. M. Posner, and J. P. Quirk. 1967. "Specific Adsorption of Anions." Nature 215:1459-1461.

- Hingston, F. J., R. J. Atkinson, A. M. Posner, and J. P. Quirk. 1968. "Specific Adsorption of Anions on Goethite." Transactions at the 9th International Congress of Soil Science 1:669-678.
- Hohl, H. and W. Stumm. 1976. "Interaction of Pb^{2+} with Hydrated $\gamma-Al_2O_3$." Journal of Colloid and Interface Science 55(2):281-288.
- Hounslow, A. W. 1980. "Ground-Water Geochemistry: Arsenic in Landfills." Groundwater 18(4):331-333.
- Howard, J. R., III. 1977. "Geochemistry of Selenium: Formation of Ferroselite and Selenium Behavior in the Vicinity of Oxidizing Sulfide and Uranium Deposits." Geochimica et Cosmochimica Acta 41:1665-1678.
- Jacobs, L. W., L. M. Walsh, and D. R. Keeney. 1970. "Arsenic Residue Toxicity to Vegetable Crops Grown on Plainfield Sand." Agron. J. 62:588-591.
- Jenne, E. A. 1977. "Trace Element Sorption by Sediments and Soil-Sites and Processes." p. 425-553. In Symposium on Molybdenum in the Environment, Volume 2, W. Chappel and K. Peterson (eds), M. Dekker, Inc., NY.
- Jenne, E. A., J. W. Ball, J. M. Burchard, D. V. Vivit, and J. H. Parks. 1980. "Geochemical Modeling: Apparent Solubility Controls on Ba, Zn, Cd, Pb, and F in Waters of the Missouri Tri-State Mining Area." In Trace Substances in Environmental Health-XIV, D. D. Hemphill, ed., University of Missouri.
- Johnson, K. S. 1982. "Solubility of Rhodochrosite ($MnCO_3$) in Water and Seawater." Geochimica et Cosmochimica Acta 46:1805-1809.
- Kaback, D. J., and D. D. Runnells. 1980. "Geochemistry of Molybdenum in Some Stream Sediments and Waters." Geochimica et Cosmochimica Acta 44:447-456.
- Karimian, N., and F. R. Fox. 1978. "Adsorption and Extractability of Molybdenum." Soil Sci. Soc. Am. J. 46:757-760.
- Lakin, H. W. 1961. Geochemistry of Selenium in Relation to Agriculture. Selenium in Agriculture. Agr. Handbook 200. USDA.
- Langmuir, D. 1969. "The Gibbs Free Energies of Substances in the System $Fe-O_2-H_2O-CO_2$ at 25°C." U.S. Geological Survey, Prof. Paper 650-B:B180-B184.
- Langmuir, D. 1971. "Particle Size Effect on the Reaction Goethite = Hematite and Water." Am. J. Sci. 271:147-156.
- Langmuir, D., and D. O. Whittemore. 1971. "Variations in the Stability of Precipitated Ferric Oxyhydroxides." In Nonequilibrium Systems in Natural Waters, ed. J. D. Hem, pp. 209-234, Adv. in Chem. Series No. 106, Am. Chem. Soc., Washington, D.C.

- Latimer, W. M. 1952. The Oxidation States of the Elements and Their Potentials in Aqueous Solutions. 2nd Ed. Prentice-Hall, Inc., Englewood Cliffs, New Jersey.
- Leckie, J. O., M. M. Benjamin, K. Hayes, G. Kaufman, and S. Altman. 1980. Adsorption/Coprecipitation of Trace Elements from Water with Iron Oxyhydroxide. EPRI CS-1513 Project 910-1. Edison Power Research Institute, Palo Alto, California.
- LeGrande, G. R., and D. D. Runnels. 1975. "Removal of Dissolved Molybdenum from Wastewaters by Precipitates of Ferric Iron." Environmental Science and Technology 9(8):744-749.
- Lindsay, W. L. 1979. Chemical Equilibria in Soils. John Wiley and Sons, New York, New York.
- Matzat, E., and K. Shirak. 1978. "Chromium." In Handbook of Geochemistry. Springer-Verlog, Heidelberg, Chapter 24.
- May, H. M., P. A. Helmke, and M. L. Jackson. 1979. "Gibbsite Solubility and Thermodynamic Properties of Hydroxy-Aluminum Ions in Aqueous Solution at 25°C." Geochimica et Cosmochimica Acta 43:861-868.
- Mayer, L. M., and L. L. Schick. 1981. "Removal of Hexavalent Chromium from Estuarine Waters by Model Substrates and Natural Sediments." Environmental Science and Technology 15(12):1482-1484.
- Means, J. L., D. A. Crerar, M. P. Boresik, and S. O. Duguid. 1978. "Adsorption of Co and Selected Actinides by Mn and Fe Oxides in Soils and Sediments." Geochimica et Cosmochimica Acta 42:1763-1773.
- Morey, G. W., R. O. Fournier, and J. J. Rowe. 1964. "The Solubility of Amorphous Silica at 25°C." Journal of Geophysical Research 69(10):1995-2002.
- Murray, J. W. 1979. "Iron Oxides," Chapter in Mineralogical Society of America, Short Course Notes, Volume 6, November 1979, pp. 47-99, Roger G. Burns (ed.).
- Nakayama, E., T. Kuwamoto, H. Tokoro, and T. Fujinaya. 1981. "Chemical Speciation of Chromium in Sea Water. Part 3. The Determination of Chromium Species." Analytica Chimica Acta 131:247-254.
- Nordstrom, D. K., E. A. Jenne, and J. W. Ball. 1979. "Redox Equilibria of Iron in Acid Mine Waters." In Chemical Modeling in Aqueous Systems. E. A. Jenne (ed.), ACS Symposium Series No. 93:51-79.
- Nordstrom, D. K. 1982. "The Effect of Sulfate on Aluminum Concentrations in Natural Waters: Some Stability Relations in the System $Al_2O_3-SO_3-H_2O$ at 298 K." Geochimica et Cosmochimica Acta 46:681-692.

- Parkhurst, D. L., D. C. Thorstenson, and L. N. Plummer. 1980. PHREEQE - A Computer Program for Geochemical Calculations. U.S. Geological Survey, Water Resources Investigations 80-96, 210 pp.
- Pasricha, N. S., and N. S. Randhawa. 1977. "Molybdenum Adsorption by Soils as Influenced by Different Cations." Agrochimica XXI:105-113.
- Peterson, S. R., and K. M. Krupka. 1981. "Contact of Clay Liner Materials with Acidic Tailings Solution. II. Geochemical Modeling." In Uranium Mill Tailings Management, Proceedings of the Fourth Symposium on Uranium Mill Tailings Management, Colorado State University, Fort Collins, Colorado, pp. 609-626, October 26-27.
- Peterson, S. R., R. L. Erikson, and G. W. Gee. 1982. The Long Term Stability of Earthen Materials in Contact with Acidic Tailings Solutions. NUREG/CR-2946 (PNL-4463), Pacific Northwest Laboratory, Richland, Washington.
- Plotnikov, V. I., and I. I. Safonov. 1979. "Radiochemical Investigation of the Coprecipitation of Microquantities of Certain Hydrolyzable Elements with Metal Hydroxides and Oxides VI, Coprecipitation of Chromium (III)." Radiokhimiya 21(3):355-359.
- Reisenauer, H. M., A. A. Tabikh, and P. R. Stout. 1962. "Molybdenum Reactions with Soils and the Hydrous Oxides of Iron, Aluminum, and Titanium." Soil Sci. Soc. Am. Proc. 26:23-27.
- Relyea, J. F., and W. J. Martin. 1982. "Evaluation of Inactive Uranium Mill Tailings Sites for Liner Requirements: Characterization and Interaction of Tailings, Soil and Liner Materials." Proceedings of the Fifth Symposium on Uranium Mill Tailings Management. Civil Engr. Dept., Colo. State University, Ft. Collins, Colorado.
- Rosenfeld, I., and O. A. Beath. 1964. Selenium: Geobotany, Biochemistry, Toxicity, and Nutrition. 411 pp. Academic Press.
- Sadiq, N., and W. L. Lindsey. 1979. Selection of Standard Free Energies of Formation for Use in Soil Chemistry. Colorado State University Experimental Station, Technical Bulletin 134, Ft. Collins, Colorado.
- Schwertmann, U., and H. Thalmann. 1976. "The Influence of Fe(II), Si and pH on the Formation of Lepidocrocite and Ferrihydrite During Oxidation of Aqueous FeCl₂ Solutions." Clay Minerals 11:184-204.
- Serne, R. J., S. R. Peterson, and G. W. Gee. 1983. Laboratory Measurements of Contaminant Attenuation of Uranium Mill Tailings Leachates by Sediments and Clay Liners. NUREG/CR-3124 (PNL-4605), Pacific Northwest Laboratory, Richland, Washington.
- Sillen, L. G., and A. E. Martell. 1964. "Stability Constants of Metal-Ion Complexes." Special Publication No. 17, The Chemical Society, London.

- Singh, S. S. 1974. "The Solubility Product of Gibbsite at 15°, 25°, and 35°C." Soil Sci. Soc. Amer. Proc. 38:415-417.
- Singh, S. S. 1976. "Chemical Equilibrium and Chemical Thermodynamic Properties of Gibbsite." Soil Science 121(6):332-336.
- Singh, M., N. Singh, and P. S. Relan. 1981. "Adsorption and Desorption of Selenite and Selenate Selenium on Different Soils." Soil Science 132(2):134-141.
- Taylor, R. M., and J. B. Giles. 1970. "The Association of Vanadium and Molybdenum with Iron Oxides in Soils." J. Soil Sci. 21(2):203-215.
- Theis, T. L., and R. O. Richter. 1979. "Chemical Speciation of Heavy Metals in Power Plant Ash Pond Leachate." Environ. Sci. Tech. 13(2):219-224.
- Theng, B. K. G. 1971. "Adsorption of Molybdate by Some Crystalline and Amorphous Soil Clays." New Zealand Journal of Science 14:1040-1056.
- Truesdell, A. H., and B. F. Jones. 1974. "WATEQ, A Computer Program for Calculating Chemical Equilibria of Natural Waters." U.S. Geol. Survey J. Res. 2:233-274.
- Udy, M. J. 1956. Chromium: Chemistry of Chromium and Its Compounds. Vol. 1, Reinhold Pub. Corp., New York.
- U.S. Environmental Protection Agency. 1978. Hazardous Waste. Proposed Guidelines and Regulations and Proposal on Identification and Listing Federal Register. 43(243):58946-59026.
- U.S. Environmental Protection Agency. 1980. Draft Environmental Impact Statement for Remedial Action Standards for Inactive Uranium Processing Sites. EPA 520/4-80-011 (40 CFR 192).
- U.S. Nuclear Regulatory Commission (USNRC). 1979. Final Environmental Statement Related to Operation of Morton Ranch Uranium Mill, United Nuclear Corporation. NUREG-0532, National Technical Information Service, Springfield, Virginia.
- Vlek, P. L. G., and W. L. Lindsay. 1977. "Thermodynamic Stability and Solubility of Molybdenum Minerals in Soils." Soil Sci. Soc. Am. J. 41:42-46.
- Wada, K., and H. Kubo. 1975. "Precipitation of Amorphous Aluminosilicates from Solutions Containing Monomeric Silica and Aluminum Ions." Journal of Soil Science 26(2):100-111.
- Wageman, R. 1978. "Some Theoretical Aspects of Stability and Solubility of Inorganic Arsenic in the Freshwater Environment." Water Research 12:139-145.

- Wagner, S. L. 1972. "Arsenic and Cadmium in the Environment." In Heavy Metals in the Environment, pp. 45-57. Oregon State University Water Resources Research Institute. SEMN WR 016.73.
- Weswig, P. H. 1972. "Selenium in the Environment." In Heavy Metals in the Environment, pp. 183-203, Oregon State University Water Resources Research Institute, SEMN WR 016.73.
- Westall, J. C., J. L. Zachary, and F. M. M. Morel. 1976. MINEQL: A Computer Program for the Calculation of Chemical Equilibrium Composition of Aqueous Systems. Tech. Note 18, Dept. Civil Eng., Massachusetts Institute of Technology, Cambridge, Massachusetts.
- Yates, D. E., S. Levine, and T. W. Healy. 1974. "Site-Binding Model of the Electrical Double Layer at the Oxide/Water Interface." Chem. Soc. Faraday. 70:1807-1818.



APPENDIX A

TABLE A.1. Chemical Analyses of Effluent Solutions from Permeability Column 1 (mg/l)

Constituents	Pore Volume					
	1.26	2.12	2.95	4.47	5.84	25.51
Li	DL	DL	0.2	0.3	0.5	DL
B	ND ^(b)	ND	ND	ND	ND	ND
HCO ₃ /CO ₃	ND	ND	ND	0.0 ^(c)	0.0	0.0
NO ₃	ND	ND	ND	ND	ND	ND
F	ND	ND	ND	ND	ND	ND
Na	229	248	315	364	415	334
Mg	360	405	689	1040	1,127	813
Al	DL ^(a)	DL	DL	29	193	958
Si	7.2	7.2	6.8	27.8	45	51
P	DL	DL	DL	7.2	9.8	3.8
SO ₄	2,445	2,690	3,833	7,147	7,984	12,200
Cl	121	97	88	100	97	100
K	ND	ND	ND	ND	ND	ND
Ca	686	703	715	660	600	517
V	ND	ND	ND	ND	ND	ND
Cr	DL	DL	DL	0.2	0.02	0.2
Mn	0.2	1.4	4.2	7.0	8.2	4.5
Fe	DL	DL	DL	645	1582	1510
Co	ND	ND	ND	ND	ND	ND
Ni	DL	DL	1.4	4.3	5.6	2.5
Cu	0.02	DL	0.5	DL	0.2	0.2
Zn	0.5	DL	3.2	7.7	7.8	11.1
As	DL	DL	DL	0.5	3.1	DL
Se	DL	DL	DL	0.8	DL	1.1
Sr	14	16	27	30	27	3.9
Mo	DL	DL	DL	DL	DL	DL
Cd	DL	DL	DL	0.4	1.1	0.7
Sb	ND	ND	ND	ND	ND	ND
Ba	ND	ND	ND	ND	ND	ND
La	ND	ND	ND	ND	ND	ND
Pb	DL	DL	DL	1.2	DL	3.0
U	DL	DL	DL	23.1	DL	DL
pH (units)	7.72	7.75	7.80	4.02	3.82	3.35
Eh (mv)	348	346	343	581	593	623

(a) DL - less than detection limit.

(b) ND - not determined.

(c) By definition HCO₃/CO₃ = 0.0 when pH < 4.3.

TABLE A.2. Chemical Analyses of Effluent Solutions from Permeability Column 5 (mg/l)

Constituents	Pore Volume							
	1.35	3.46	5.54	6.24	7.91	8.89	10.39	11.17
Li	DL ^(a)	0.4	1.2	1.0	1.1	1.4	1.4	1.3
B	ND ^(b)	ND	ND	ND	ND	ND	ND	ND
HCO ₃ /CO ₃	ND	ND	ND	0.0 ^(c)	0.0	0.0	0.0	0.0
NO ₃	ND	ND	ND	ND	ND	ND	ND	ND
F	ND	ND	ND	ND	ND	ND	ND	ND
Na	158	283	424	308	296	332	329	319
Mg	203	519	1,420	1,554	1,771	1,738	1,601	1,420
Al	DL	DL	DL	47	167	392	564	703
Si	3.2	7.2	15.2	23.2	28.8	40	43	45
P	DL	DL	1.5	2.1	2.1	3.0	3.8	3.8
SO ₄	2,220	3,704	7,864	9,492	12,192	13,900	14,800	10,100
Cl	132	292	402	303	306	389	355	333
K	ND	ND	ND	ND	ND	ND	ND	ND
Ca	657	612	820	512	467	507	528	517
V	ND	ND	ND	ND	ND	ND	ND	ND
Cr	DL	DL	0.08	0.1	0.1	0.5	0.5	0.5
Mn	DL	2.4	41.2	64.4	89.6	101	101	96
Fe	DL	DL	127	538	950	1,330	1,560	1,720
Co	ND	ND	ND	ND	ND	ND	ND	ND
Ni	0.2	0.5	4.1	0.8	10.9	12.9	12.4	10.8
Cu	DL	DL	0.09	0.1	0.2	0.2	0.3	0.3
Zn	0.5	0.7	9.1	15	21	29.5	31.8	29.5
As	DL	DL	DL	0.6	0.7	DL	DL	DL
Se	DL	DL	DL	DL	DL	1.6	2.1	2.1
Sr	14	19	38	32	31	31	25	19
Mo	DL	DL	DL	DL	DL	DL	DL	DL
Cd	DL	DL	0.2	0.4	0.9	0.8	1.0	1.0
Sb	ND	ND	ND	ND	ND	ND	ND	ND
Ba	ND	ND	ND	ND	ND	ND	ND	ND
La	ND	ND	ND	ND	ND	ND	ND	ND
Pb	DL	DL	DL	DL	0.5	2	2	2
U	0.4	0.6	DL	DL	DL	19.7	23.8	27.2
pH (units)	8.20	8.00	4.80	4.20	3.80	3.53	3.70	3.42
Eh (mv)	318	331	532	570	594	612	601	618

(a) DL - less than detection limit.

(b) ND - not determined.

(c) By definition HCO₃/CO₃ = 0.0 when pH < 4.3.

TABLE A.3. Chemical Analyses of Effluent Solutions from Permeability Column 8 (mg/l)

Constituents	Pore Volume						
	0.84	1.75	2.59	3.24	4.03	8.77	10.55
Li	DL	0.3	0.7	0.6	1.0	1.3	1.2
B	ND	ND	ND	ND	ND	ND	ND
HCO ₃ /CO ₃	ND	ND	ND	ND	ND	0.0	0.0
NO ₃	ND	ND	ND	ND	ND	ND	ND
F	ND	ND	ND	ND	ND	ND	ND
Na	85	218	308	310	314	300	291
Mg	89	473	781	1,099	1,467	1,147	1,018
Al	DL	DL	5.5	DL	93	976	1,061
Si	6.4	12.3	17.0	15.2	39	104	158
P	DL	DL	7.8	1.5	0.9	0.6	1.2
SO ₄	783	3,793	4,518	5,752	8,492	13,700	13,972
Cl	52	216	347	326	296	303	306
K	ND	ND	ND	ND	ND	ND	ND
Ca	306	1,577	904	800	546	480	500
V	ND	ND	ND	ND	ND	ND	ND
Cr	0.01	DL	0.1	DL	0.12	1.0	1.6
Mn	0.04	0.3	7.6	32.8	62.7	75.6	74
Fe	DL	DL	0.1	1.2	146	90	112
Co	ND	ND	ND	ND	ND	ND	ND
Ni	0.09	DL	0.6	1.4	3.6	5.0	4.1
Cu	0.04	0.1	0.02	0.04	0.2	1.3	2.7
Zn	0.7	0.4	0.5	3.2	9.5	14	14
As	DL	DL	0.7	DL	1.0	5.7	7.2
Se	DL	DL	0.9	DL	DL	DL	DL
Sr	5.3	25	22	26	27	15	12
Mo	DL	DL	0.2	DL	DL	DL	DL
Cd	DL	DL	DL	0.04	0.2	0.2	0.2
Sb	ND	ND	ND	ND	ND	ND	ND
Ba	ND	ND	ND	ND	ND	ND	ND
La	ND	ND	ND	ND	ND	ND	ND
Pb	0.2	DL	0.5	DL	DL	DL	DL
U	2.1	6.8	4.4	DL	DL	DL	DL
pH (units)	7.95	8.10	8.10	5.80	4.40	3.70	3.00
Eh (mv)	5.64	5.47	5.47	7.92	9.41	10.15	10.90

(a) DL - less than detection limit.
 (b) ND - not determined.
 (c) By definition HCO₃/CO₃ = 0.0 when pH < 4.3.

TABLE A.4. Chemical Analyses of Effluent Solutions from Vacuum Extractor Columns 1-6 (mg/l)

Constituents	Pore Volume										
	1.36	3.04	4.04	5.19	6.28	7.66	9.21	10.43	11.75	13.21	16.05
Li	0.28	0.91	1.0	1.1	0.92	0.79	0.66	0.32	0.37	0.24	0.20
B	0.12	0.11	0.30	0.58	0.52	0.52	0.42	0.28	0.20	0.18	0.12
HCO ₃ /CO ₃	ND ^(a)	ND	ND	ND	ND	0.0 ^(b)	0.0 ^(b)	0.0 ^(b)	0.0 ^(b)	0.0 ^(b)	0.0 ^(b)
NO ₃	43.6	25.0	28.2	28.2	32.0	33.8	31.2	26.2	ND	23.8	25.0
F	4.0	3.8	9	9	7.8	13.4	5.6	3.2	ND	2.2	1.8
Na	174	451	439	481	462	388	352	136	90	76	74
Mg	307	409	1,260	1,320	1,010	765	584	290	186	160	112
Al	0.20	0.05	0.29	23.1	46.6	171	444	250	147	128	91
Si	15.2	13.3	17.7	27.0	59.7	106	126	108	89	89	76
P	0.81	<0.5	<0.5	<0.5	<0.5	<0.5	<0.5	1.1	<0.5	<0.5	<0.5
SO ₄	2,600	3,400	6,540	7,400	7,880	8,480	8,480	4,540	3,880	2,780	2,420
Cl	320	280	320	320	320	320	220	92	66	58	56
K	122	74.8	160	211	112	36.4	11.6	6.5	10.8	4.9	3.0
Ca	913	830	607	534	503	466	482	514	483	566	554
V	<0.1	<0.1	<0.1	<0.1	<0.1	<0.1	<0.1	<0.1	ND	<0.1	<0.1
Cr	<0.06	<0.06	<0.06	<0.06	<0.06	0.11	0.12	0.08	ND	0.06	<0.06
Mn	0.42	1.78	4.50	44.5	130	72.8	53.6	25.4	15.6	13.5	9.6
Fe	0.16	<0.10	14.7	108.2	852	1,266	948	466	236 ^(c)	256	192
Co	<0.1	<0.1	0.2	1.0	6.9	4.1	2.1	1.0	0.7	0.6	0.4
Ni	<0.2	<0.2	0.18	1.45	11.8	7.5	3.7	1.7	1.0	0.8	0.6
Cu	0.02	0.01	0.02	0.07	0.23	0.43	0.78	0.76	0.62	0.64	0.59
Zn	1.88	0.29	0.78	2.74	20.9	17.8	9.2	4.1	2.6	2.5	1.8
As	<0.1	<0.1	<0.1	<0.1	<0.1	<0.1	0.31	0.15	ND	0.10	<0.10
Se	1.57	0.42	0.73	0.97	1.05	1.43	1.04	0.35	ND	0.23	0.22
Sr	16.3	17.8	30.9	29.3	18.1	11.9	9.1	6.1	4.9	5.0	4.6
Mo	0.28	<0.06	<0.06	<0.06	<0.06	<0.06	0.06	<0.06	<0.06 ^(c)	<0.06	<0.06
Cd	<0.02	<0.02	<0.02	0.024	0.218	0.276	0.068	0.026	ND	<0.02	<0.02
Sb	<0.5	<0.5	<0.5	<0.5	<0.5	0.6	0.9	0.8	0.5	0.6	<0.5
Ba	0.17	0.11	0.09	0.07	0.10	0.09	0.10	0.08	0.07	0.08	0.05
La	7.7	7.2	5.4	4.9	4.7	5.4	6.4	5.4	0.71	5.5	5.0
Pb	<0.04	<0.04	<0.04	<0.04	<0.04	<0.04	0.07	0.05	ND	0.04	0.04
U	0.17	0.15	0.09	0.40	0.82	1.16	3.80	3.60	ND	1.90	2.20
pH (units)	7.86	7.79	7.33	6.51	4.72	4.22	3.95	3.94	3.95	3.96	3.97
Eh (mv)	+421	+418	+165	+254	+439	+459	+470	+455	+453	+442	+441
Radionuclides (cms/ml)											
⁵¹ Cr	DL ^(b)	DL	DL	DL	0.132	1.12	0.277	0.165	0.092	0.086	0.046
⁵⁴ Mn	DL	1.319	3.38	36.72	112.5	67.236	47.626	23.36	14.266	17.714	28.187
⁵⁹ Fe	DL	DL	0.016	0.115	0.832	1.703	1.377	0.655	0.374	0.333	0.317
⁷³ As	DL	DL	DL	DL	DL	DL	DL	DL	DL	DL	DL
⁷⁵ Se	0.514	0.269	0.408	0.530	0.653	1.061	1.273	0.832	0.751	0.840	0.922
^{110m} Ag	DL	DL	DL	DL	DL	DL	DL	DL	DL	DL	DL
¹⁰⁹ Cd	DL	0.016	0.265	0.722	7.22	11.11	6.616	2.727	1.564	1.885	2.807
²¹⁰ Pb	DL	DL	DL	DL	DL	DL	DL	DL	DL	DL	DL

(a) ND - not determined.

(b) Not measured but by definition = 0 as pH < 4.3.

(c) Analysis reported was obtained on ICP but atomic absorption/graphite furnace is preferred method.

(d) DL - activity was below detection limit as determined by PEAK SEARCH® Nuclear Data, Inc., Schaumburg, IL 60196, December 22, 1978 version.

TABLE A.5. Chemical Analyses of Effluent Solutions from Vacuum Extractor Columns 8-12 (mg/l)

Constituents	Cumulative Pore Volume						
	1.91	4.06	4.70	5.37	6.11	6.80	7.59
Li	0.60	0.94	0.81	0.80	0.35	0.26	0.28
B	0.10	0.44	0.54	0.51	0.29	0.26	0.27
HCO ₃ /CO ₃	ND ^(a)	ND	ND	ND	ND	ND	ND
NO ₃	26.2	28.8	23.8	ND	21.2	22.6	22.6
F	3.8	9.4	8.0	ND	3.6	2.8	2.4
Na	360	390	315	205	106	80	76
Mg	296	1,354	1,133	758	456	345	287
Al	0.9	1.0	0.6	2.3	0.9	2.8	2.9
Si	14.3	17.1	19.8	27.6	31.7	40.1	39.5
P	<0.5	<0.5	<0.5	<0.5	<0.5	<0.5	<0.5
SO ₄	2,960	7,980	6,780	5,860	4,060	3,460	3,220
Cl	300	260	170	84	66	66	66
K	67	183	171	116	63	39	27
Ca	868	558	494	486	468	505	526
V	<0.10	<0.10	<0.1	<0.1	<0.1	<0.1	<0.1
Cr	<0.06	<0.06	<0.06	ND	<0.06	<0.06	<0.06
Mn	1.94	12.6	36.2	67.2	69.2	49.8	29.2
Fe	9.6	12.3	46.4	93.9 ^(c)	155	202	226
Co	0.22	0.46	0.94	2.1	2.6	3.20	3.48
Ni	0.24	0.44	1.35	3.1	4.0	5.1	5.75
Cu	0.12	0.10	0.07	0.08	0.05	0.07	0.08
Zn	0.56	1.02	2.17	4.70	6.02	7.83	9.36
As	<0.10	<0.1	<0.1	ND	<0.1	<0.1	<0.10
Se	0.60	1.06	0.78	ND	0.20	0.19	0.21
Sr	15.2	30.2	25.2	16.2	10.1	8.3	7.5
Mo	0.07	<0.06	<0.06	<0.06 ^(c)	<0.06	<0.06	<0.06
Cd	<0.02	<0.02	0.024	ND	0.07	0.11	0.07
Sb	0.6	<0.5	<0.5	<0.5	<0.5	0.50	<0.5
Ba	0.16	0.10	0.09	0.09	0.08	0.09	0.08
La	7.7	5.14	4.4	4.10	4.2	4.4	4.5
Pb	<0.04	<0.04	<0.04	ND	<0.04	<0.04	<0.04
U	0.19	0.09	0.04	ND	0.05	0.02	0.002
pH (units)	7.49	7.30	7.16	6.77	6.23	5.02	4.68
Eh (mv)	+211	+268	+161	+150	+234	+369	+404
<u>Radionuclides (cps/ml)</u>							
⁵¹ Cr	DL ^(b)	DL	DL	DL	DL	DL	DL
⁵⁴ Mn	1.349	8.943	29.166	55.543	62.805	43.316	24.912
⁵⁹ Fe	DL	0.005	0.061	0.122	0.155	0.164	0.209
⁷³ As	DL	DL	DL	DL	DL	DL	DL
⁷⁵ Se	0.302	0.498	0.457	0.726	0.783	0.767	0.849
^{110m} Ag	DL	DL	DL	DL	DL	DL	DL
¹⁰⁹ Cd	0.100	0.132	0.724	1.169	1.870	2.338	2.734
²¹⁰ Pb	DL	DL	DL	DL	DL	DL	DL

(a) ND - not determined.

(b) DL - activity was below detection limit as determined by PEAK SEARCH® Nuclear Data, Inc., Schaumburg, IL 60196, December 22, 1978 version.

(c) Analysis reported was obtained on ICP but atomic absorption/graphite furnace is preferred method.

TABLE A.6. Chemical Analyses of Effluent Solutions from Vacuum Extractor Columns 15-18 (mg/l)

Constituents	Cumulative Pore Volume					
	0.47	1.85	2.36	2.87	3.33	3.85
Li	0.26	0.43	0.86	1.70	0.97	0.66
B	0.04	0.03	0.06	0.48	0.38	0.23
HCO ₃ /CO ₃	ND ^(a)	ND	ND	ND	ND	ND
NO ₃	43.8	26.2	ND	ND	ND	20.0
F	2.4	3.4	ND	ND	ND	6.4
Na	123	466	425	382	342	259
Mg	281	310	306	504	1,080	1,040
Al	<0.3	<0.3	0.44	0.92	0.76	<0.3
Si	18.1	15.3	14.3	15.4	16.0	14.3
P	<0.5	<0.5	<0.5	<0.5	<0.5	<0.5
SO ₄	2,300	3,340	3,820	4,820	6,660	6,120
Cl	380	360	316	242	146	92
K	71	76	62	77	113	142
Ca	877	841	820	759	576	494
V	<0.10	<0.10	ND	ND	ND	<0.1
Cr	<0.06	<0.06	0.06 ^(c)	ND	ND	<0.06
Mn	0.12	0.28	0.22	1.23	0.54	1.18
Fe	0.14	0.09	0.11 ^(c)	0.87 ^(c)	0.38 ^(c)	2.12
Co	<0.1	<0.1	<0.05	0.1	0.09	0.05
Ni	<0.2	<0.2	<0.1	<0.1	<0.1	<0.1
Cu	<0.05	<0.05	0.03 ^(c)	0.08 ^(c)	<0.03 ^(c)	<0.03
Zn	0.57	0.32	0.18	0.25	0.24	0.44
As	<0.10	<0.10	ND	ND	ND	<0.10
Se	1.92	0.60	ND	ND	ND	0.28
Sr	15.0	15.4	15.2	18.2	25.3	24.2
Mo	0.45	0.09	<0.05 ^(c)	<0.05 ^(c)	<0.05 ^(c)	<0.06
Cd	<0.02	<0.02	ND	ND	ND	<0.02
Sb	<0.5	<0.5	<0.3	<0.3	<0.3	0.26
Ba	0.21	0.15	0.14	0.14	0.11	0.08
La	7.2	7.0	0.5	0.5	0.4	4.3
Pb	<0.04	<0.04	ND	ND	ND	<0.04
U	0.06	0.14	ND	ND	ND	0.04
pH (units)	7.58	7.62	7.69	7.57	7.52	7.51
Eh (mv)	+434	+409	401	+324	+373	+270
<u>Radionuclides (cps/ml)</u>						
⁵¹ Cr	DL ^(c)	DL	0.008	DL	DL	DL
⁵⁴ Mn	0.013	0.125	0.082	0.698	0.203	0.700
⁵⁹ Fe	DL	DL	DL	DL	0.009	0.008
⁷³ As	DL	DL	DL	DL	DL	DL
⁷⁵ Se	0.310	0.261	0.441	0.490	0.457	0.384
^{110m} Ag	DL	DL	DL	DL	DL	DL
¹⁰⁹ Cd	DL	DL	DL	DL	0.021	0.026
²¹⁰ Pb	DL	DL	DL	DL	DL	DL

(a) ND - not determined.

(b) DL - activity was below detection limit as determined by PEAK SEARCH® Nuclear Data, Inc., Schaumburg, IL 60196, December 22, 1978 version.

(c) Analysis reported was obtained on ICP but atomic absorption/graphite furnace is preferred method.

APPENDIX B

TABLE B.1. Values of Log AP/K Calculated by MINTEQ for Original and Synthetic Leaching Solutions and Column Experiment 1 (AP = activity product of solid phase components; K = solubility product of solid phase)

Minerals	H. M. Tailings		1/5 Strength	Sythetic	Permeability					
	H. M. Tailings Solution No. 1	Solution No. 2 - Radiotraced No. 1	H. M. Tailings Solution No. 2 - Radiotraced No. 1	Tailings Solution	Column No. 1 P.V. = 1.26	Column No. 1 P.V. = 2.12	Column No. 1 P.V. = 2.95	Column No. 1 P.V. = 4.47	Column No. 1 P.V. = 5.89	Column No. 1 P.V. = 25.51
B-UO ₂ (OH) ₂	-6.791	-6.882	-5.723					-4.050		
Schoepite	-6.661	-6.744	-5.583					-3.911		
Uranophane	-22.971	-22.436	-20.617					-14.902		
Al(OH) ₃ (A)	-8.120	-7.243	-5.371	-7.592				-2.880	-2.608	-3.441
Al(OH) ₃ (C)	-0.153	0.063	0.185	0.046				0.755	1.373	1.574
Alunite	-4.540	-5.950	-3.062					2.844	4.147	3.227
Barite	1.527	-0.879	-1.047							
Bohemite	-6.308	-5.440	-3.570	-5.788				-1.077	-0.804	-1.630
Brucite	-15.371	-14.814	-13.908	-15.014	-3.686	-3.603	-3.306	-10.780	-11.131	-12.263
Celestine	0.128	-0.074	-0.915		0.025	0.103	0.388	0.557	0.427	-0.351
Chalcedony	1.491	1.505	0.796		-0.062	-0.046	-0.081	0.543	0.758	0.832
Sepiolite(c)	-19.182	-18.013	-18.326		-0.455	-0.254	0.246	-12.831	-12.890	-14.940
Ferrihydrite	-3.052	2.633	-0.803	-2.649				1.277	1.269	0.262
Fe ₃ (OH) ₈	-18.833	-15.276	-10.486	-14.422				-2.514	-2.549	-5.590
Fluorite	-7.80	-7.156	-12.629							
Gibbsite(c)	-6.510	-5.633	-3.762	-5.982				-1.270	-0.998	-1.831
Gypsum	0.243	0.304	-0.522	0.312	0.300	0.310	0.377	0.428	0.347	0.308
New Gypsum	-0.005	0.056	-0.0770	0.064	0.052	0.062	0.129	0.180	0.099	0.060
Na-Jarosite	5.253	5.64	7.646	6.017				11.828	12.350	10.821
K-Jarosite	7.650	4.866	7.632					12.303	12.765	11.326
H-Jarosite	6.310	6.262	8.257	6.878				10.652	11.319	10.352
SiO ₂ (A,G1)	0.986	1.000	0.291		-0.567	-0.551	-0.586	0.038	0.253	0.327
SiO ₂ (A,PT)	0.678	0.692	-0.017		-0.875	-0.859	-0.894	-0.270	-0.055	0.019
Strengite	1.474	1.646	2.365					4.043	4.695	3.520
Willemite	-19.431	-18.639	-17.274		0.547		2.294	-11.688	-12.220	-13.845
Halloysite	-8.528	-6.755	-4.432					0.047	1.021	-0.489
MnHPO ₄	-1.368	-1.032	-1.222					0.325	0.662	-0.752
Tyuyamunite	-4.931	-4.828	-3.276							
Carnotite	-5.029	-7.998	-6.129							
Powellite	-4.708	-6.887	-6.013							
Wulfenite										
Kaolinite	-5.260	-3.487	-1.164					3.315	4.289	2.779
Anhydrite	0.051	0.096	-0.732	0.105	0.090	0.115	0.167	0.220	0.139	0.116
Hausmannite	-27.220	-30.081	-25.918		-5.919	-3.295	-1.691	-23.528	-24.482	-28.164
Wairakite	-21.400	-18.902	-17.078					-10.229	-24.482	-28.164

B.1

TABLE B.2. Values of Log AP/K Calculated by MINTEQ for Permeability Column 5
(AP = activity product; K = solubility product.)

Minerals	Perm. Column #5 P.V. = 1.35	Perm. Column #5 P.V. = 3.46	Perm. Column #5 P.V. = 5.54	Perm. Column #5 P.V. = 6.24	Perm. Column #5 P.V. = 7.91	Perm. Column #5 P.V. = 8.89	Perm. Column #5 P.V. = 10.39	Perm. Column #5 P.V. = 11.17
B-UO ₂ (OH) ₂	0.264	0.244				-4.097	-3.768	-3.857
Schoepite	0.396	0.375				-3.966	-3.638	-3.726
Uranhophane	0.354	0.524				-15.787	-14.709	-15.324
Al(OH) ₃ (A)				-2.270	-2.997	-3.441	-2.784	-3.238
AlOHSO ₄				1.102	1.229	1.325	1.649	1.514
Alunite				4.305	3.419	2.892	4.365	3.382
Barite								
Bohemite				-0.459	-1.185	-1.630	-0.972	-1.427
Brucite	-2.982	-3.052	-9.111	-10.305	-11.077	-11.627	-11.325	-11.837
Celestite	0.062	0.286	0.655	0.635	0.648	0.638	0.546	0.194
Chalcedony	-0.409	-0.047	0.299	0.485	0.586	0.733	0.767	0.781
Sepiolite(c)	-0.101	0.846	-10.236	-12.065	-13.307	-13.965	-13.263	-14.244
Ferrihydrite			2.006	1.486	0.898	0.520	0.914	0.492
Fe ₃ (OH) ₈			-0.279	-1.881	-3.643	-4.816	-3.615	-4.893
Fluorite								
Gibbsite(c)				-0.660	-1.387	-1.831	-1.174	-1.628
Gypsum	0.287	0.323	0.510	0.338	0.320	0.353	0.373	0.229
New Gypsum	0.039	0.075	0.262	0.090	0.072	0.281	0.125	-0.019
Na-Jarosite			11.787	12.017	11.537	11.263	11.942	11.034
K-Jarosite			12.194	12.559	12.091	11.764	12.446	11.559
H-Jarosite			9.762	10.737	10.681	10.628	11.141	10.514
SiO ₂ (A,Gl)	-0.914	-0.552	-0.206	-0.020	0.081	0.228	0.262	0.276
SiO ₂ (A,PT)	-1.222	-0.860	-0.514	-0.328	-0.227	-0.080	-0.046	-0.032
Strengite			4.269	4.302	0.586	3.444	3.642	3.429
Willemite	2.030	1.742	-8.719	-10.604	-11.910	-12.557	-11.790	-12.641
Halloysite				1.160	-0.092	-0.686	0.695	-0.185
MnHPO ₄			2.128	1.643	1.117	0.567	0.707	0.429
Tyuyamunite								
Carnotite								
Powellite								
Wulfenite								
Kaolinite				4.428	3.176	2.582	3.963	3.083
Anhydrite	0.062	0.286	0.655	0.635	0.648	0.638	0.546	0.194
Hausmannite		-1.277	-16.699	-19.736	-21.806	-23.207	-22.240	-23.682
Wairakite				-9.037	-10.957	-11.764	-9.961	-11.278

B.2

TABLE B.3. Values of Log AP/K Calculated by MINTEQ for Permeability Column 8
(AP = activity product; K = solubility product)

Minerals	Perm. Column #8 P.V. = 0.84	Perm. Column #8 P.V. = 1.75	Perm. Column #8 P.V. = 2.59	Perm. Column #8 P.V. = 3.24	Perm. Column #8 P.V. = 4.03	Perm. Column #8 P.V. = 8.77	Perm. Column #8 P.V. = 10.55
B-UO ₂ (OH) ₂	0.433	0.639	-3.134				
Schoepite	0.565	0.770	-3.003				
Urahopane	0.610	2.421	-5.127				
Al(OH) ₃ (A)			0.694		-1.322	-2.508	-4.564
AlOHSO ₄			-3.969		1.611	1.906	1.245
Alunite			1.065		6.479	5.167	1.091
Barite							
Boehemite			2.504		0.489	-0.696	-2.752
Brucite	-3.704	-2.867	-2.689	-7.174	-9.909	-11.457	-12.907
Celestite	-0.585	0.265	0.311	0.431	0.537	0.333	0.232
Chalcedony	-0.106	0.188	0.329	0.293	0.708	1.142	1.324
Sepiolite(c)	-0.635	1.919	2.698	-6.381	-10.604	-12.400	-14.753
Ferrihydrite			2.424	1.594	1.317	-0.295	-1.645
Fe ₃ (OH) ₈			1.195	-1.447	-2.368	-7.243	-11.343
Fluorite							
Gibbsite(c)			2.304		0.288	-0.898	-2.954
Gypsum	-0.216	0.651	0.474	0.456	0.349	0.328	0.344
New Gypsum	-0.464	0.403	0.226	0.208	0.101	0.080	0.096
Na-Jarosite			2.689	7.236	10.844	8.242	6.270
K-Jarosite			3.244	7.784	11.381	8.792	6.834
H-Jarosite			-2.515	4.336	9.351	7.476	6.216
SiO ₂ (A,GI)	-0.611	-0.317	-0.176	-0.212	0.203	0.637	0.819
SiO ₂ (A,PT)	-0.919	-0.625	-0.484	-0.520	-0.105	0.329	0.511
Stroengite			0.319	2.840	3.757	2.672	2.132
Willemite	2.008	1.942	2.174	-5.485	-9.910	-12.077	-14.686
Halloysite			6.774		3.502	1.999	-1.749
MnHPO ₄			3.716	3.065	1.678	0.841	0.245
Tyuyamunite							
Carnotite							
Powellite			-0.618				
Wulfenite			2.962				
Kaolinite			10.042		6.770	5.267	1.519
Anhydrite	-0.412	0.457	0.280	0.263	0.156	0.136	6.152
Hausmannite	-6.225	-3.367	0.728	-10.978	-18.543	-22.555	-26.675
Walrakitite			4.434		-5.798	-7.933	-12.697

B.3

TABLE B.4. Values of Log AP/K Calculated by MINTEQ for Vacuum Extractor Columns 1-6 (pore volumes = 1.36 to 7.66)

Minerals	Columns 1-6 P.V. = 1.36	Columns 1-6 P.V. = 3.04	Columns 1-6 P.V. = 4.04	Columns 1-6 P.V. = 5.19	Columns 1-6 P.V. = 6.28	Columns 1-6 P.V. = 7.66
B-UO ₂ (OH) ₂	0.001	-0.047	-0.389	-0.442	-2.846	-3.699
Schoepite	0.140	0.092	-0.250	-0.303	-2.708	-3.560
Urahopane	0.619	0.185	-1.380	-2.831	-10.563	-12.812
Al(OH) ₃ (A)	-0.519	-1.063	-0.043	2.174	-0.749	-1.638
Al(OH) ₃ (A)	-4.877	-5.174	-3.057	0.847	1.522	-1.655
Alunite	0.215	-1.216	3.876	13.194	9.554	7.939
Barite	1.409	1.305	1.324	1.250	1.417	1.392
Boehemite	1.284	0.740	1.760	3.977	1.055	0.166
Brucite	-3.483	-3.543	-4.066	-5.707	-9.412	-10.543
Celestite	0.075	0.198	0.544	0.556	0.359	0.197
Chalcedony	0.264	0.209	0.345	0.531	0.878	1.128
Sepiolite(c)	0.925	0.641	0.001	-2.720	-9.091	-10.602
Ferrihydrite	2.640	0.417 Fe _L	2.589	2.476	1.125	0.199
Fe ₃ (OH) ₈	0.434	-6.114 Fe _L	5.131	4.112	-1.280	-4.128
Fluorite	0.956	0.782	1.004	-1.348	-4.554	-5.279
Gibbsite(c)	1.091	0.547	1.567	3.784	0.861	-0.028
Gypsum	0.415	0.434	0.376	0.343	0.326	0.304
New Gypsum	0.167	0.186	0.128	0.095	0.078	0.056
Na-Jarosite	3.481	2.358	5.858	8.108	9.443	7.891
K-Jarosite	6.678	0.211	8.758	11.086	12.162	10.198
H-Jarosite	1.246	7.420	1.289	4.324	7.468	6.493
SiO ₂ (A,G1)	-0.241	-0.296	-0.160	0.026	0.373	0.623
SiO ₂ (A,PT)	-0.549	-0.604	-0.468	-0.282	0.065	0.315
Strenigite	-1.952 P _L	-4.071 P _L	-1.258 P _L	-0.461 P _L	0.919 P _L	0.459 P _L
Willemite	2.557	0.511	-0.605	-2.672	-7.749	-9.669
Halloysite	4.211	3.012	5.325	10.132	4.980	3.701
MnHPO ₄	-0.419 P _L	0.104 P _L	0.162 P _L	0.392 P _L	-0.001 P _L	-0.716 P _L
Tyuyamunite	1.318 V _L	1.251 V _L	0.995 V _L	0.996 V _L	-1.448 V _L	-2.687 V _L
Carnotite	1.581 V _L	1.336 V _L	1.454 V _L	1.649 V _L	-1.057 V _L	-2.764 V _L
Powellite	-0.262	-3.166 Mo _L	-3.455 Mo _L	-3.543 Mo _L	-3.638 Mo _L	-3.818 Mo _L
Wulfenite	0.286	-2.572 Mo _L	-2.712 Mo _L	-2.739 Mo _L	-2.811 Mo _L	-2.965 Mo _L
Kaolinite	7.479	6.280	8.593	13.400	8.248	6.969
Anhydrite	0.206	0.224	0.168	0.135	0.117	0.096
Hausmannite	-1.410	-0.391	-11.600	-12.279	-18.972	-23.095
Weirakite	1.354	-0.183	1.247	4.709	-3.365	-5.188

L - less than values were used for the specified element

TABLE B.5. Values of Log AP/K Calculated by MINTEQ for Vacuum Extractor Columns 8-12 [pore volumes (accumulative) = 1.90 to 7.59]

Minerals	Columns 8-12 P.V. = 1.90	Columns 8-12 P.V. = 4.06	Columns 8-12 P.V. = 4.70	Columns 8-12 P.V. = 5.37	Columns 8-12 P.V. = 6.11	Columns 8-12 P.V. = 6.80	Columns 8-12 P.V. = 7.59
B-UO ₂ (OH) ₂	-0.125	-0.393	-0.914		-1.857	-3.872	-5.318
Schoepite	0.014	-0.254	-0.776		-1.718	-3.732	-5.179
Uranophane	-0.467	-1.552	-2.757		-6.088	-12.274	-15.831
Al(OH) ₃ (A)	0.431	0.469	0.249	1.262	-0.881	-1.637	-2.413
Al(OH) ₃ (A)	-3.122	-2.396	-2.379	-0.586	-1.751	-0.140	-0.256
Alunite	4.040	5.725	5.389	9.431	4.173	5.224	3.717
Barite	1.441	1.445	1.422	1.406	1.298	1.313	1.249
Boehmite	2.233	2.272	2.053	3.065	0.921	0.165	-0.610
Brucite	-4.263	-4.137	-4.463	-5.415	-6.658	-9.170	-9.919
Celestite	0.103	0.609	0.513	0.345	0.085	-0.038	-0.097
Chalcedony	0.241	0.333	0.402	0.537	0.589	0.689	0.682
Sepiolite(c)	-0.704	-0.176	-0.621	-2.119	-4.448	-9.172	-10.690
Ferrihydrite	3.657	3.868	2.499	1.461	1.542	0.336	-0.033
Fe ₃ (OH) ₈	7.406	7.259	5.101	2.567	1.929	-2.758	-4.115
Fluorite	0.870	0.928	0.802		-0.042	-2.433	-2.765
Gibbsite(c)	2.041	2.079	1.859	2.872	0.729	-0.027	-0.803
Gypsum	0.434	0.384	0.321	0.317	0.262	0.272	0.280
New Gypsum	0.186	0.136	0.073	0.069	0.014	0.024	0.032
Na-Jarosite	8.087 Fe _L	9.905	6.055	3.920	5.307	5.099	4.950
K-Jarosite	10.708 Fe _L	12.911	9.125	7.014	8.429	8.132	7.843
H-Jarosite	3.419 Fe _L	5.425	1.791	0.238	2.437	3.555	3.765
SiO ₂ (A,Gl)	-0.264	-0.172	-0.103	0.032	0.084	0.184	0.177
SiO ₂ (A,PT)	-0.572	-0.480	-0.411	-0.276	-0.224	-0.124	-0.131
Strengite	-0.422 P _L	0.058 P _L	-0.932 P _L	-0.824 P _L	-0.427 P _L	0.181 P _L	0.193 P _L
Willemite	-0.046	-0.633	-0.369	-1.117	-2.836	-7.269	-8.450
Halloysite	6.063	6.324	6.023	8.319	4.136	2.825	1.260
MnPO ₄	-0.006 P _L	0.534 P _L	1.125 P _L	1.767 P _L	1.079 P _L	0.359 P _L	-0.160 P _L
Tyuyamunite	1.335 V _L	0.916 V _L	0.428 V _L		-0.379 V _L	-2.375 V _L	-3.866 V _L
Carnotite	1.359 V _L	1.503 V _L	1.013 V _L		-0.266 V _L	-2.458 V _L	-4.124 V _L
Powellite	-0.936	-3.447	-3.454 Mo _L	-3.438 Mo _L	-3.357 Mo _L	-3.309 Mo _L	-3.314 Mo _L
Wulfenite	-0.316	-2.691	-2.630		-2.457 Mo _L	-2.426 Pb _L , Mo _L	-2.442 Mo _L , Pb _L
Kaolinite	9.331	9.952	9.291	11.587	7.404	6.093	4.528
Anhydrite	0.224	0.176	0.113	0.108	0.052	0.062	0.070
Hausmannite	-9.547	-7.177	-10.440	-13.112	-14.364	-19.825	-22.024
Wairakite	2.372	2.082	1.620	3.400	-1.713	-5.181	-7.410

L - less than values were used for the specified element

TABLE B.6. Values of Log AP/K Calculated by MINTEQA for Vacuum Extractor Columns 15-18 [pore volumes (accumulative) = 0.47 to 3.85]

Minerals	Columns 15-18					
	P.V. = 0.47	P.V. = 1.85	P.V. = 2.36	P.V. = 2.87	P.V. = 3.33	P.V. = 3.85
B-UO ₂ (OH) ₂	-0.357					0.505
Schoepite	-0.218	0.009				-0.366
Uranophane	-0.502	-0.196			-	-1.540
Al(OH) ₃ (A)	-2.877 Al _L	-2.916 Al _L	-0.030	0.387	0.338	-2.847 Al _L
Al(OH) ₃ (A)	-6.719 Al _L	-6.675 Al _L	-3.859	-3.128	-3.009	-6.196 Al _L
Alunite	-6.38 Al _L	-6.235 Al _L	2.260	4.103	4.343	-5.073 Al _L
Barite	1.467	1.457	1.493	1.545	1.470	1.321
Boehmite	-1.075 Al _L	-1.114 Al _L	1.773	2.190	2.141	-1.044 Al _L
Brucite	-4.064		-3.898	-3.958	-3.768	-3.793
Celestite	0.005	0.153	0.213	0.343	0.516	0.486
Chalcedony	0.341	0.270	0.241	0.276	0.298	0.248
Sepiolite(c)	-0.005	-0.100	0.028	0.014	0.458	0.257
Ferrinhydrite	2.480	0.350 Fe _L	2.424	3.248	2.862	3.478
Fe ₃ (OH) ₈	0.013		0.295	4.187	2.251	5.847
Fluorite	0.526	0.741				0.712
Gibbsite(c)	-1.267 Al _L	-1.306 Al _L	1.580	1.997	1.948	-1.237 Al _L
Gypsum	0.374	0.449	0.479	0.479	0.384	0.309
New Gypsum						
Na-Jarosite	3.607	-2.008	4.097	7.022	6.094	7.809
K-Jarosite	6.720	-0.553	6.609	9.671	8.952	10.888
H-Jarosite	-0.692	-6.915	-0.836	2.263	1.444	3.286
SiO ₂ (A,Gl)	-0.164	-0.235	-0.264	-0.229	-0.207	-0.257
SiO ₂ (A,PT)	-0.472	-0.543	-0.572	-0.537	-0.515	-0.565
Strengite	-1.613 P _L	-3.881 P _L	-1.456 P _L	-0.438 P _L	0.846 P _L	-0.527 P _L
Willemite	0.532	-0.049	-0.377	-0.634	-0.968	-0.492
Halloysite	-0.352 Al _L	-0.572 Al _L	5.142	6.049	5.994	-0.477 Al _L
Mn ₃ PO ₄	-1.008 P _L	-0.762 P _L	-0.401 P _L	0.262 P _L	-0.263 P _L	-0.225 P _L
Tyuyamunite	1.101 V _L	1.255 V _L				0.736 V _L
Carnotite	1.133 V _L	1.345 V _L				1.236 V _L
Powellite	-0.077	-0.886	-3.105 Mo _L	-3.196 Mo _L	-3.390 Mo _L	-3.435 Mo _L
Wulfenite	0.539 Pb _L	-0.279 Pb _L				-2.614 Mo _L Pb _L
Kaolinite	2.916 Al _L	2.696 Al _L	8.410	9.317	9.262	2.791 Al _L
Anhydrite	0.164	0.240	0.270	0.270	0.175	0.100
Hausmannite	-4.791		-4.513	-5.945	-5.892	-8.390
Wairakite	-3.614		1.775	2.439	2.164	-4.481

APPENDIX C



**TABLE C.1. Measured and Predicted Effluent Values for Permeability
Column 5 (mg/l, except for pH and pe)**

Pore Volume	Measured Values							
	1.35	3.46	5.54	6.24	7.91	8.89	10.39	11.17
Al	DL	DL	DL	47	167	392	564	703
Fe	DL	DL	127	538	950	1,330	1,560	1,720
Mn	DL	2.4	41.2	64.4	89.6	101	101	96
SO ₄	2,200	3,704	7,864	9,492	12,192	13,900	14,800	10,100
Mg	203	519	1,420	1,554	1,771	1,738	1,601	1,420
Sr	14	19	38	32	31	31.3	25.3	19.0
Ca	657	612	820	512	467	507	528	517
Si	1.35	3.46	5.54	6.24	7.91	8.89	10.39	11.17
U	0.4	0.56	DL	DL	DL	19.7	23.8	27.2
pH	8.20	8.00	4.80	4.20	3.80	3.53	3.70	3.42
pe	5.37*	5.59*	8.99*	9.63*	10.03*	10.34*	10.15*	10.44*

Pore Volume	Predicted Values								
	1.0	2.0	3.0	4.0	5.0	6.0	7.0	8.0	9.0
Al	0.4	0.5	51	89	89	89	89	27	747
Fe	0.0	0.0	479	3,809	3,809	3,809	3,809	3,001	2,254
Mn	16	24	154	65	65	65	65	65	65
SO ₄	2,305	7,470	7,428	11,128	11,128	11,128	11,128	11,897	13,540
Mg	608	2,102	881	701	701	701	701	700	700
Sr	16	10	14	12	12	12	12	12	12
Ca	824	513	605	506	506	506	506	532	535
Si	52	50	52	51	51	51	51	52	51
U	41	41	41	41	41	41	41	41	41
pH	7.66	7.66	3.05	2.83	2.83	2.83	2.83	2.28	1.87
pe	2.21	2.22	14.16	14.81	14.81	14.81	14.81	15.01	15.29

DL - less than detection limit.
* - estimated values.

TABLE C.2. Measured and Predicted Effluent Values for Permeability Column 8 (mg/l, except for pH and pe)

Pore Volume	Measured Values						
	0.84	1.75	2.59	3.24	4.03	8.77	10.55
Al	DL	DL	5.5	DL	93	976	1,061
Fe	DL	DL	0.1	1.2	146	90	112
Mn	0.04	0.3	7.6	32.8	62.7	75.6	74
SO ₄	783	3,793	4,518	5,752	8,492	13,700	13,972
Mg	89	473	781	1,099	1,467	1,147	1,018
Sr	5.3	25	22	26	27	15	12
Ca	306	1,577	904	800	546	480	500
U	2.1	6.8	4.4	DL	DL	DL	DL
pH	7.95	8.10	8.10	5.80	4.40	3.70	3.00
pe	5.64*	5.47*	5.47*	7.92*	9.41*	10.15*	10.90*

Pore Volume	Predicted Values					
	1.0	2.0	3.0	4.0	5.0	6.0
Al	0.5	68	89	89	352	747
Fe	0.01	1,446	3,809	3,809	2,885	2,254
Mn	20	110	65	65	65	65
SO ₄	4,525	6,754	11,128	11,128	12,137	13,540
Mg	1,313	878	701	701	701	701
Sr	13	12	12	12	12	12
Ca	588	557	506	506	533	535
U	41	41	41	41	41	41
pH	7.65	2.92	2.83	2.83	2.19	1.87
pe	2.21	14.48	14.81	14.81	15.05	15.29

DL - less than detection limit.
 * - estimated values.

TABLE C.3. Measured and Predicted Effluent Values for Vacuum
Extractor Columns 1-6 (mg/l, except for pH and pe)

Pore Volume	Measured Values										
	1.36	3.04	4.04	5.19	6.28	7.66	9.21	10.43	11.75	13.21	16.05
Al	0.20	0.05	0.29	23.1	46.6	171	444	250	147	128	91
Fe	0.16	<0.10	14.7	108.2	852	1,266	948	466	236	256	192
Mn	0.42	1.78	4.50	44.5	130	72.8	53.6	25.4	15.6	13.5	9.6
SO ₄	2,600	3,400	6,540	7,400	7,880	8,480	8,480	4,540	3,880	2,780	2,420
Mg	307	409	1,260	1,320	1,010	765	584	290	186	160	112
Sr	16.3	17.8	30.9	29.3	18.1	11.9	9.1	6.1	4.9	5.0	4.6
Ca	913	830	607	534	503	466	482	514	483	566	554
U	0.17	0.15	0.09	0.40	0.82	1.16	3.80	3.60	ND	1.90	2.20
pH	7.86	7.79	7.33	6.51	4.72	4.22	3.95	3.94	3.95	3.96	3.97
pe	421	418	165	254	439	459	470	455	453	442	441

Pore Volume	Predicted Values								
	1.0	2.0	3.0	4.0	5.0	6.0	7.0	8.0	9.0
Al	0.66	0.58	3.02	31.6	58.6	58.6	58.6	111.2	372.3
Fe	6.31	10.6	88	192	1173	1173	1173	1027	567
Mn	8.52	14.5	107.7	43.5	43.5	43.5	43.5	43.5	43.6
SO ₄	4121	6763	5696	5264	7829	7829	7829	8021	8972
Mg	340	1019	659	445	445	445	445	445	445
Sr	6.68	6.68	6.68	6.68	6.68	6.68	6.68	6.68	6.68
Ca	437	413	417	425	421	421	421	425	437
UO ₂	8.29	8.29	8.32	8.29	8.32	8.32	8.32	8.32	8.32
pH	7.85	7.77	5.85	3.28	2.99	2.99	2.99	2.70	2.16
pe	12.67	-1.04	-0.96	3.88	11.91	12.80	12.80	12.81	12.68

ND - not determined



DISTRIBUTION

<u>No. of Copies</u>		<u>No. of Copies</u>
485	U.S. Nuclear Regulatory Commission Division of Technical Information and Document Control 7920 Norfolk Avenue Bethesda, MD 20014 Gary Beall Radian Corporation 8500 Shoal Creek Austin, TX 78766 G. F. Birchard NRC Office of Nuclear Regulatory Research Washington, DC 20555 D. G. Brookins Department of Geology University of New Mexico Albuquerque, NM 87131 Jess Cleveland Denver Federal Center U.S. Geological Survey P.O. Box 25046 MS-412 Lakewood, CO 80225 George Condrat Dames & Moore Suite 200 250 E. Broadway Salt Lake City, UT 84717 J. J. Davis NRC Office of Nuclear Regulatory Research Washington, DC 20555 W. K. Eister DOE Office of Waste Isolation Washington, DC 20545	B. R. Erdal Los Alamos Scientific Laboratory CNC-11, MS-514 Los Alamos, NM 87545 P. J. Garica NRC Office of Nuclear Material Safety and Safeguards Washington, DC 20555 G. Gnugnoli Uranium Recovery Licencing Branch Division of Waste Management Nuclear Regulatory Commission MS-467-SS Washington, DC 20555 D. F. Harmon NRC Office of Nuclear Regulatory Research Washington, DC 20555 Dana Isherwood Lawrence Livermore Laboratory P.O. Box 808 MSL-224 Livermore, CA 94550 Don Langmuir Dept. of Chemistry and Geochemistry Colorado School of Mines Golden, CO 80401 Lawrence Berkeley Laboratory Reference Library University of California Berkeley, CA 94720 Lawrence Livermore Laboratory Reference Library P.O. Box 808 Livermore, CA 94550

No. of
Copies

Los Alamos Scientific Laboratory
Reference Library
P.O. Box 1663
Los Alamos, NM 87544

Mark Matthews
UMTRAP
DOE Albuquerque Operations
Office
P.O. Box 5400
Albuquerque, NM 87115

Robert E. Meyer
Oak Ridge National Laboratory
P.O. Box X
Oak Ridge, TN 37830

Thomas Nicholson
Nuclear Regulatory Agency
Earth Science Division
MS 1130 SS
Office of Nuclear Materials,
Safety and Safeguards
Washington, DC 20555

G. A. Parks
Stanford University
Department of Applied Earth
Sciences
Stanford, CA 94305

Savannah River Laboratory
Reference Library
Aiken, SC 29801

Martin Seitz
Argonne National Laboratory
9700 S. Cass Avenue
Argonne, IL 60439

Dan Siefken
Nuclear Regulatory Agency
Office of Nuclear Materials,
Safety and Safeguards
Washington, DC 20555

No. of
Copies

Robert Silva
Lawrence Berkeley Laboratory
University of California
One Cyclotron Road
Building 70A/1160
Berkeley, CA 94720

Daryl Tweeton
U.S. Bureau of Mines
P.O. Box 1660
Twin Cities, MN 55111

K. L. Weaver
Radiation Control Division
Colorado Department of Health
4210 E. 11th Avenue
Denver, CO 80220

W. A. Williams
Office of Radiation Programs
Environmental Protection Agency
Washington, DC 20460

T. J. Wolery
Lawrence Livermore Laboratory
P.O. Box 808
Livermore, CA 94550

Kurt Wolfsberg
Los Alamos Scientific Laboratory
CNC-11, MS-514
Los Alamos, NM 97545

Rockwell Hanford Operations

G. S. Barney

50 Pacific Northwest Laboratory

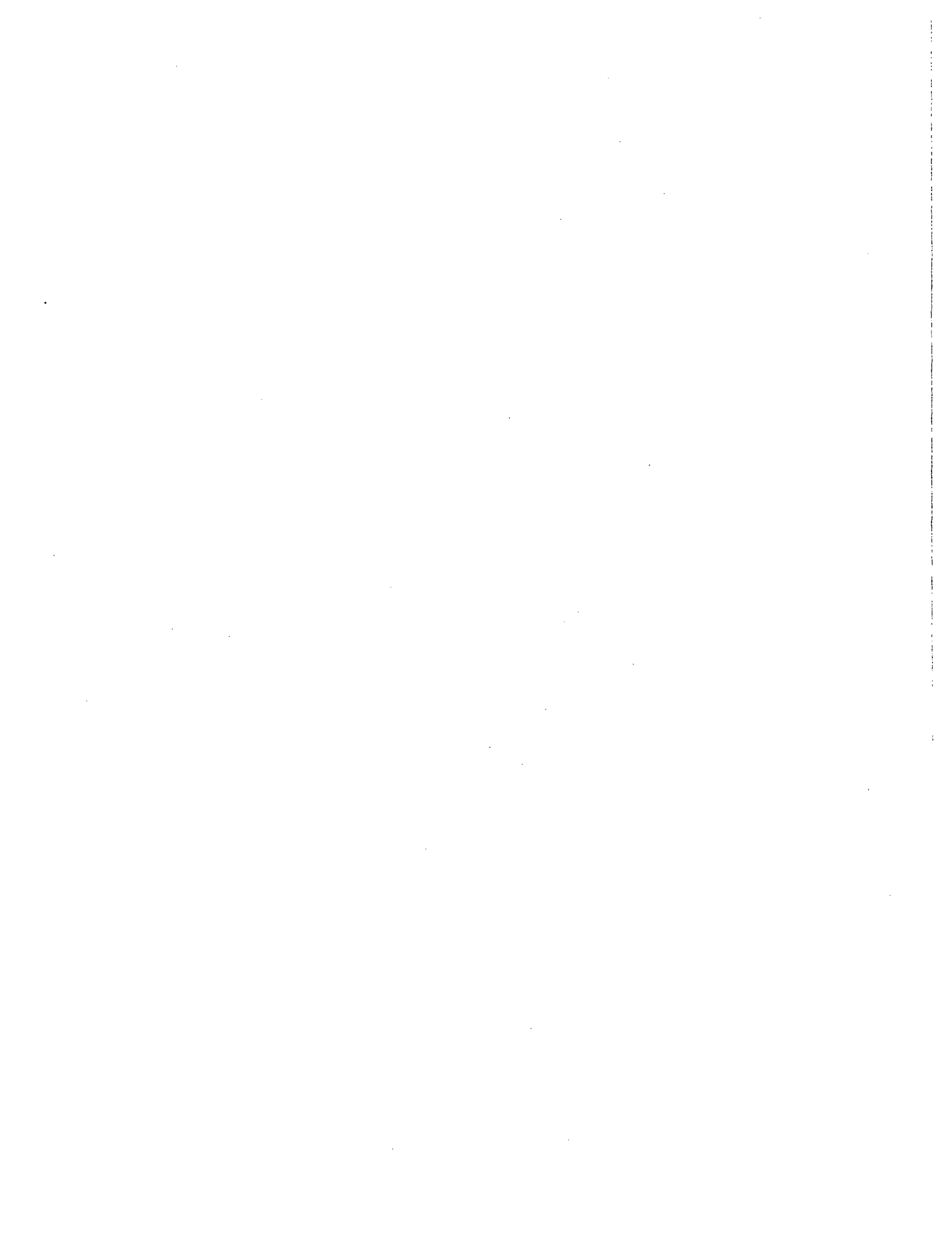
W. J. Deutsch
M. E. Dodson
D. W. Dragnich
C. E. Elderkin
R. L. Erikson
A. R. Felmy

No. of
Copies

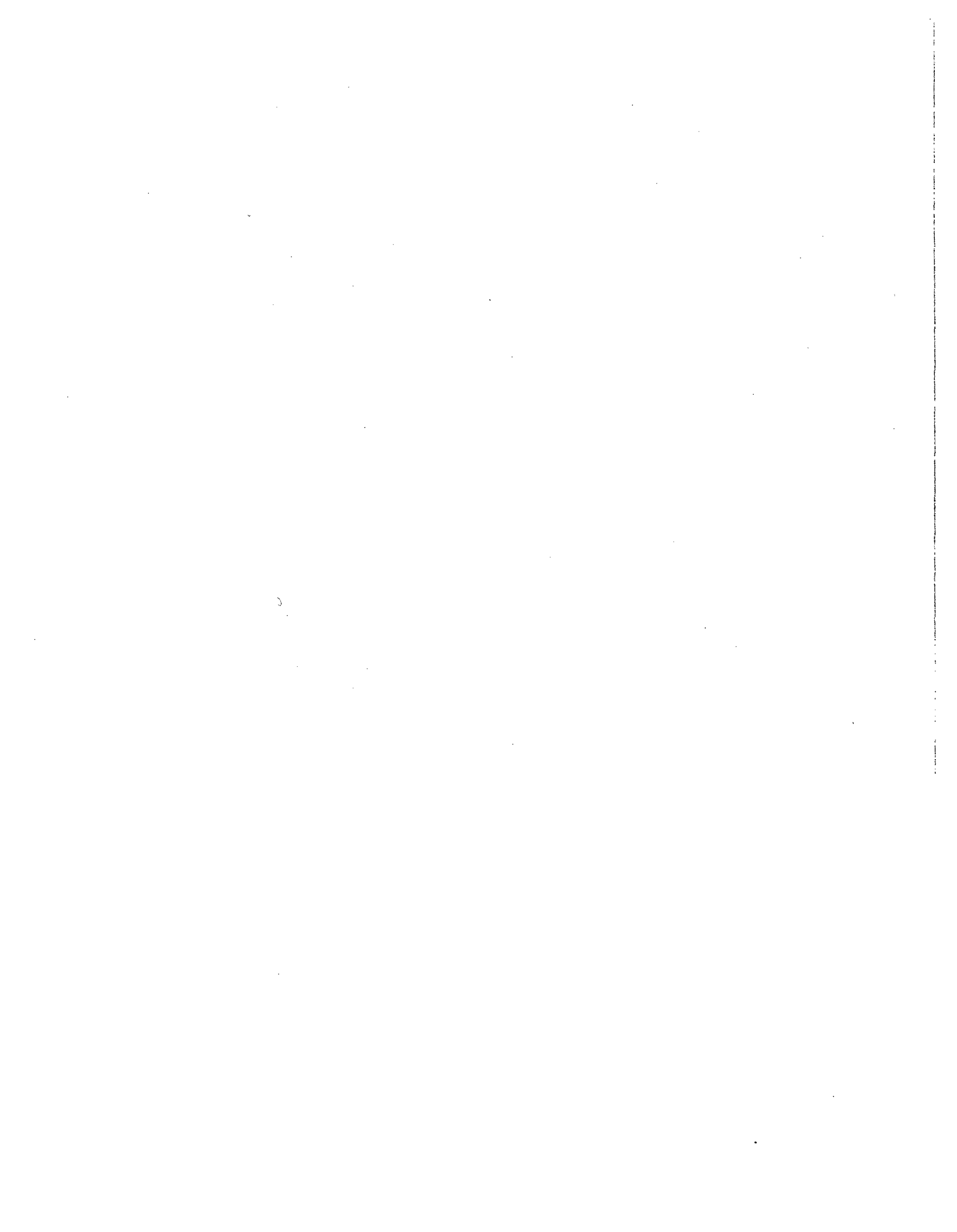
M. G. Foley
J. S. Fruchter
G. W. Gee
J. N. Hartley
C. T. Kincaid
D. R. Kalkwarf
W. J. Martin
R. W. Nelson
B. E. Opitz
P. R. Partch (19)
R. W. Perkins

No. of
Copies

S. R. Peterson
J. F. Relyea
R. J. Serne
D. R. Sherwood
J. A. Stottlemire
V. T. Thomas
W. C. Weimer
N. A. Wogman
Technical Information (5)
Publicating Coordination BE(2)



NRC FORM 335 (11-81)		U.S. NUCLEAR REGULATORY COMMISSION BIBLIOGRAPHIC DATA SHEET		1. REPORT NUMBER (Assigned by DDC) NUREG/CR-3404 PNL-4782	
4. TITLE AND SUBTITLE (Add Volume No. if appropriate) Predictive Geochemical Modeling of Interactions Between Uranium Mill Tailings Solutions and Sediments in a Flow-Through System Model Formulations and Preliminary Results				2. (Leave blank)	
7. AUTHOR(S) S.R. Peterson, A.R. Felmy, R.J. Serne, G.W. Gee				5. DATE REPORT COMPLETED MONTH July YEAR 1983	
9. PERFORMING ORGANIZATION NAME AND MAILING ADDRESS (Include Zip Code) Pacific Northwest Laboratory Richland, WA 99352				DATE REPORT ISSUED MONTH August YEAR 1983	
12. SPONSORING ORGANIZATION NAME AND MAILING ADDRESS (Include Zip Code) Division of Health, Siting and Waste Management Office of Nuclear Regulatory Research U.S. Nuclear Regulatory Commission Washington, DC 20555				10. PROJECT/TASK/WORK UNIT NO.	
13. TYPE OF REPORT				PERIOD COVERED (Inclusive dates) November 1982 - May 1983	
15. SUPPLEMENTARY NOTES				14. (Leave blank)	
16. ABSTRACT (200 words or less) An equilibrium thermodynamic conceptual model consisting of minerals and solid phases was developed to represent a soil column. A computer program was used as a tool to solve the system of mathematical equations imposed by the conceptual chemical model. The combined conceptual model and computer program were used to predict aqueous phase compositions of effluent solutions from permeability cells packed with geologic materials and percolated with uranium mill tailings solutions. Initial calculations of ion speciation and mineral solubility and our understanding of the chemical processes occurring in the model. The modeling predictions were compared to the analytically determined column effluent concentrations. Hypotheses were formed, based on modeling predictions and laboratory evaluations, as to the probable mechanisms controlling the migration of selected contaminants. An assemblage of minerals and other solid phases could be used to predict the concentrations of several of the macro constituents (e.g., Ca, SO ₄ , Al, Fe, and Mn) but could not be used to predict trace element concentrations. These modeling conclusions are applicable to situations where uranium mill tailings solutions of low pH and high total dissolved solids encounter either clay liners or natural geologic materials that contain inherent acid neutralizing capacities.					
17. KEY WORDS AND DOCUMENT ANALYSIS			17a. DESCRIPTORS		
Predictive Geochemical Modeling, precipitation, dissolution, uranium mill tailings, permeability columns					
17b. IDENTIFIERS/OPEN-ENDED TERMS					
18. AVAILABILITY STATEMENT Unlimited			19. SECURITY CLASS (This report) Unclassified		21. NO OF PAGES
			20. SECURITY CLASS (This page) Unclassified		22. PRICE \$



PAGE: 1

U.S. NUCLEAR REGULATORY COMMISSION
PACKING SLIP

DATE: 10/16/86

USNRC
MICHAEL YOUNG
623SS

ORDER NUMB: A18836-00013
ORDER TYPE: 2

DOCUMENT NO.	QTY @	COST	TOTAL COST	COMMENTS
NUREGCR1494	1			
NUREGCR2383	1			
NUREGCR3124	1			
NUREGCR3404	1			

TOTAL DOCUMENTS ORDERED : 4
TOTAL DOCUMENTS ENCLOSED: 4

UNITED STATES
NUCLEAR REGULATORY COMMISSION
WASHINGTON, D.C. 20555

OFFICIAL BUSINESS
PENALTY FOR PRIVATE USE, \$300

FOURTH-CLASS MAIL
POSTAGE & FEES PAID
USNRC
WASH. D. C.
PERMIT No. 667